III International Symposium

TOPICAL PROBLEMS OF BIOPHOTONICS

NEUROIMAGING AND NEURODYNAMICS

Chairs

Alexander Dityatev, Italian Institute of Technology, Genova, Italy; University of Nizhny Novgorod, Russia

Victor Kazantsev, Institute of Applied Physics RAS, University of Nizhny Novgorod, Russia

Alexey Semyanov, RIKEN Brain Science Institute, Japan; University of Nizhny Novgorod, Russia

Program Committee

Pavel Balaban, Institute of Higher Nervous Activity and Neurophysiology RAS, Russia

Luca Berdondini, Italian Institute of Technology, Italy

Christian Henneberger, University College London, UK

Alexander Kleschevnikov, University of California, San Diego, USA

Vladimir Nekorkin, Institute of Applied Physics RAS, Russia

Evgeny Nikolsky, Kazan State University, Russia

Ivan Pavlov, University College London, UK

Dmitri Rusakov, University College London, UK

Constanze Seidenbecher, Leibniz Institute for Neurobiology, Germany

Kirill Volynski, University College London, UK

Vladimir Yakhno, Institute of Applied Physics RAS, Russia

Invited

STUDY OF MITOCHONDRIAL PHYSIOLOGY IN NEURONS AND ASTROCYTES USING FLASH PHOTOLYSIS OF CAGED CALCIUM

A.Y. Abramov

Department of Molecular Neuroscience, UCL Institute of Neurology, London
a.abramov@ucl.ac.uk

The most prominent and disabling features in patients with mitochondrial disease are often due to neuronal dysfunction and neurodegeneration. Mitochondrial dysfunction is shown to be associated with most common age related neurodegenerative diseases, such as Alzheimer's and Parkinson's Diseases.

Mitochondrial dysfunction is originally implicated in PD pathogenesis because exposure to environmental toxins that inhibit mitochondrial respiration and promote production of reactive oxygen species (ROS) cause loss of dopaminergic neurons in humans and animal models. Indeed, the most established model of PD is induced by mitochondrial complex I inhibitor – rotenone and mptp/mpp [1, 2]. Recent demonstrations that *pink1* and *DJ-1 are* located in mitochondria also have an effect on mitochondrial function [3], reinforce the importance of these themes in PD pathogenesis and have enabled understanding of these processes at the mechanistic level.

One of the major mitochondrial functions is buffering of Ca^{2+} in physiological calcium signaling. Mitochondrial Ca^{2+} overload is critically important as a determinant of irreversible cell injury by inducing the permeability transition pore (mPTP) opening. This results in rapid depolarization of the mitochondrial membrane and cessation of mitochondrial oxidative phosphorylation. Prevention of mPTP opening can prevent cells from dying during ischaemia and reperfusion injury.

When cytosolic Ca^{2+} rises mitochondria accumulate Ca^{2+}, which moves down its electrochemical gradient through an electrogenic uniporter that facilitates Ca^{2+} transport across the inner mitochondrial membrane into the matrix. Mitochondrial Ca^{2+} release in neurons is regulated primarily by a Na^{+}/Ca^{2+} exchanger [4]. The maximal rate of release is much lower than the maximal rate of uptake, which is why continuous mitochondrial calcium accumulation is observed when the cytosolic Ca^{2+} is high. The net effect of the mitochondrial Ca^{2+} transport pathways is that this organelle contains little calcium in resting cells, but abruptly begins to accumulate large amounts of calcium during stimulated Ca^{2+} entry, and to release this calcium load during recovery. Net Ca^{2+} accumulation will occur when the rate of influx exceeds the capacity of the exchangers to remove Ca^{2+}.

Measurement of mitochondrial uptake Ca^{2+} capacity (or the threshold for mPTP opening) is therefore important for understanding the mechanisms of the pathology and also for testing neuroprotective drugs. Many approaches use isolated mitochondria or bulk measurements from permeabilised cells and titration of the Ca^{2+} capacity by the progressive application of external Ca^{2+}. We have devised an approach that allows these measurements to be made at the level of a single cell, where this approach is a requirement of the experimental system. Thus, the experimental system demands that these measurements are made at the level of single cells when cell numbers are small, the population is heterogeneous, or when a modest proportion of cells are transfected and express a protein of interest.

Furthermore, it is important to bear in mind that, as mitochondrial Ca^{2+} uptake depends on $\Delta\psi_m$, comparative studies of mPTP threshold may be biased by differences in effective Ca^{2+} uptake in populations in which $\Delta\psi_m$ varies. We have therefore devised an approach that delivers Ca^{2+} directly to the matrix of mitochondria independent of uptake and therefore independent of $\Delta\psi_m$, which allows a direct study of the efflux pathway and the specific sensitivity of mPTP to Ca^{2+}. This is achieved by using flash photolysis of caged Ca^{2+} compounds such as *o*-nitrophenyl EGTA which are introduced into the cell as the acetoxymethyl (AM) ester (NP-EGTA, AM). This method can be used in intact and permeabilized cells, although results in intact cells can be misinterpreted because Ca^{2+} will be released both in the cytosol and in the mitochondrial matrix. Permeabilization of cells with digitonin in a pseudo intracellular solution localizes the caged Ca^{2+} signal to the matrix of mitochondria only.

The principle of the 'caged' Ca^{2+} is that NPEGTA is a photolabile Ca^{2+} chelator, whose affinity diminishes greatly following exposure to UV light (the Kd changes in the time of UV flash from 80 nM to >1 mM). Thus, NPEGTA acts as a chelator that binds Ca^{2+}avidly when loaded into cells, but will release Ca^{2+}as the affinity falls following a UV flash.

Measurement of mPTP opening can be achieved using cells co-loaded with a fluorescent Ca^{2+}-indicator and with probes for mitochondrial membrane potential (fluo-4 and TMRM respectively). The loss of mitochondrial membrane potential in response to a rise in $[Ca^{2+}]_c$ in intact or permeabilized cells can be attributed to mPTP opening, if it can be prevented by cyclosporine A (CsA), the archetypal inhibitor of the mPTP [5].

Delivery of Ca^{2+} into the matrix of mitochondria independent of calcium uniporter can also be used for investigation of the activity of mitochondrial Na^+/Ca^{2+} exchanger [6] and for mild activation of mitochondrial respiration.

References

1. J.T. Greenamyre and T.G. Hastings, *Science*, 2004, **304**, 1120-1122.
2. M.W. Dodson, M. Guo, *Curr Opin Neurobiol*., 2007, **17**(3), 331-7.
3. A. Wood-Kaczmar, S. Gandhi, N.W. Wood, *Trends Mol Med*., 2006, **12**(11), 521-8.
4. M. Crompton, R Moser, H. Ludi, and E. Carafoli, *Eur J Biochem*, 1978, **82**, 25-31.
5. K.M. Broekemeier, M.E. Dempsey, D.R. Pfeiffer, *Journal of Biological Chemistry,* 1989, **264**, 7826-7830.
6. S. Gandhi, A. Wood-Kaczmar, Z. Yao, H. Plun-Favreau, E. Deas, K. Klupsch, J. Downward, D.S. Latchman, S.J. Tabrizi, N.W. Wood, M.R. Duchen, A.Y. Abramov, *Molecular Cell*, 2009, **33**, 627-638.

SUBCELLULAR CA^{2+} DYNAMICS IN SPATIALLY EXTENDED MODEL OF ASTROCYTE

S.Yu. Asatryan[1,2], **V.B. Kazantsev**[1,2], and **A.V. Semyanov**[1,3]

[1] Nizhny Novgorod State University, Russia, asatryan@neuro.nnov.ru
[2] Institute of Applied Physics RAS, Nizhny Novgorod, Russia
[3] RIKEN Brain Science Institute, Wako-shi, Japan

Calcium signaling in astrocytes is one of the mechanisms for neuron-glia communication [1]. In particular, the astrocytes using their branching processes can detect the activation of neighboring synapses through neurotransmitter (for example, glutamate) diffused from the synaptic cleft. Activation of metabotropic glutamate receptors triggers the production of inositol 1, 4, 5-trisphosphate (IP3). In turn, the IP3 may activate the IP3 receptors in the endoplasmic reticulum (ER), leading to Ca^{2+} release from the ER to cytosol. This mechanism is described in detail in many theoretical models [3, 4]. It is still unclear, however, how calcium signals correlate with complex morphology of astrocyte processes that may have generally different subcellular structure between distal processes and somatic compartment. Recent experimental findings have demonstrated that calcium responses in different compartments may have different characteristics [2]. In particular, most of calcium "sparks" may be localized in distal processes and may not necessarily trigger generalized response in soma. In other words, local events may not trigger the propagation of intracellular calcium waves in the astrocyte compartments.

In this work we developed a mathematical model of calcium signaling taking into account spatially extended astrocyte morphology and the details of subcellular structure for different cell compartments. The model is schematically shown in Fig. 1A. For each compartment we used three equations (modified from [4]) describing changes of intracellular calcium concentration due to active and passive fluxes through plasmatic and ER membrane. We considered each astrocyte compartment as a cylinder defining the total cell volume with inserted cylinder defining the volume of ER. First, we analyzed the characteristics of spontaneous signals depending on the geometry. To generate spontaneous calcium "sparks" we introduced a noise component in the equation for IP3 concentration that describes its overall fluctuations due to, for example, spontaneous activation of metabotropic glutamate receptors. Figure 1B illustrates how the frequency of spontaneous calcium "sparks" changes for different sizes of cell compartments. Here we fixed the ratio between the ER and cell radii and vareid the radius of the ER. The frequency of calcium "sparks" was much higher for smaller processes.

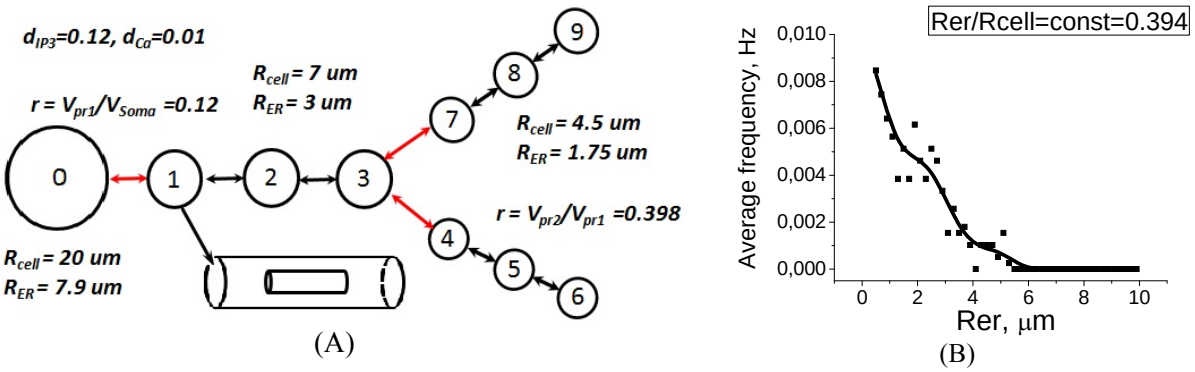

Fig. 1. A – Qualitive view of astrocyte model structure. The model consists of soma (compartment №0) and 3 processes. Compartments connected with each other by the diffusion of key intracellular chemicals (IP3 and Ca^{2+}). B – Average frequency of spontaneous calcium spikes for different sizes of ER

Another problem is the propagation of the activity from distal processes to proximal ones. To address this issue we introduced into the model calcium and IP3 diffusive fluxes between the compartments:

$$J_{ij}^{IP3diff} = \frac{d_{IP3}}{r_{ij}}([IP3]_j - [IP3]_i), \qquad J_{ij}^{Cadiff} = \frac{d_{Ca}}{r_{ij}}([Ca]_j - [Ca]_i). \tag{1}$$

Here, parameters d_{IP3} and d_{Ca} are the diffusion constants for IP3 and for calcium, respectively; r_{ij} is the ratio of volumes between the compartments. Figure 2 shows typical results of simulation of the model composed of 10 interconnected compartments. Note that spontaneous calcium "sparks" were quite localized and the diffusion did not lead to their propagation. Typical frequency of spontaneous calcium "sparks" was higher for smaller size compartments. Thus, local events generated in distal processes had no direct correlation with generalize calcium signals generated and detected in somatic region.

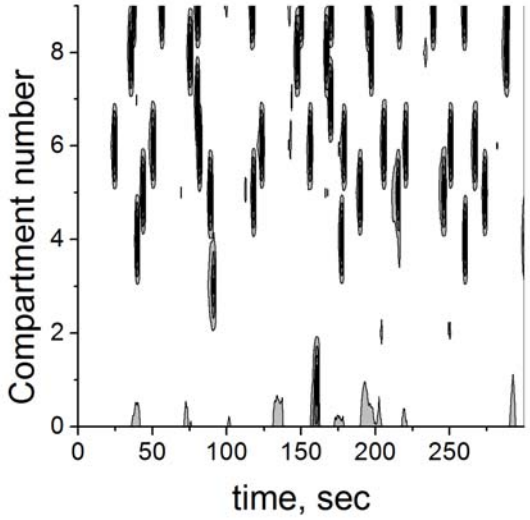

Fig. 2. Binary mapped distribution of calcium "sparks" in the model composed of 10 interconnected compartments. The number of compartments on the binary map corresponds to numbering in the schematic view of the model in figure 1

In summary, the model predicts that the peripheral compartments of the astrocyte may communicate with synapses independent of activation of the whole astrocyte. Therefore, a generalized calcium transient typically recorded in astrocytes may not effectively correlate with activation of particular synaptic pathways. The generalized transient might be connected only with highly synchronized (brain rhythms or epileptic-like discharges) activation of neuronal groups surrounding the astrocyte.

Acknowledgements

This work was supported by the Russian Federal Program (grants 16.512.11.2136, 14.740.11.0075) and by the grant of the President of the Russian Federation (MD-5096.2011.2).

References

1. A. Verkhratsky, Butt A. Glial, *Neurobiology – Wiley: John Wiley&Sons*, 2007, **83**.
2. W.J. Nett, S.H. Oloff, *Journal of Neurophysiology*, 2002, **87**, 529.
3. G.W.D. Young, J. Keizer, *Proc.Natl. Acad. Sci.*, 1992, **89**, 9895-9899.
4. G. Ullah, P. Jung, and A.H. Cornell-Bell, *Cell Calcium*, 2006, **39**, 197-208.

Invited

IMAGING NEURODYNAMICS WITH HIGH-RESOLUTION ELECTRODE ARRAYS

L. Berdondini and **A. Maccione**

[1] Neuroscience and Brain Technology Department, Fondazione Istituto Italiano di Tecnologia (IIT)
Genova, Italy, e-mail: Luca.Berdondini@iit.it

Microelectrode arrays (MEAs) is an increasingly used methodology for investigating the ongoing or evoked neurodynamics on cultured neuronal networks or brain tissue and it is a valuable technological candidate for developing effective high-throughput instrumentation for in-vitro drug screenings [1]. Developed at the end of the seventies [2–4], these devices are conventionally realized by thin-film micro-machining approaches and were constantly improved over the years, by modifying the electrode materials and morphologies or by completing the on-chip functionalities [5–9]. This methodology enabled for example to investigate neuronal signaling expressed by complex in-vitro experimental models [10, 11], to explore coding and learning basic mechanisms at the neuronal population and cellular levels [12, 13] and to study the effects of neuro-active compounds [14] on the global network activity.

Conventional and commercially available MEAs systems (e.g. Multi Channel Systems, Reutlingen, Germany; Panasonic, Osaka, Japan; Ayanda Biosystems, Lausanne, Switzerland) manage acquisitions from typically 64–256 microelectrodes. This provides a global view of the network activity at a typical spatial resolution of 100 μm (typical value for inter electrode distances) and at sampling frequencies of 10–50 kHz. However, experimental variability affecting the significance of first order statistical parameters to describe the network activity, e.g. Mean Firing Rate (MFR), Inter Spike Intervals (ISI), Mean Bursting Rate (MBR); lack of single neuron activity resolution in large networks and the lower extracellular signal quality compared to intracellular recordings are some of the key issues affecting the extensive use of this methodology.

While pioneering developments in enabling neuro-electrode couplings to sense intracellular like signals were recently reported [15], in our work we are extending the potential capabilities, yet under-exploited, of the MEAs methodology by adopting technological concepts originally developed for light-imaging sensors. Indeed, the access to a detailed spatial-temporal view of the global network electrophysiological signaling has become feasible only recently with the development of MEAs based on Complementary Metal Oxide Semiconductor (CMOS) technology, providing on large active areas, recording site separations in the range of (or below) soma dimensions [16–18]. Our recent development of an Active Pixel Sensor based MEA platform (APS-MEA) integrating 4096 microelectrodes at spatial resolution of 21 μm and enabling to achieve a sampling rate of 7.7 kHz/channel when recording from the full active area of 2.5 x 2.5 mm^2 [19], allowed to observe the propagation of spontaneous activity patterns over large neuronal networks at cellular resolution and was recently applied to acute brain tissue to investigate retinal development and epileptogenic signaling in cortico-hippocampal brain slices (Figure 1).

This innovative experimental capability brings the MEA methodology into the imaging field [20] and settles innovative challenges in the representation and analysis of spatiotemporal activity patterns acquired form very large electrode arrays.

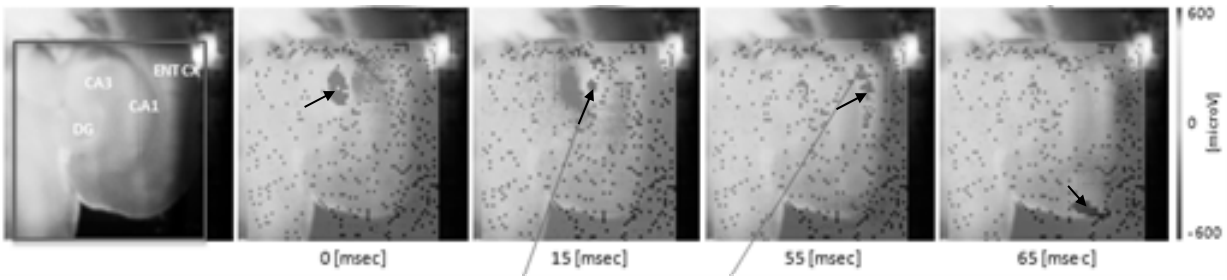

Fig. 1. Imaging on a 4096 electrode array of an epileptogenic LFP propagation in the cortico-hippocampal circuit, induced by application of the convulsant agent 4-aminopyridine and in combination with bicuculline (full-frame rate at 7.8 kHz/electrode, inter-electrode separation of 21 μm)

References

1. M. Baker, "From promising to practical: tools to study networks of neurons", *Nat. Methods*, 2010, **7**(11), 877-883.
2. J. Pine, "Recording action potentials from cultured neurons with extracellular microcircuit electrodes", *J. Neurosci. Meth.*, 1980, **2**, 19-31.
3. G.W. Gross, "Simultaneous single unit recording in vitro with a photoetched laser deinsulated gold multielectrode surface", *IEEE Trans. Bio-Med. Eng.*, 1979, **26**, 273-9.
4. C.A. Thomas, P.A. Springer, L.M. Okun, Y. Berwaldn, and G.E. Loeb, "Miniature Microelectrode Array to Monitor Bioelectric Activity of Cultured Cells", *Exp. Cell Res.*, 1972, **74**, 61.
5. L. Rowe, M. Almasri, K. Lee, N. Fogleman, G.J. Brewer, Y. Nam, B.C. Wheeler, J. Vukasinovic, A. Glezer, and A.B. Frazier, "Active 3-D microscaffold system with fluid perfusion for culturing *in vitro* neuronal networks", *Lab. Chip*., 2007, **7**, 475-82.
6. T. Kraus, E. Verpoorte, V. Linder, W. Franks, A. Hierlemann, F. Heer, S. Hafizovic, T. Fujii, N.F. de Rooij, and S. Koster, "Characterization of a microfluidic dispensing system for localised stimulation of cellular networks", *Lab. Chip.,* 2006, **6**, 218-29.
7. M.O. Heuschkel, M. Fejtl, M. Raggenbass, D. Bertrand, and P. Renaud, "A three-dimensional multi-electrode array for multi-site stimulation and recording in acute brain slices", *J. Neurosci. Meth.,* 2002, **114**, 135-48.
8. W.H. Baumann, M. Lehmann, A. Schwinde, R. Ehret, M. Brischwein, and B. Wolf, "Microelectronic sensor system for microphysiological application on living cells", *Sensor Actuat B-Chem*., 1999, **55**, 77-89.
9. P. Thiébaud, N.F. de Rooij, M. Koudelka-Hep, and L. Stoppini, "Microelectrode arrays for electrophysiological monitoring of hippocampal organotypic slice cultures", *IEEE Trans. Bio-Med. Eng*., 1997, **44**, 1159-63.
10. M. Chiappalone, M. Bove, A. Vato, M. Tedesco, and S. Martinoia, "Dissociated cortical networks show spontaneously correlated activity patterns during in vitro development", *Brain Res*., 2006, **1093**, 41-53.
11. D.A. Wagenaar, Z. Nadasdy, and S.M. Potter, "Persistent dynamic attractors in activity patterns of cultured neuronal networks", *Phys. Rev. E.,* 2006, **73**.
12. S. Marom and D. Eytan, "Learning in *ex-vivo* developing networks of cortical neurons", *Prog. Brain Res.,* 2005, **147**, 189-99.
13. Y. Jimbo, Y. Tateno, and H.P.C. Robinson, "Simultaneous induction of pathway-specific potentiation and depression in networks of cortical neurons", *Biophys J.,* 1999, **76**, 670-8.
14. E.W. Keefer, A. Gramowski, D.A. Stenger, J.J. Pancrazio, and G.W. Gross, "Characterization of acute neurotoxic effects of trimethylolpropane phosphate via neuronal network biosensors", *Biosens Bioelectron.*, 2001, **16**, 513-25.
15. A. Hai, J. Shappir, and M.E. Spira, "In-Cell recordings by extracellular microelectrodes", *Nat. Methods,* 2010, **7**, 200-202.
16. B. Eversmann, M. Jenkner, F. Hofmann, C. Paulus, R. Brederlow, B. Holzapfl, P. Fromherz, M. Merz, M. Brenner, M. Schreiter, R. Gabl, K. Plehnert, M. Steinhauser, G. Eckstein, D. Schmitt-Landsiedel, and R. Thewes, "A 128x128 CMOS biosensor array for extracellular recording of neural activity", *IEEE J. Solid-St Circ.*, 2003, **38**, 2306-17.
17. F. Heer, S. Hafizovic, T. Ugniwenko, U. Frey, W. Franks, E. Perriard, J.-C. Perriard, A. Blau, C. Ziegler, and A. Hierlemann, "Single-chip microelectronic system to interface with living cells", *Biosens & Bioelectron*., 2007, **22**, 2546–53.
18. L. Berdondini, K. Imfeld, A. Maccione, M. Tedesco, S. Neukom, M. Koudelka-Hep, and S. Martinoia, "Active pixel sensor array for high spatio-temporal resolution electrophysiological recordings from single cell to large scale neuronal networks", *Lab. Chip.*, 2009.
19. K. Imfeld, S. Neukom, A. Maccione, Y. Bornat, S. Martinoia, P.A. Farine, M. Koudelka-Hep, and L. Berdondini, "Large-Scale, High-Resolution Data Acquisition System for Extracellular Recording of Electrophysiological Activity", *IEEE Trans Bio-Med Eng*., 2008, **55**, 2064-73.
20. M. Gandolfo, A. Maccione, M. Tedesco, S. Martinoia, and L. Berdondini, "Tracking burst patterns in hippocampal cultures with high-density CMOS-MEAs", *J. Neural Engineering*, 2010, **7**, Issue 5.

Invited

SYNAPTIC COMPUTATION OF VISUAL CONTRAST IN THE RETINA

N.W. Oesch and **J.S. Diamond**

Synaptic Physiology Section
National Institute of Neurological Disorders and Stroke
National Institutes of Health Bethesda, MD USA,
DiamondJ@ninds.nih.gov

Adaptation is a common computational tool used throughout the nervous system. In some cases, adaptive processes modulate the gain of synaptic connections, thereby avoiding saturation and enabling them to encode inputs over a range that greatly exceeds their intrinsic output (Rieke and Rudd, 2009). One strategy to avoid saturation is to respond selectively to changes in input (i.e., contrast; Shapley and Enroth-Cugell, 1984). Among sensory systems, where physiological inputs can range over more than ten orders of magnitude and the danger of saturation is particularly acute, the rod pathway in the mammalian retina (the neural circuitry that mediates night vision) has become a model system in which to study adaptation in neural networks. This circuitry adapts strongly to light stimuli, allowing it to encode both contrast and luminance across a range of background levels. Despite extensive description of the properties of adaptation within this circuit, the specific mechanisms that allow the retinal circuitry to accomplish this important task of early visual processing remain poorly understood (Green, 1986; Laughlin, 1989; Rieke, 2009).

In the rod pathway, the gain of responses to luminance are modulated over a range of background light levels, and the site of this adaptation has been localized to the excitatory synapse between the rod bipolar cell (RBC) and the AII amacrine cell (AII) (Dunn, et al., 2006). Here, we show that this ribbon synapse encodes luminance and computes temporal contrast through changes in the occupancy of its readily releasable vesicle pool (RRP). We compared light-evoked excitatory postsynaptic responses in RBCs and AII amacrine cells, which receive synaptic input from RBCs. We found that synaptic release from RBC ribbon synapses adapts to step increases in light levels, thereby generating a transient component in the AII light response that encodes contrast over a range of background light levels. The sustained component of the AII response faithfully represents the RBC light response and provides a reliable measure of luminance regardless of stimulus history. Paired recordings from synaptically coupled RBC-AII pairs indicated that rapid, partial depletion of the RRP underlies the transient component of the AII EPSC and adaptation to increased stimuli; subsequent release from and replenishment to the partially depleted RRP produces a sustained rate of release that encodes the RBC luminance signal independently of stimulus history. A simple model of RRP release indicated that depletion and replenishment of a single, kinetically homogeneous pool of vesicles can account for this behavior. These results indicate that tightly regulated occupancy of a finite RRP constitutes an intrinsic synaptic mechanism that enables RBC ribbon synapses to parse visual information into multiple streams.

Acknowledgements

This research was supported by the National Institute of Neurological Disorders and Stroke Intramural Research Program.

References

1. L.F. Abbott, J.A. Varela, K. Sen, & S.B. Nelson, *Science,* 1997, **275**, 220-224.
2. F.A. Dunn, T. Doan, A.P. Sampath, & F. Rieke, *J Neurosci.,* 2006*,* **26**, 3959-3970.
3. D.G. Green, *Vision Res.,* 1986*,* **26**, 1417-1429.
4. F. Rieke, & M.E. Rudd, *Neuron,* 2009*,* **64**, 605-616.
5. R. Shapley, & C. Enroth-Cugell, "Visual adaptation and retinal gain controls", *Prog. Ret. Res.*, 1984, **3**, 263-346.

Invited

NEURODYNAMICS AND EXTRACELLULAR MATRIX

A. Dityatev

Laboratory for Brain Extracellular Matrix Research, University of Nizhny Novgorod, Russia
dityatev@neuro.nnov.ru
Department of Neuroscience and Brain Technologies, Istituto Italiano di Tecnologia, Genova, Italy

Neurodynamics of neural networks is determined by composition and functional properties of its cellular elements, such as excitatory and inhibitory neurons and glial cells, and by connectivity between them. Additionally, neural cells secrete diverse molecules, which accumulate in the extracellular space and form the extracellular matrix (ECM). The ECM of the central nervous system is well recognized as a migration and diffusion barrier that allows for the trapping and presentation of growth factors to their receptors at the cell surface, and hence for controls of cell migration and differentiation, determining cellular composition of neural networks. Recent data highlight the importance of ECM molecules as synaptic and perisynaptic scaffolds that direct synapse formation and the clustering of neurotransmitter receptors in the postsynaptic compartment [1]. Thus, neural ECM shapes neuronal wiring. Furthermore, ECM molecules regulate various aspects of synaptic function and plasticity, and recent data strengthened a link between the ECM and learning and memory. New findings also support the view that the ECM is important for homeostatic processes, such as scaling of synaptic responses, metaplasticity and stabilization of synaptic connectivity [2].

Importantly, ECM structures are slowly formed and remodeled in an activity-dependent manner, including molecular signatures of both glial and synaptic elements. The ECM can respond to network activity by incorporating either secreted molecules or shed extracellular domains of transmembrane molecules, or by freeing products of ECM proteolytic cleavage as signaling messengers. This highlights the ECM as a substrate for long-term storage and retrieval of information and suggests that the ECM is a fourth essential element of synapses that could be hence viewed as "tetrapartite" systems containing the pre- and postsynaptic compartments, glial processes and ECM [3].

ECM glycoprotein tenascin-R and regulation of perisomatic inhibition

The most prominent accumulations of ECM molecules in the brain are found in the so-called perineuronal nets. They are enriched in hyaluronic acid, link proteins, CSPGs, and glycoprotein tenascin-R (TNR) [4]. Initial studies revealed a role of HNK-1 carbohydrate (human natural killer cell glycan) carried by TNR in regulation of GABAergic transmission [5, 6]. Mice deficient in TNR exhibited elevated basal excitatory synaptic transmission and reduced perisomatic GABAergic inhibition in the CA1 region [7]. Analysis of density and spatial arrangement of synaptic vesicles in the synaptic terminals provided ultrastructural evidence for reduced perisomatic inhibition in TNR-deficient mice [8]. This reduction in perisomatic inhibition induces a metaplastic shift (increase) in the threshold for induction of long-term potentiation (LTP) in the CA1 region [9]. The threshold and levels of LTP induced by theta burst stimulation are restored in TNR-deficient mice by pre-treatment of hippocampal slices with the $GABA_A$ receptor agonist zolpidem, indicating that disinhibition is a cause of metaplasticity in these mice. The mechanisms of metaplasticity that are downstream of disinhibition involve elevated activities of L-VDCCs and serine/threonine protein phosphatase 1 and/or 2A [9].

TNR-deficient mice show brain subregion-specific synaptic abnormalities: in these mice, whereas perisomatic innervation of principal neurons by GABAergic interneurons is reduced in area CA1, it is normal in area CA3 and increased in the dentate gyrus [10]. *In vivo*, this abnormality in the dentate gyrus leads to a $GABA_A$ receptor-dependent reduction in LTP and an enhanced excitability of granule cells following tetanic stimulation of entorhinal cortex axons projecting to the dentate gyrus. Behaviourally, TNR-deficient mice show enhanced reversal learning, improved working memory and enhanced reactivity to novelty than wild-type littermates. Faster reversal learning rates correlate with increased ratios of parvalbumin-positive interneurons to granule cells and increased densities of parvalbumin-positive terminals on somata of granule cells, which indicate increased perisomatic GABAergic inhibition in the dentate gyrus [10]. These data demonstrate that modification of the ECM by ablation of TNR leads to a new structural and functional design of the dentate gyrus, with enhanced

GABAergic innervation and altered plasticity that promote working memory and reversal learning. Enhanced inhibition in the dentate gyrus probably increases the signal-to-noise ratio by suppressing the background firing of neurons and/or by increasing the activity-dependent disinhibition of neurons that encode task-relevant features of the environment. Such changes therefore improve the filtering of sensory information and allow the discrimination of biologically relevant features.

Regulation of Ca^{2+} channels by ECM molecules tenascin-C and hyalurionic acid

NMDA receptors and L-type voltage-dependent Ca^{2+} channels (L-VDCCs) are known to contribute to the increase in postsynaptic Ca^{2+} concentration, particularly during strong or repetitive high-frequency stimulations, and therefore to induce some forms of LTP. The importance of ECM molecules for the amplification of L-VDCC activity in neurons was originally found using mice deficient in the ECM molecule TNC [11]. This glycoprotein is most prominently expressed during development of the nervous system and its expression is up-regulated following synaptic stimulation. Mice deficient in TNC show impairment in several forms of synaptic plasticity, which are known to involve L-VDCCs. Injection of TNC fibronectin repeats 6-8 in the hippocampal slices impairs LTP in the CA1 area [12]. Recent data show that L-VDCC activity and LTP are regulated by hyaluronic acid [13], a key ECM glycosaminoglycan that is synthesized in neural cells by a class of integral membrane proteins. Hyaluronic acid is extruded through the cell membrane into the extracellular space, where it serves as a scaffold for the assembly of the ECM. Although evidence for a direct physical interaction between L-VDCC and TNC or hyaluronic acid is lacking, both ECM molecules are expressed perisynaptically in close proximity to L-VDCC-immunopositive dendritic domains and interact with CSPGs. It is therefore possible that these ECM molecules are constituents of a functional complex. Consistent with this notion, LTP at CA3-CA1 synapses is similarly impaired by genetic ablation of TNC, removal of hyaluronic acid by the exogenous, highly specific enzyme hyaluronidase or by inhibiting L-VDCCs. The deficit in synaptic plasticity after hyaluronidase treatment is rescued by re-introduction of hyaluronic acid or by pharmacological potentiation of L-VDCCs. Removal of hyaluronic acid reduces Ca^{2+} transients in dendritic spines of hippocampal pyramidal neurons due to impaired activity of L-VDCCs, prevents somatic translocation of the phosphorylated extracellular signal-regulated kinases ERK1 and ERK2 in area CA1, prevents activation of the cyclic AMP-responsive element-binding protein (CREB), and reduces hippocampus-mediated contextual fear conditioning [13].

Recordings in a heterologous expression system demonstrated that hyaluronic acid potentiates the activity of the $Ca_v1.2$ but not the $Ca_v1.3$ $\alpha1$ subunit of L-VDCCs [13]. This is consistent with the predominant expression of the $Ca_v1.2$ subunit in the hippocampus and its reported role in LTP and phosphorylation of ERK1, ERK2 and CREB. As other ECM components, such as heparin, laminin, fibronectin and retinoschisin, also potentiate the activity of L-VDCCs in different cell types, this seems to be a common signalling mechanism by which ECM molecules modulate Ca^{2+} signalling.

Acknowledgements

This work was supported by a grant from the Government of the Russian Federation and by the Italian Institute of Technology.

References

1. A. Dityatev, C.I. Seidenbecher, and M. Schachner, *Trends Neurosci.*, 2010, **33**, 503.
2. A. Dityatev, M. Schachner, and P. Sonderegger, *Nat. Rev. Neurosci.,* 2010, **11**, 735.
3. A. Dityatev and D.A. Rusakov, *Curr. Opin. Neurobiol.*, 2011, **21**, 353.
4. C.M. Galtrey and J.W. Fawcett, *Brain. Res. Rev.,* 2007, **54**, 1.
5. A.K. Saghatelyan, S. Gorissen, M. Albert, et al., *Eur. J. Neurosci.m,* 2000, **12**, 3331.
6. A. K. Saghatelyan, M. Snapyan, S. Gorissen, et al., *Mol. Cell. Neurosci.,* 2003, **24**, 271.
7. A. K. Saghatelyan, A. Dityatev, S. Schmidt, et al., *Mol. Cell. Neurosci.,* 2001, **17**, 226.
8. A. Nikonenko, S. Schmidt, G. Skibo, et al., *J. Comp. Neurol.,* 2003, **456**, 338.
9. O. Bukalo, M. Schachner, and A. Dityatev, *J. Neurosci.,* 2007, **27**, 6019.
10. F. Morellini, E. Sivukhina, L. Stoenica, et al., *Cereb. Cortex,* 2010, **20**, 2712.
11. M. R. Evers, B. Salmen, O. Bukalo, et al., *J. Neurosci.* **22**, 2002, 7177.
12. T. Strekalova, M. Sun, M. Sibbe, et al., *Mol. Cell. Neurosci.,* 2002, **21**, 173.
13. G. Kochlamazashvili, C. Henneberger, O. Bukalo, et al., *Neuron,* 2010, **67**, 116.

Invited

SYNAPTIC PLASTICITY INDUCED DYNAMICS OF PRESYNAPTIC CYTOMATRIX AT THE ACTIVE ZONE

V. Lazarevic[1,2], C. Schöne[1,3], M. Heine[3], Eckart D. Gundelfinger[1], and **A. Fejtova[1]**

[1] Department of Neurochemistry and Molecular Biology, Leibniz Institute for Neurobiology Magdeburg, Germany, afejtova@ifn-magdeburg.de
[2] German Center for Neurodegenerative Disorders (DZNE), Magdeburg Branch, Magdeburg, Germany
[3] Research Group Molecular Physiology, Leibniz Institute for Neurobiology, Magdeburg, Germany

Communication between brain cellular units and neurons occurs through specialized cell-cell contacts, named synapses, by means of secretion of messenger molecules, neurotransmitters (NT), by presynaptic neurons staying upstream in signal transmission flow and their recognition by specialized receptor apparatus of postsynaptic neurons downstream. Neurons are able to adjust the strength of their synaptic transmission depending on the history of their activity. This probably most remarkable feature of neuronal cells represents cellular bases of neuronal plasticity, which is the fundamental mechanism of complex brain functions such as learning and memory formation [1]. Synaptic strength can be adjusted by regulating efficacy of presynaptic NT release or by modulating sensitivity of its detection by postsynaptic receptor apparatus. In the proposed project I would like to concentrate my attention on the cellular and molecular mechanisms underlying plasticity of presynaptic efficacy.

The presynaptic endings function as sources of NTs, which are stored in small synaptic vesicles (SVs). SVs cluster above the active zone of NT release, where they can dock and eventually fuse to release their content. The evoked fusion of SV is triggered by calcium influx through voltage-dependent calcium channels, which are activated upon action potential-driven depolarization of axonal plasma membrane. After the fusion, the SV membrane recycles by means of compensatory endocytosis forming new SVs, which can be refilled with NT and used in the next SV cycle. To assure synaptic transmission occurring in frame of millisecond and with high fidelity the described SV cycle has to be precisely controlled in time and space. The important role in the spatial organization and functional regulation of multiple steps of SV cycle was ascribed to the components of cytormatrix at the active zone (CAZ), i.e. Bassoon, Piccolo, ELKS/CAST, RIM, Munc13 and liprin-alpha [2].

Although there was considerable progress in understanding the molecular mechanisms of basic synaptic function, our knowledge of mechanisms underlying the experience-induced or homeostatic synaptic plasticity are still not sufficient. As already discussed above the changes of presynaptic efficacy of NT release are important mechanisms underlying synaptic plasticity. Mechanistically, the functional changes in the presynaptic efficacy have to be coupled with molecular remodeling of protein machineries involved. Following this hypothesis we investigated molecular remodeling of presynaptic release apparatus upon pharmacological blockade of the network activity in cultures of dissociated cortical neurons. It has been shown previously that activity blockage induces compensatory changes in the efficacy of neurotransmitter release [3]. This homeostatic plasticity serves to keep network activity within a physiologically meaningful frame and is therefore a prerequisite for effective learning-induced plasticity [4].

Presynaptic CAZ proteins are important modulators of release efficiency during Hebbians' plasticity; however, to date their role in homeostatic plasticity was neglected. I will present you our approach where we have investigated whether and how the altered synaptic network activity influences the molecular composition of the presynaptic active zone (AZ) [5]. We used primary cultures of cortical neurons as a convenient model system allowing pharmacological manipulations and found significant down-regulation of cellular expression levels of presynaptic scaffolding proteins Bassoon, Piccolo, ELKS/CAST, Munc13, RIM, liprin-α and synapsin upon prolonged (48-hrs) activity depletion. This was accompanied by a general reduction of Bassoon, Piccolo, ELKS/CAST, Munc13 and synapsin levels at synaptic sites. Interestingly, RIM was up-regulated in a subpopulation of synapses. Analysis at the level of individual synapses revealed that RIM quantities correlated well with synaptic activity and that a constant relationship between RIM levels and synaptic activity was preserved upon activity silencing. Silencing also induced synaptic enrichment of other previously identified regulators of presynaptic release probability, i.e. synaptotagmin-1, SV2B and P/Q-type calcium channels. Seeking for responsible cellular mechanisms we revealed a complex role of the ubiquitin-proteasome system in the functional presynaptic remodeling and enhanced degradation rates

of Bassoon and liprin-α upon silencing. Despite the fact that pharmacological inhibition of the UPS induced a complex pattern of regulation of presynaptic scaffolding proteins, it did not affect presynaptic neurotransmitter release probability in silenced networks. Altogether, our data indicate a significant molecular reorganization of the presynaptic release apparatus during homeostatic adaptation to network inactivity and identify RIM, synaptotagmin1, Cav2.1 and SV2B as molecular candidates underlying the main silencing-induced functional hallmark at presynapse, i.e. increase of neurotransmitter release probability.

Acknowledgements

This work was supported by Deutsche Forschungsgemeinschaft (SFB779/B9 and GRK 1167 to EDG and HE 3604/2-1 to MH) and the European Community (HEALTH-2007-22918, REPLACES) and the European Regional Development Fonds and the Land Saxony-Anhalt (EFRE/LSA 2007-2013) to EDG.

References

1. G. Neves, S.F. Cooke, T.V. Bliss, "Synaptic plasticity, memory and the hippocampus: a neural network approach to causality", *Nat. Rev. Neurosci*., 2008, **9**, 65-75.
2. A. Fejtova, E.D. Gundelfinger, "Molecular organization and assembly of the presynaptic active zone of neurotransmitter release", *Results Probl. Cell Differ*., 2006, **43**, 49-68.
3. V.N. Murthy, T. Schikorski, C.F. Stevens, Y. Zhu, "Inactivity produces increases in neurotransmitter release and synapse size", *Neuron*, 2001, **32**, 673-682.
4. K. Pozo, Y. Goda, "Unraveling mechanisms of homeostatic synaptic plasticity", *Neuron*, 2010, **66**, 337-351.
5. V. Lazarevic, C. Schone, M. Heine, E.D. Gundelfinger, A. Fejtova, "Extensive remodeling of the presynaptic cytomatrix upon homeostatic adaptation to network activity silencing", *J. Neurosci.*, in press.

Invited

HOW REMODELING OF THE BRAIN PERINEURONAL NETS INFLUENCES CELL SURFACE TRAFFICKING OF POSTSYNAPTIC GLUTAMATE

R. Frischknecht, **Y. Klyueva, A. Bikbaev,** and **M. Heine**

Leibniz Institute for Neurobiology, Magdeburg, Germany, rfrischk@ifn-magdeburg.de

Brain synapses are wrapped by a dense meshwork of extracellular matrix (ECM), which consists of glycoproteins and proteglycans of both glial and neuronal origin. Most neurons in the brain are surrounded by ECM, however the most prominent form of the ECM the so called peri-neuronal nets (PNN) are only present on a subset of neurons, which have been identified to be mainly parvalbumin-positive (PV) interneurons. This specific ECM has already been discovered more than 100 years ago by the pioneers in neuroscience Ramón y Cajal and Camillo Golgi and is thought to be critical for the development as well as for the function of brain synapses [1].

The major organizing polysaccharide of the brain's extracellular matrix is the polymeric carbohydrate hyaluronic acid (HA). It forms the backbone of a meshwork consisting of CNS proteoglycans belonging mainly to the lectican family of chondroitin sulfate proteoglycans (CSPG; [2]). This family comprises 4 abundant components of brain ECM: aggrecan and versican, which are ubiquitinously expressed and neurocan and brevican, which are nervous system-specific family members. Versican and neurocan can be considered as genuine components of juvenile ECM, and aggrecan and brevican (a lectican that is primarily contributed by glial cells) are most prominent in the mature nervous system. Lecticans can be considered as connectors between neural surfaces, where they are able to bind to cell surface components with their C-terminal globular domains, and to ECM structures via HA, which specifically associates with the N-terminal globular domains of the CSPGs. Thus, the lecticans together with link proteins, HA and glycoproteins like the tenascins, form huge carbohydrate-protein aggregates and tie them up to the cell surfaces and thereby may compartmentalize the neuronal surface.

The distribution of the lecticans throughout the brain is not even; while brevican is found on PNN-like structures on most excitatory as well as inhibitory cells aggrecan is mainly found on PV-positive interneurons, labeling the classical PNN. Interestingly these structures do not only form *in vivo* but also in cell culture within a similar time course and reaching same composition [3], which makes dissociated neurons a valuable tool to study ECM function.

The ECM of the brain surrounds cell bodies and proximal dendrites in a mesh-like structure that interdigitates with synaptic contacts. For example, brevican localizes perisynaptically in close vicinity to the synaptic cleft [4]. Biochemical fractionation revealed an enrichment of membrane-bound brevican in synaptic fractions [5], suggesting a role at chemical synapses.

In fact, a number of mice lacking different components of the ECM show deficits in synaptic plasticity. Maintenance of long-term potentiation (LTP) is dramatically impaired in brevican mutants, a phenotype that can be mimicked by application of anti-brevican antibody [6]. Also tenascin-R mutants exhibit deficits in both LTP and in long-term depression (LTD). Treatment of hippocampal slices with the bacterial enzyme chondroitinase ABC (ChABC), which removes chondroitin sulfates from CSPGs, leads to a reduction in LTP expression [7].

Experimental removal of the ECM affects not only synaptic transmission but also structural plasticity as it was well documented in rat visual cortex. Monocular deprivation during a critical period leads to an ocular dominance combined with reduced spine density at the contralateral side. This dominance is persistent in the adult due to loss of the required juvenile conditions for neuronal plasticity. However, injections of ChABC into the visual cortex in deprived adult rats abolish the ocular dominance and differences in spine densities in the contra- compared to the ipsi-lateral side (Pizzorusso et al., 2006). These results indicate that on one hand the PNN are blocking synaptic plasticity by stabilizing synaptic contacts and preventing synaptogenesis in the adult, and on the other hand they provide important instructive information necessary for LTP, a measure for synaptic plasticity. Accordingly, it is hypothesized that the appearance of PNN, marks and is functionally involved in the switch from developmental to adult modes of synaptic plasticity.

In our recent work we have found an additional function of the ECM. Removal of the ECM using the glycosidase hyaluronidase (Hyase) that digests hyaluronic acid, the backbone of the ECM alters short-term plasticity in dissociated hippocampal neurons [8]. Hyaluronidase-treated cells exhibited

decreased paired-pulse ratio as compared to control cells, which showed paired-pulse depression (PPD) upon a pulse interval ≤ 50 ms. This result was obtained by paired-patch recording and reproduced using iontophoretic application of glutamate directly onto the postsynapse, indicating a postsynaptic mechanism responsible for the escape from PPD.

Indeed, we have identified in a previous work lateral diffusion of AMPA-receptors within the postsynaptic membrane as a modulator of short-term plasticity [9]. We found that desensitized postsynaptic receptors emerging after presynaptic or iontophoretic glutamate release are rapidly exchanged for naïve functional ones by lateral diffusion. This mechanism guarantees a repertoire of functional receptors in the postsynaptic density and thus a high synaptic fidelity. At high firing rates lateral diffusion no longer fully compensate desensitization and synapses show subsequently PPD [9]. Thus, mechanisms leading to a higher or lower lateral diffusion and consequently altering exchange of synaptic receptor are very likely to modulate short-term plasticity. In line with this finding, enzymatic removal of the ECM increased lateral mobility of extrasynaptic AMPA-receptors, thereby augmented exchange of synaptic receptors and led to decreased paired-pulse depression [8]. We concluded that the function of the ECM was to control lateral diffusion and synaptic access of AMPA-receptors. Thus, local changes in the structure or density of the ECM represent an attractive mechanism, how cells may alter AMPA-receptors diffusion and modulate short-term plasticity. However, these studies have been carried out on spiny, excitatory neurons. In a follow up study we now analyse lateral diffusion of AMPA receptors selectively on aspiny GABA-ergic neurons and compare diffusion rates to those found on excitatory neurons. Further we test for the impact of the PNN on lateral diffusion and short-term plasticity after enzymatic removal of this specialized form of the ECM. Together these results will provide insight to what extend the ECM modifies excitatory input on excitatory and inhibitory neurons, which differ not only in their morphology but also in their ECM content.

Acknowledgements

This work is supported by the ERA-NET NEURON project “Moddifsin” and the DFG project GU230-5/1-3. We thank Daniel Choquet for material and fruitful discussions. We thank Eckart Gundelfinger and Constanze Seidenbecher for their support and helpful discussions.

References

1. O. Bukalo, A. Dityatev, *Methods Enzymol.,* 2006, **417**, 52.
2. Y. Yamaguchi, *Cell Mol Life Sci.,* Feb, 2000, **57**, 276.
3. N. John *et al.*, *Mol Cell Neurosci.,* Apr, 2006, **31**, 774.
4. C. Seidenbecher, K. Richter, E. D. Gundelfinger, in *Neurochemistry,* A. W. Teelken, J. Korf, Eds. (Plenum Press, New York, 1997), pp. 901-04.
5. C.I. Seidenbecher, K.H. Smalla, N. Fischer, E.D. Gundelfinger, M.R. Kreutz, *J. Neurochem.,* Nov, 2002, **83**, 738.
6. C. Brakebusch *et al.*, *Mol Cell Biol.,* Nov, 2002, **22**, 7417.
7. O. Bukalo, M. Schachner, A. Dityatev, *Neuroscience,* 2001, **104**, 359.
8. R. Frischknecht *et al.*, *Nat. Neurosci.,* Jul. 2009, **12**, 897.
9. M. Heine *et al.*, *Science,* Apr11, 2008, **320**, 201.

ULTRASTRUCTURAL FEATURES OF REPARATIVE PROCESSES IN CULTURED NEURONS EXPOSED TO GLUTAMATE EXCITOTOXICITY

L.E. Frumkina, A.A. Lizhin, and **L.G. Khaspekov**

Research Centre of Neurology RAMS, Moscow, Russia, khaspekleon@mail.ru

One of the actual goals in contemporary experimental and clinical neurology is the investigation of neuronal destructive and reparative processes in cerebral ischemia. The appropriate methodological approach to achieve this goal is the study in vitro of the glutamate excitotoxicity which is the main pathogenic factor of ischemic neuronal damage [1]. To reveal the potential capacity of neurons for maintaining their viability in excitotoxic conditions, we investigated the ultrastructure of cultured cerebellar granule cells after toxic glutamate exposure.

Cerebellar cell cultures were prepared following the procedure described in [2]. After 7 days in vitro cultured cells were exposed for 15 min to 100 mcM glutamate. Then the 1st group of cultures was fixed in 2.5% glutaraldehyde immediately after glutamate application, whereas the 2nd group was maintained in nutrient medium for 3 hours, following which was also fixed. After fixation, all cultures were treated with standard procedure for transmission electron microscopy.

Immediately after glutamate exposure, the irreversible damage of some neurons is characterized by total chromatolysis and disappearance of cytoplasmic organelles (Fig. 1A). After 3 hours sparse dead neurons surrounded by glial cells are present (Fig. 1B). At the same time, among the neurons of the 1st group the cells with comparatively insignificant ultrastructural changes, such as weak cytoplasmic swelling and nuclear transparency ("clear" type, Fig. 1C) or hyperchromatosis ("dark" type, Fig. 1D) dominated.

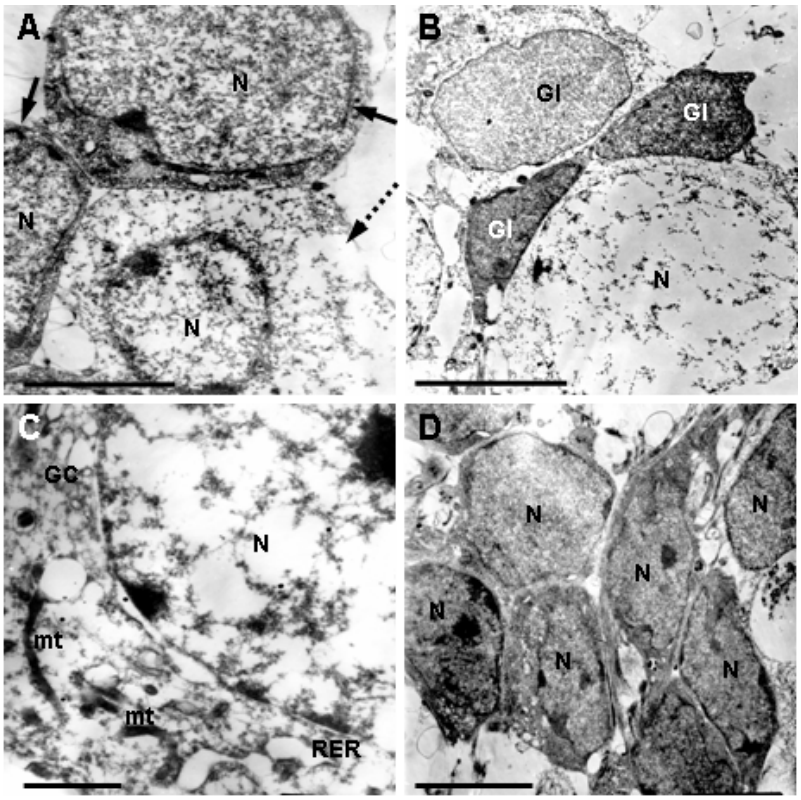

Fig. 1. Fine structure of cultured cerebellar granule cells immediately after 15 min glutamate exposure.
A: Among normochromic neurons (solid arrows), the swollen neuron (dotted arrow) with total chromatolysis and the absence of cytoplasmic organelles is seen. **B:** Dead neuron ("cell-shadow") surrounded by glial cells, that is the sign of neuronophagia. **C:** "Clear" neuron undergoing the transient state of edema-swelling; localized dilatations between nuclear membranes and swollen endoplasmic organelles are seen. **D:** "Dark" neurons with homogenization of cytoplasm, clamping of nuclear chromatin and disaggregation of polysomes.
N – nucleus; mt – mitochondrion; RER – rough endoplasmic reticulum; GC – Golgi complex; G – glial cells.
Scale: 5 mcM (A, B), 2 mcM (C), 10 mcM (D)

Three hours after glutamate exposure, in "clear" neurons (Fig. 2A) new formed nuclear heterochromatin is localized on the inner nuclear membrane, in the zone of tight contact with smooth endoplasmic reticulum cisterns which shaped from external nuclear membrane. Cytoplasm contains numerous polysomal rosettes, branched or budding mitochondria (Fig. 2B), as well as other organelles, which contact with each other and nucleus, indicating activation of metabolic interactions between the nucleus and the cytoplasm.

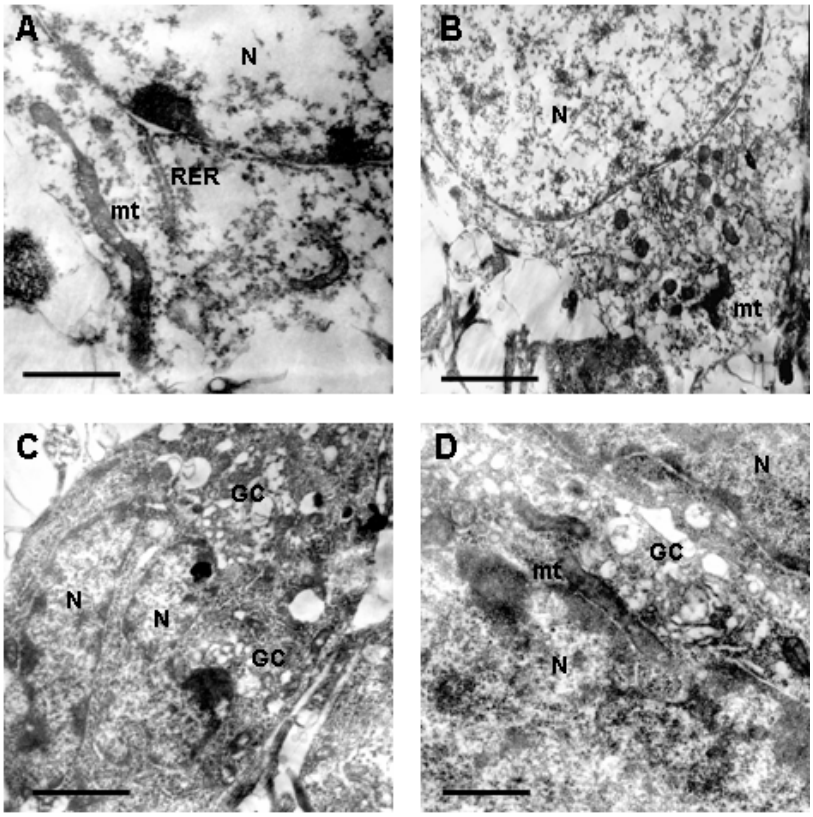

Fig. 2. Fine structure of cultured cerebellar granule cells 3 hours after glutamate exposure.
A, B: Reparative processes in "clear" neurons. A – formation of cisterns of rough endoplasmic reticulum from outer nuclear membrane, mitochondrial hyperplasia; B – local clusters of cytoplasmic organelles and their contacts with each other and with nucleus.
C, D: Plastic reorganization of ultrastructure of "dark" neurons. C – binuclear neuron with hyperplasia of Golgi complex elements; D – hypertrophy of mitochondria and their intimate contact with nucleus.
The indications are the same as in Fig. 1. Scale 2 mcM

Among hyperchromic ("dark") neurons, binuclear cells, as well as neurons with multiblade nuclei, folded nuclear membrane, its invagination containing cytoplasmic organelles, heterochromatic clusters with inner nuclear membrane are present (Fig. 2C). Cytoplasm contains giant and divisible mitochondria (Fig. 2D) which contact with nucleus, each other and other organelles, that is the evidence of mitochondrial new formation and functional activation.

The mentioned above ultrastructural intraneuronal reorganization, occurring during postglutamate period, reflects the intensive intraneuronal reparative processes in neurons, which provide the so-called "compensatory-plastic answer" [3]. Thus, the remodeling of ultrastructure of neurons exposed to excitotoxicity suggests their capacity for maintaining viability after ischemic damage.

References

1. M. Arundin, M. Tymianski, *Cell. Mol. Life Sci.,* 2004, **61,** 657-668.
2. N. Andreeva, B. Khodorov, E. Stelmashook, E. Cragoe, I. Victorov, *Brain Res.,* 1991, **548**, 322-325.
3. D.F. Marrone, T.L. Petit, *Brain Res. Rev.,* 2002, **38,** 291-308.

Invited

PROBING ASTROGLIAL BIOLOGY WITH LIGHT

A.V. Gourine[1] and **S. Kasparov**[2]

[1] Neuroscience, Physiology & Pharmacology, University College London, London WC1E 6BT
a.gourine@ucl.ac.uk
[2] Department of Physiology and Pharmacology, University of Bristol, Bristol BS8 1TD, United Kingdom

The mammalian central nervous circuitry that generates respiratory activity is silent in the absence of CO_2 and requires a threshold level of CO_2 to operate. Arterial PCO_2 is monitored by the central chemosensors located in the lower brainstem and the peripheral chemoreceptors of the carotid and aortic bodies. It is estimated that up to 80% of the overall ventilatory response to CO_2 is mediated via its action on the respiratory chemosensors located within the CNS. The anatomical location of these sensors, their cellular identity and the mechanisms of how changes in blood and brain pH and PCO_2 are transmitted into a modified pattern of breathing remain controversial. Although previous reports suggested that astrocytes could be potentially important for chemoreception [1], it is generally believed that central respiratory chemosensitivity is a feature of one or several highly specialized neuronal populations located in the medulla oblongata and pons [2]. On the basis of our earlier observations of a rapid and profound central release of ATP (a key gliotransmitter) in response to increases in inspired CO_2 [3], we previously proposed that activation of glial cells by chemosensory stimuli may underlie this release. Recently, using novel optogenetic tools developed to monitor and control astroglial Ca^{2+}-excitability *in vitro* and *in vivo* we were able to test this hypothesis directly. The data obtained provide strong evidence that brainstem astrocytes have the ability to sense physiological changes in PCO_2 and pH and then impart these changes into a modified pattern of breathing to adjust lung ventilation accordingly [4, 5].

Because astrocytes are electrically non-excitable, but display Ca^{2+} excitability (reactive increases in cytosolic $[Ca^{2+}]_i$ concentration), we studied their behavior using genetically encoded Ca^{2+} indicator – *Case12*. *Case12* was expressed in astrocytes residing at and near the classical chemosensitive area of the ventral surface of the medulla oblongata of rats using an adenoviral vector with enhanced shortened glial fibrillatory acidic protein (GFAP) promoter.

It was found that astrocytes which reside within the "classical" chemoreceptor areas located at and near the ventral surface of the medulla oblongata are highly chemosensitive. This chemosensitivity is intrinsic and operates in the absence of the neuronal input. Both *in vitro* and *in vivo* ventral medullary astrocytes respond to small physiological decreases in pH with vigorous elevations in intracellular Ca^{2+} and exocytotic release of ATP [5]. ATP propagates Ca^{2+} excitation across the ventral medullary astrocytes and these responses are markedly attenuated in the presence of ATP receptor antagonists or ATP degrading enzyme apyrase. Interestingly, high pH-sensitivity appears to be a distinctive feature of astrocytes residing within the classical chemosensitive areas of the ventral surface of the brainstem, while astrocytes from the cerebral cortex or dorsal brainstem are insensitive to acidification and do not release ATP in response to pH changes within the physiological range [5].

ATP has been identified as the key gliotransmitter responsible for astrocytic modulation of the respiratory network. Activation of individual respiratory neurones as well as the rhythm generating respiratory circuits in response to application of exogenous ATP have been demonstrated. In our experiments Ca^{2+} imaging and patch clamp recordings from Phox2b-expressing putative chemoreceptor neurones within the retrotrapezoid nucleus (RTN) located in the ventrolateral region of the medulla oblongata revealed that responses of these "chemosensitive" neurones to changes in pH are largely mediated by prior release of ATP [5].

In order to mimic Ca^{2+} excitation of astrocytes we generated an adenoviral vector where a mutant of the light-sensitive channelrhodopsin-2 (ChR2-H134R) is fused to a far red-shifted fluorescent protein Katushka1.3 and expressed using enhanced GFAP promoter. In primary cultures and in brainstem slices of adult rats astrocytes transduced with this construct displayed robust increases in $[Ca^{2+}]_i$ in response to 470 nm light. Optogenetic activation of VS astrocytes transduced with AVV-sGFAP-ChR2(H134R)-Katushka1.3 in organotypic brainstem slices triggered immediate ATP release and evoked long-lasting depolarizations of all recorded DsRed-labeled RTN neurons. Furthermore, mimicking pH-evoked Ca^{2+} excitation of astrocytes by selective optogenetic stimulation was found to trigger robust activations of the respiratory network *in vivo* [5]. Together these data indicate that

astrocytes are capable of sensing pH/PCO_2 level of the arterial blood entering the brainstem integrating it with pH/PCO_2 level of the brain parenchyma and then imparting this information on the activity of the brainstem respiratory network.

It is well known since the first historical observations and drawings by Ramón y Cajal that close association of astrocytes with cerebral vasculature and multiple neurones is one of the key anatomical features of these glial cells. Astrocytes therefore are ideally positioned to rapidly detect changes in chemical or physical properties of both brain circulation and neuropil. Accumulating evidence obtained using recent advances in optogenetics indicates that brain astrocytes indeed respond to different sensory modalities known to activate central interoceptive pathways. Astrocytes are capable of transmitting sensory information (via regulated release of gliotransmitters or lactate) to the adjacent neural networks controlling vital behaviours and therefore fulfil key criteria to be considered as functional central interoceptors.

Acknowledgements

We are grateful to The Wellcome Trust and British Heart Foundation for financial support.

References

1. Y. Fukuda, Y. Honda, M. Schlafke, and H.H. Loeschcke, *Pflugers Archive*, 1978, **376**, 229-235.
2. E. Nattie, and A. Li, *J. Appl. Physiol.,* 2009, **106**, 1464-1466.
3. A.V. Gourine, E. Llaudet, N. Dale, and K.M. Spyer, *Nature*, 2005, **436**, 108-111.
4. R. Huckstepp, R. id Bihi R. Eason, K.M. Spyer, N. Dicke, K. Willecke, N. Marina, A.V. Gourine, and N. Dale, *J. Physiol.*, 2010, **588**, 3901-3920.
5. A.V. Gourine, V. Kasymov, N. Marina, F. Tang, M. Figueiredo, S. Lane, A.G. Teschemacher, K.M. Spyer, K. Deisseroth, and S. Kasparov, *Science*, 2010, **329**, 571-575.

Invited

STRUCTURAL PHASE TRANSITIONS IN NEURONAL NETWORKS

D.I. Iudin[1,2], V.B. Kazantsev[2], and **I.Y. Tukin[3]**

[1] Radiophysical Research Institute, Nizhny Novgorod, Russia, iudin_di@nirfi.sci-nnov.ru
[2] Institute of Applied Physics RAS, Nizhny Novgorod, Russia
[3] University of Leicester, Leicester, Great Britain

Living neuronal networks in dissociated neuronal cultures are known to demonstrate highly robust activity patterns recorded in different experimental conditions. Such patterns are often treated as neuronal avalanches satisfying power scaling law and demonstrate a bright example of self-organized criticality (SOC) in living systems [1–3]. It is clear that the properties of such activity have to be associated with the dynamics of network topology of developing neuronal culture. Here we demonstrate how such patterns can be realized in neuronal network model with developing morphological architecture. Being supplied by the energy feedback the morphological growth of the network stops near the edge of network percolation transition. This network state is self-sustainable and represents a kind of energetic balance between the morphological processes and the spontaneous activity. We also show that the activity in this state is represented by the population bursts satisfying the scaling avalanche conditions. Striking examples of SOC-like behavior have been found in experimental studies of neuronal cultures [4, 5]. The cultures grow autonomously and form synaptically coupled networks of living cells. After a period of initial growth and development the cultures start to generate spontaneous activity patterns in the form of population bursts. These bursts are shown to satisfy the power scaling law and hence are often referred to as neuronal avalanches [4]. Since then a number of mathematical models have been proposed for simulation and analysis of spontaneous burst generation in neuronal networks. The spectrum of network's features linked to emergence of persistent bursts includes, but is not limited to, e.g. re-wiring, delays [6, 7], frequency dependent and spike timing dependent synaptic plasticity [8–10]. With regards to the mathematical frameworks describing neuronal avalanches, models of network's growth [11] and stochastic networks [12] have been put forward. Despite these results advance substantially our understanding of the phenomenon, underlying macroscopic physical mechanisms (expressed e.g. in terms of energy balances) robustly driving living neuronal networks to the burst multiscale dynamics are still unclear.

In this presentation we contribute to the idea that neural network SOC-like behavior (e.g. the neuronal avalanches) is tightly related to the interplay between the network's growth and degeneration regulated by an energy supply. Behavior of each neuron is described by a phenomenological model comprising a triple of variables I_j, s_j, E_j). Variables I_j, s_j are binary; I_j = 1when the j-th neuron generates a spike and $I_j = 0$ otherwise, and the value of $s_j =$ - 1 for inhibitory neurons and $s_j = 0$ for the excitatory ones. Variable E_j models the neuron's energy resource. This energy resource is supposed to be supported by external driving associated with metabolic activity. The energy is needed for generating spikes. Yet, each time when the neuron generates a spike its energy decreases by a fixed amount, an energy quant. Taking these considerations into account, we can write the energy balance equation as follows:

$$\frac{dE_j}{dt} = -\beta\left(E_j - E_0\right) - \mathcal{H}\left(E_j - E'\right)\mathcal{E}\sum_i \delta(t - t_i),$$

where $\beta > 0$ is a relaxation constant, E_0 is an equilibrium (homeostatic) energy level and E is the spike energy consumption which the j-th neuron pays for generating a spike at $t = t_i$; E' is an emergency energy ($0 < E' < E_0$, H(x) is the Heaviside function), reflecting the supposition that the j-th neuron cannot generate spikes if $E_j < E$'. Let n be an average number of circle centers enclosed in unit area, i.e. the cell density on a 2D plate. The percolation transition of the randomly distributed circles depends on the mean number of circle centers that are kept inside a circle of radius R: $\Theta = \pi R^2 n$. Morphological growth of the network is assumed to be linear yet saturated by the overall spiking activity depending on strength of the energy feedback.

Figure 1 shows how the model network evolves from the uncoupled state. The presence of inhibitory neurons increases the critical value (dashed curve in Fig. 1). At the critical state the spiking rate dramatically increases and the energy feedback is effectively activated saturating the growth. Hence, the energy feedback balances the system geometry to evolve at the edge of the percolation

transition. Network bulk energy characterizing the overall activity also stops to grow, oscillating near some saturation level. For the excitatory network ($Q = 0$) the critical point for the geometrical transition directly defines the energy saturation level.

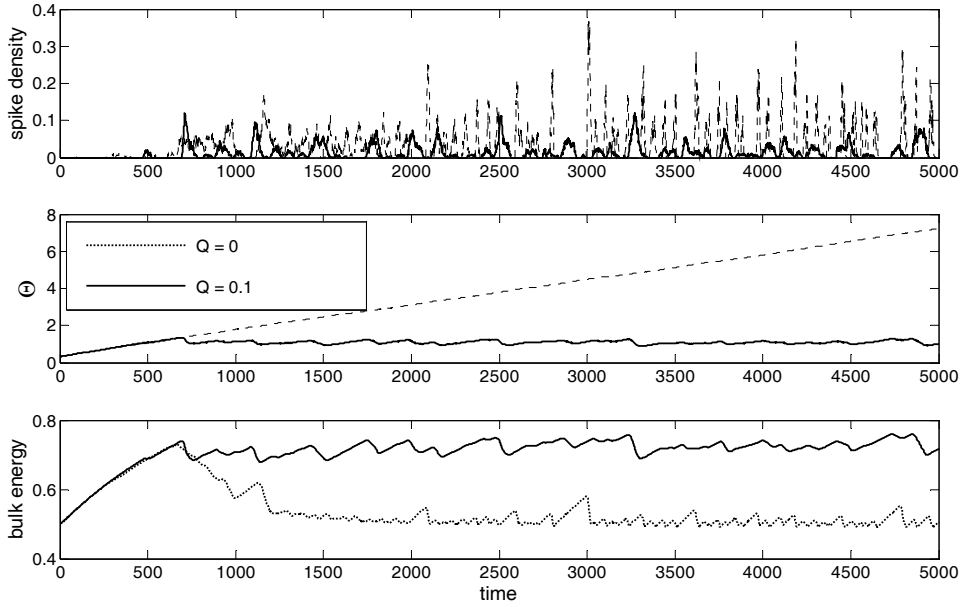

Fig. 1. Spontaneous evolution of the network starting from the uncoupled state without inhibitory neurons (solid curves) and with the fraction $Q = 0.1$ of inhibitory neurons (dashed curves). Top panel: average spike density. In the middle: critical parameter Θ describing network geometry. Bottom plate: network bulk energy

Surprisingly, the influence of the inhibitory neurons apparently divides the critical conditions for the geometrical (percolation) transition and for the energetic balance (Fig. 1). For $Q = 0.1$ (dashed curves in Fig. 1) the first network burst generated at the edge of the circle percolation activates the inhibitory neurons that suppress the activity in addition to the energetic feedback. The energy goes to lower values which, in turn, reduces the feedback to the morphological growth. So, parameter Θ continues the quasilinear increase up to the values corresponding to the saturated energy level (the middle panel in Fig. 1). Finally, the network dynamics converges to its stationary (e.g. homeostatic) state when three mechanisms including the morphological growth, the energy balance and the signal suppression due to the inhibition come into balance.

Acknowledgements

This work is partly supported by the Russian Foundation for Basic Research (project No. 10-01-00690-a), by Russian Federal Programs (No. 16.740.11.0488) and the Ministry of education and science of Russian Federation (project No. 2.1.1/6020).

References

1. P. Bak, *How Nature Works (The Science of Self-organized Criticality)*, Oxford Univ. Press, 1997, p. 287.
2. K. Christensen, R. Donangelo, B. Koiller, K. Sneppen, *PhysRevLett.*, 1998, **81**, doi 10.1103, 2380.
3. S. Bornholdt, T. Rohlf, *Phys. Rev. Lett*., 2000, **84**, doi 10.1103, 6114-6117.
4. J. Beggs, D. Plenz, *J Neurosci*., 2003, **23**, 11167; *J Neurosci*., 2004, **24**, 5216.
5. V. Pasqualea, P. Massobriob, L.L. Bolognaa, M. Chiappalonea & S. Martinoia, *Neuroscience*, 2008, **153**(4), 1354.
6. P. Gong, C. van Leeuwen, *Europhysics Letters*, 2004, **67**(2), 328.
7. P. Gong, C. van Leeuwen, *Europhysics Letters*, 2007, **98**, 048104-1.
8. M. Tsodyks, A. Uziel, H. Markram, *J. Neuroscience*, 2000, **20**, RC50.
9. E.M. Izhikevich, J.A. Gally, G.M. Edelman, *Cereb Cortex*, 2004, **14**, 933.
10. E.M. Izhikevich, *Neural Comput*., 2006, **18**, 245.
11. L. Abbott, R. Rohrkemper, *Prog Brain Res*, 2007, **165**, 13.
12. M. Benayoun, J.D. Cowan, W. van Drongelen, E. Wallace, *PLOS Computational Biology*, 2010, **6**, e1000846.

REPEATABILITY OF BURST ACTIVATION PATHWAYS IN STDP DRIVEN NEURONAL NETWORK MODEL

I.A. Kastalskiy[1], **S.A. Lobov**[2], **A.S. Pimashkin**[1], and **V.B. Kazantsev**[1,2]

[1] Lobachevsky State University, Nizhny Novgorod, Russia, www.unn.ru
[2] Institute of Applied Physics, Russian Academy of Sciences, Nizhny Novgorod, Russia, www.iapras.ru

Cellular and network mechanisms of activity pattern generation and sustainability in living neuronal systems are the subjects of intensive discussions in modern neuroscience. Cultured neuronal networks formed in development represent one of the basic models to investigate the effects of network organization and plasticity [1–3]. It has been observed in many culture preparations that after certain time of spontaneous development in vitro the culture network dynamics converges to the so-called burst population discharges characterized by a robust precisely timed pattern. The mechanisms of the burst dynamics can be associated with the presence of quite stable network morphology and synaptic connectivity activating particular pathways of excitation propagation. Typical intervals of burst durations may be explained by short term frequency dependent synaptic depression [4]. However, the characteristics of intraburst spiking patterns that generally reflect activated synaptic pathways are still the subject of debates. On the one hand, the bursts are characterized by certain activation patterns repeating in the consequent bursts and forming certain groups or motifs [5]. On the other hand, spontaneous bursts may be treated as neuronal avalanches developed at the edge of self-organized criticality [2, 3]. Theoretically they contain a huge number of possible pathways of excitation propagation at different space and time scaling.

In our work we develop a caricature mathematical model of culture network and analyze the correspondence between the profile of intraburst spiking patterns and network connectivity. The model contains hundreds of neurons distributed on 2D surface with cell positions randomly assigned. Each neuron is described by the Izhikevich model generating spikes if total synaptic input exceeds certain threshold [6]. Neurons (80% of excitatory and 20% of inhibitory) are connected with probability monotonically decreasing as a function of distance between cells. Synapses are supplied by frequency dependent short term depression and spike timing dependent plasticity (STDP) learning rule. Being initialized from a Gaussian distribution of synaptic strengths spontaneous network connectivity converges to some asymmetric distribution of synaptic weights selected by the STDP. Then, the network displays series of quite well shaped population bursts similarly to those observed in culture experiments [1–3]. We investigate if there is a repeatability in the burst activation profile by calculating the quantity (modified from [5]):

$$S(p,q) = \sqrt{\sum_{i=1}^{N=N_{\max}} \left(t_i^p - t_i^q\right)^2} \,. \qquad (1)$$

It defines the distance between two bursts in the sequence as time interval between the first spikes generated by same neurons and burst initiation time. Collecting the statistics from the model data and comparing it with shuffled surrogates we have found that there is no any repeatability in the burst activation patterns. It means that the bursts can be initiated along different signaling pathways not statistically repeated.

Next, we analyze how the network is structured in terms of significance of particular neurons participating in the activity. Stimulating one excitatory neuron by a short pulse stimulus we followed the network response. Surprisingly, there exists a small fraction of neurons leading to prolonged network dynamics after the stimulus relative to the other ones (Fig. 1A). These cells were then treated as "activity hubs" routing the network signals within certain STDP driven synaptic architecture. Note that such cells are not necessarily having much more topological connections relative to the others (e.g. topological hubs). Collecting the activity hubs we applied the repeatability test (1) and found that the burst activation profiles are statistically similar to each other relative to surrogates (Fig. 1B). Thus, burst generation is determined by the certain order of hub activations reflecting principle signal transmission pathways in the STDP driven network dynamics. Such pathways may coexist with many other signaling routes involving other neurons and developing at different time and spatial scaling in accordance with the neuronal avalanche concept.

In conclusion, we summarize the key findings of our analysis. Following the STDP driven model dynamics we identify the formation of network hubs repetitively activated in the consequent bursts. The activation profile of the other network neurons occurs statistically at random with no apparent repeatability. On the one hand, this fits the statistics of self-organized criticality [1,5]. On the other hand, the presence of burst similarly agrees with the analysis of activation patterns in culture discharges [2, 3]. Based on the model results, we hypothesize that generation of different spikes recorded in culture networks may have different level of "functional significance" for network dynamics.

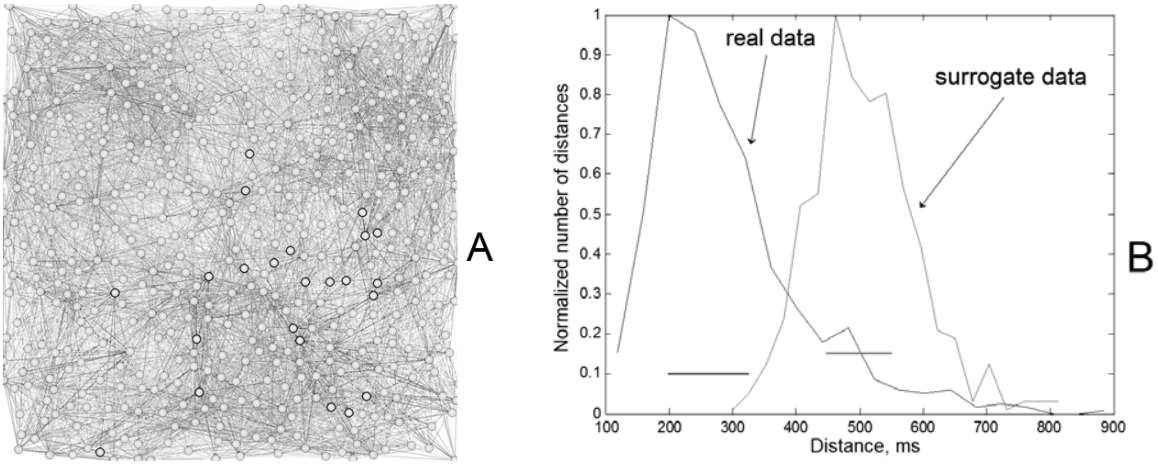

Fig. 1. A: A fragment of network connectivity in the STDP driven model. Connection weights are shown as gray degree: from white (weight = 0) to black (weight = 1). Hubs are circled solid black lines. **B:** Distribution of distance (1) between pair of bursts generated by the STDP driven network calculated for the activity hubs. Two horizontal lines illustrate the median absolute deviation of the model data from the left and right distribution medians, respectively

Acknowledgements

This work was supported by the Federal Agency of Science and Innovations (government contracts Nos. 14.740.11.0075, 16.512.11.2136), by the grant of the President of the Russian Federation (grant No. MD-5096.2011.2), by the RAS Presidium program "Molecular and cellular biology".

References

1. J.D. Rolston, D.A. Wagenaar, S.M. Potter, *Neuroscience*, 2007, **148**, 294.
2. V. Pasquale, P. Massobrio, L.L. Bologna et al., *Neuroscience*, 2008, **4**, 1354.
3. J.M. Beggs & D. Plenz, *J. Neurosci*., 2004, **24**(22), 5216.
4. M. Tsodyks, A. Uziel, H. Markram, *The Journal of Neuroscience*, 2000, **20**, RC50.
5. N. Raichman, E. Ben-Jacob, *Journal of Neuroscience Methods*, 2008, **170**, 96-110.
6. E.M. Izhikevich, J.A. Gally, G.M. Edelman, *Cereb. Cortex*., 2004, **14**, 933-944.

Invited

STDP-BASED SPIKING PHASE BINDING IN SYNAPTICALLY COUPLED NEURONAL OSCILLATORS

V.B. Kazantsev[1,2] and **I.Yu. Tyukin**[3]

[1] Nizhny Novgorod State University, Russia, vkazan@neuron.sci-appl.nnov.ru
[2] Institute of Applied Physics RAS, Nizhny Novgorod, Russia
[3] University of Leicester, Leicester, UK

Spike timing dependent plasticity (STDP) is one of the key mechanisms driving signal transmission in neuronal networks. Various forms of STDP have been discovered to date and a large number of models describing the phenomenon with different degrees of biophysical detail have been proposed and used in simulations of neural circuits. At the cellular level, being served by different molecular mechanisms of postsynaptic modulation, the STDP can be viewed as a kind of feedback regulating the efficacy of signal transmission depending on timing between post- and presynaptic spikes. Many forms of STDP have been found experimentally and explained theoretically [1]. One of the basic mechanisms of STDP is related to postsynaptic changes mediated by calcium flux through the NMDA receptors located in the spine [2]. Such changes may induce long term potentiation or depression depending on the relative timing of post- and presynaptic spikes. In modeling, thanks to the phenomenological description of the STDP in terms of increased synaptic efficacy, the STDP is implemented as dynamic variations of synaptic weights accounting for the mere strength of the synaptic transmission. At this phenomenological level of description, complex postsynaptic molecular machinery in individual cells is typically reduced to the so-called STDP curves regulating the feedback and tuned according to experimental observations [3]. At the level of cell populations, e.g. network level, major consequence of the STDP is thus limited to facilitation or to depression of particular signal transmission pathways implementing, in fact, Hebbian plasticity (learning) rule.

Recent experimental findings based on multi-neuron recordings (optical and electrophysiological), revealed that spike transmission in networks is characterized not only by firing rates but also by repeated spike sequences with precise timing [4, 5]. In other words, there is a correspondence in post- to presynaptic spiking which is rather stable, persistent, and robust in different experimental conditions. The mechanism responsible for such correspondence is still not fully established and, as a consequence, understood. One candidate of such mechanisms was hypothesized in [6]. In particular, it was suggested that it is the network's morphology, by providing axonal delays of inter-neuron spike transmission, which may be responsible for inducing coherent activation in cells with certain polychronous groups or activity clusters [6]. Here we discuss if there is a purely synaptic mechanism that might give rise to persistent maintenance of post- to presynaptic spike timing in neuronal networks.

We propose a phenomenological model of STDP postsynaptic feedback and show that it may serve as a built-in postsynaptic mechanism of binding post- and presynaptic relative spiking times. The model is schematically shown in Fig. 1.

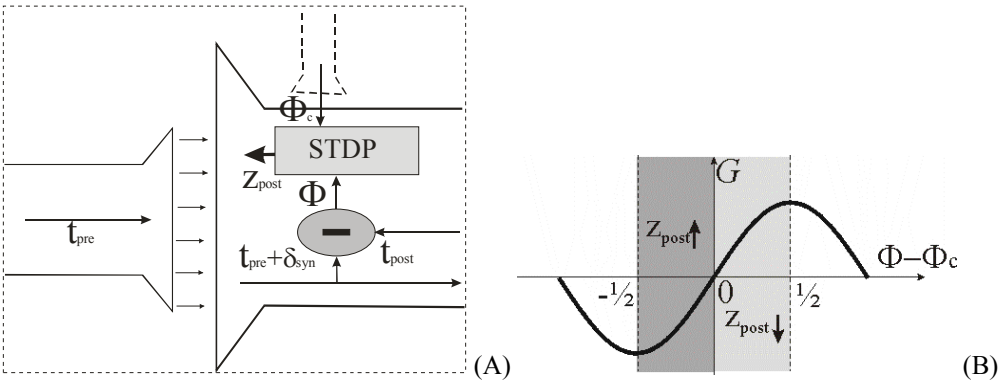

Fig. 1. A Schematic view of STDP feedback. B. STDP curve facilitating or depressing a synaptic variable z_{post} depending on the difference between actual, Φ, and "desired", Φ_c, values of post- to presynaptic spike timings

Spikes arriving at the terminal of presynaptic neurons cause the release of a neurotransmitter. It reaches the postsynaptic neuron resulting in the generation of postsynaptic potential (EPSP) with latency time $\delta_{syn}<<T_s$, where T_s is a characteristic time scale of the spike train. The EPSP, in turn, may cause the generation of the response spike (e.g. action potential). This event can then be detected in the postsynaptic terminal as a chemical or electrical back-propagating signal. Thus, the difference between presynaptic and postsynaptic spikes, e.g. the *relative phase shift*, Φ, can be extracted. Comparing the latter with some "task" or "reference" signal, which may be projected from other neurons using another synapse or extracellular modulation, the STDP generates a chemical signal compensating for the phase mismatch. Note that such feedback circuit, in fact, modifies the traditional STDP rule by extending it with embedding an error-compensating mechanism into the circuit.

In order to illustrate the updated STDP model we consider a pair of synaptically coupled neuronal oscillators described by the Rowat-Selverston equations [7]. This model represents a simplified version of Hodgkin-Huxley equations used in modeling studies to test synchronization. The STDP is implemented in the following form

$$\frac{dz_{post}}{dt} = -\alpha(z_{post} - I) + kG(\Phi)\,. \qquad (1)$$

Here, the variable z_{post} describes the additional current generated by the STDP (hence, the strength of the synaptic connection) with the feedback strength k. Parameter I defines the equilibrium level of the synaptic variable, α defines the characteristic time scale of the synaptic changes. In simulations we run two spiking oscillators with different natural frequencies so that the post- to presynaptic timing (e.g. the relative spiking phase) is fluctuating with the rate proportional to frequency mismatch (Fig. 2). Switching the STDP "on" we find that the feedback eventually stabilizes the spiking phase to the values of Φ_c. Note that the task phase Φ_c may take any desired value within the characteristic time scale T_s (here T_s is the oscillation period).

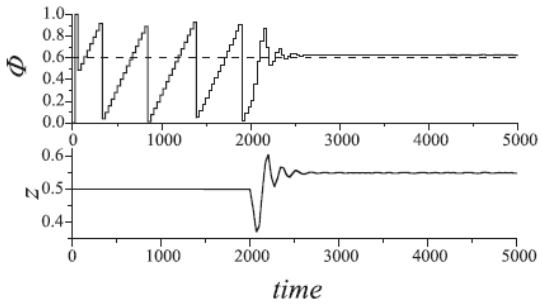

Fig. 2. Oscillation phase binding in a pair of STDP driven synaptically coupled neuronal oscillators. From 0 to 2000 the oscillators are uncoupled and the phase is fluctuating. From t = 2000 the STDP is switched on and stabilizes the phase to a desired value Φ_c = 0.6

In summary, the spike timing dependent plasticity may provide spiking phase selectivity in synaptic transmission. In the phenomenological model presented here the STDP-based feedback may potentiate or depress synapses to achieve a precise locking in post- to presynaptic timing. Moreover, specific values of timing in the system can be induced by means of external association/command, coming, for instance, from other (sensory) neurons controlling the state of synapses in relation with certain task.

Acknowledgements

This work was supported by the Russian Federal Program (grants 16.512.11.2136, 14.740.11.0075) and by the grant of the President of the Russian Federation (MD-5096.2011.2).

References

1. P.J. Sjostrom, E.A. Rancz, A. Roth, M. Hausser, *Physiological Reviews*, 2008, **88**, 769-840.
2. H.J. Koester, B. Sakmann, *Proc Natl Acad Sci USA*., 2008, **95**, 9596-9601.
3. A. Morrison, M. Diesmann, W. Gerstner, *Biol. Cyber*., 2008, **98**, 459-478.
4. J.D. Rolston, D.A. Wagenaar, S.M. Potter, *Neuroscience*, 2007, **148**, 294-303.
5. Y. Ikegaya, et al., *Science*, 2004, **304**, 559-564.
6. E.M. Izhikevich, *Neural Computation*, 2006, **18**, 245-282.
7. P.F. Rowat, A.I. Selverston, *J. Neurophysiology*, 2003, **70**(3), 1030-1053.

MODULATION OF SPONTANEOUS NETWORK ACTIVITY IN HIPPOCAMPAL CELL CULTURE BY GLUTAMATE AND N-ARACHIDONOYL DOPAMINE

L.G. Khaspekov[1], **S.A. Korotchenko**[2], **M.V. Vedunova**[2], **E.A. Koryagina**[2], **M.Yu. Bobrov**[1,3], **E.E. Genrikhs**[1], and **I.V. Mukhina**[2]

[1] Research Centre of Neurology RAMS, Moscow, Russia, khaspekleon@mail.ru
[2] Nizhny Novgorod State Medical Academy, Nizhny Novgorod, Russia
[3] Shemyakin-Ovchinnikov Institute of Bioorganic Chemistry RAS, Moscow, Russia

The modulation of neuronal spontaneous network activity (SNA) is one of important problems in modern neurobiology. The most extended neurotransmitter which realizes the informational exchange in brain neuronal networks is glutamate. At the same time, in some pathological conditions (e.g., in stroke), hyperstimulation of postsynaptic glutamate receptors on account of strengthened glutamate release from presynaptic terminals (the so-called glutamate excitotoxicity) results in abundant intracellular calcium accumulation inducing pathogenetic cascade of lipo- and proteolitic reactions causing neuronal death [3].

Therefore, neuromodulatory regulation of glutamatergic network neurotransmission may contribute to removal of negative consequences of its disturbation. Effective neuromodulators of excitatory synaptic activity are endogenous cannabinoids (EC), since their retrograde interaction with presynaptic cannabinoid receptors may inhibits the excessive release of neurotransmitter from axon terminals reducing intracellular calcium overload [1, 2].

In our work, the effects of glutamate and synthetic EC analog N-arachidonoyl dopamine (N-ADA) on hippocampal SNA in cell cultures developing on multielectrode array (MED64, Alpha Med Sciences, Japan) containing 64 microelectrodes were investigated. Dissociated hippocampal cells have been taken from the brain of E18mice embryos and cultured with density 1500-2000 cell/mm^2 in Neurobasal/B27 culture medium directly on MED64 probe during 14 days at 35.5^{o}C in an atmosphere of 5%CO_2 and 95% air. Spontaneous spike activity was detected in a 20-min recording period as the number of spikes with amplitude exceeding five times the standard deviation of the baseline noise. For statistical analysis a suite of problem program BioStat (AnalystSoft) was used. The data were represented in descriptive statistic forms, M and SD, where M is average, and SD is mean-square deviation.

As we have recently shown [4], hippocampal cells cultured on MEA64 form during the first 14 days in vitro functional network generating synchronous SNA which is characterized by determined burst quantity and determined spike frequency in every burst.

Application of increasing subtoxic glutamate concentrations results in dose-dependent raising of SNA level (Table 1).

Table 1. Effect of glutamate application on SNA parameters in hippocampal cell cultures on MEA64.

Parameter		Glutamate concentration, mcM						
		0	0,5	1	2	10	50	100
Burst quantity/ 5 min	M	16,7	34,8*	59,5*, **	61,8*	72,06*	60,5*	62,4*
	SD	3,34	2,88	3,23	2,55	5,52	2,77	4,12
Spike quantity/ burst	M	2987	1655*	1120*, **	1008*	1104*	420*, **	350*
	SD	466	438	227	269	186	86	62

* – significant difference from basal level (p<0,05); ** – significant difference from previous value, p < 0,05

An analysis of raster plots revealed dose dependent increasing the SNA level after 1–2 μM glutamate application. On the other hand, the exposure of cultures to 10-100 μM glutamate resulted in transient SNA blockade (Fig. 1, A-C), apparently on account of glutamate receptor desensitization. Moreover, application of high glutamate concentrations resulted in full or partial SNA suppression on some electrodes (e.g., 7-9, 31-33, 38, 54-56, Fig. 1 C), probably as a consequence of hyperactivation of inhibitory GABA interneurons connected synapticaly with principal hippocampal neurons.

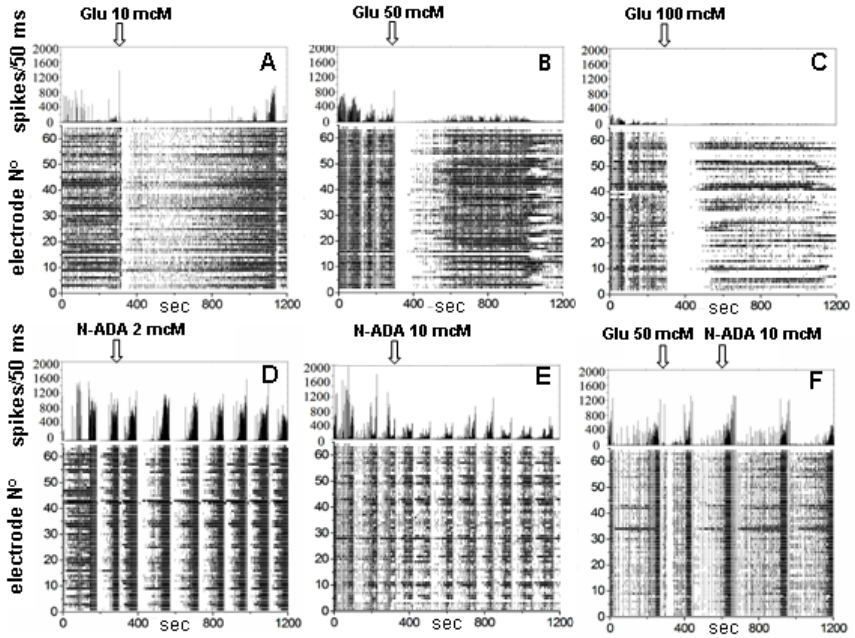

Fig. 1. Raster plots of SNA (bottom chart) and spike quantity/50 msec (upper chart) in hippocampal cell cultures on MEA64 (14 DIV) exposed to application of 10 (A), 50 (B) and 100 (C) mcM glutamate, 2 (D) and 10 (E) mcM N-АДА and to co-application of 50 mcM glutamate and 10 mcM N-АДА (F)

Exposure of cultures to 0.5-5 mcM N-ADA did not result in significant changes of main SNA parameters (Table 2). On the other hand, 10 mcM N-ADA lowered gradually the SNA level. Moreover, under N-АДА application, the network pattern of activity, i.e. burst frequency and quantity of spikes in burst, was changed (Fig. 1D,E).

Table 2. Effect of N-ADA application on SNA parameters in hippocampal cell cultures on MEA64.

Parameter		N-ADA concentration, mcM						
		0	0,5	1	2	5	7	10
Burst quantity/ 5 min	M	18,5	17,9	18,5	16,4	15,7	15	16
	SD	3,55	4,37	5,23	3,67	3,47	5,12	2,85
Spike quantity/ burst	M	2005	1675	1358	1469	1623	1050*, **	645*
	SD	423	328	312	387	233	148	134

* – significant difference from basal level ($p < 0,05$); ** – significant difference from previous value, $p < 0,05$

A combined exposure of 50 μM glutamate and 10 μM N-ADA accelerated SNA recovery to basal level, as compared with its recovery after exposure of 50 μM glutamate without N-ADA (Fig. 1F).

In conclusion, our data showed that glutamate exposure results in dose dependent increasing the SNA level in hippocampal cell culture maintained on multielectrode array. At the same time, application of cannabinoid receptor ligand after glutamate exposure provides positive modulatory effect, recovering SNA to basal level.

Acknowledgements

The research is supported by the Russian Federal Department of Education and Science N^{o} 21.1/6223.

References

1. Y. Hashimotodani, T. Ohno-Shosaku and M. Kano, *Neuroscientist*, 2007, **13**, 127-137.
2. L.G. Khaspekov and M.Yu. Bobrov, *Neurochemical J.*, 2007, **1**, 93-112.
3. P. Lipton, *Physiol Rev.,* 1999, **79,** 1431-1568.
4. I.V. Mukhina, V.B. Kazantsev, L.G. Khaspekov, Yu.N. Zakharov, M.V. Vedunova, E.V. Mitroshina, S.A. Korotchenko, and E.A. Koryagina, *Modern Technologies in Medicine*, 2009, **1**, 8-15 (In Russian).

Invited

OPTICAL MONITORING OF ACTIVITY-EVOKED pH CHANGES IN HIPPOCAMPAL SLICES FROM Ts65Dn MICE, A MODEL OF DOWN SYNDROME

A.M. Kleschevnikov

University of California San Diego, La Jolla, CA, USA, akleschevnikov@ucsd.edu

Down syndrome (DS) is a developmental disorder caused by full or partial triplication of chromosome 21. The incidence of DS is about 1:1000. The presence of one extra copy of approximately 300 genes results in a number of severe clinical phenotypes including mental retardation, congenital heart disease, acute megakaryoblastic leukemia, abnormalities in learning and memory and age-related Alzheimer's type neurodegeneration by the age of 40 [1]. At present, there is no effective treatment for DS-related CNS abnormalities.

Mouse genetic models provide the opportunity to better define abnormal molecular and cellular mechanisms in DS and to link these abnormalities to increased dosage of a specific gene(s). Genes orthologous to those on human chromosome 21 are found on three mouse chromosomes: chr. 16 (~50% of all orthologous genes), chr.10 and chr. 17. In the Ts65Dn mouse the region of chromosome 16 extending from *Gabpa* to *Mx1* (~140 genes) is triplicated [2]. This region contains genes responsible for many DS phenotypes, including mental retardation. Indeed, Ts65Dn mice exhibit a number of features typical of DS, including impairment of hippocampal function, as evidenced by impaired spatial and working memory (e.g. [3]). Mice with shorter triplicated regions of chromosome 10, 16 and 17 (Ts1Cje, Ms1Ts65, etc), and those overexpressing single DS-related genes (*SOD1*, *APP* and others) are also used as models of DS.

Regulation of extra- and intracellular pH levels is vital for normal function of many receptors, enzymes and channels. There are several systems controlling intra- and extracellular acidic and alkaline shifts in species- and tissue-specific manner. Some of these systems could be affected in DS. (i) Critical role in pH regulation in biological systems plays the carbonic acid reaction ($H_2CO_3 <=> H^+ + HCO_3^-$). Bicarbonate ions ($HCO_3^-$) contribute significantly to currents through the $GABA_A$ receptor/channel complex. Because the equilibrium potential for HCO_3^- is about 0 mV, activation of the $GABA_A$ receptors results in efflux of the bicarbonate ions and, hence, intracellular acidification and extracellular alkalization. Since the efficiency of GABAergic neurotransmission is significantly enhanced in DS model mice [4], $GABA_A$ receptor-associated pH transients could be increased. (ii) Several Na^+/H^+ exchangers (NHE1, NHE4 and NHE5) are highly expressed in the hippocampus and could be affected in DS due to abnormalities in Na^+ channels in trisomy 16 mice [5]. (iii) Several members of Cl^-/HCO_3^- anion exchanger (AE) family are highly expressed in the CNS, including the hippocampus. The efficiency of these exchangers could be affected due to greater $GABA_A$ receptors-mediated currents and hyperpolarized membrane potential (the latter is caused by increased signaling through the postsynaptic $GABA_B$ receptors). (iv) Na^+/ HCO_3^- co-transporters (NBC). These transporters are highly expressed in several regions of the brain, including dentate gyrus. Changes in the activity of these transporters could be affected due to enhanced activation of the $GABA_A$ receptors in Ts65Dn. (v) Triplication of the copper-zinc super-oxide dismutase 1 (SOD1) gene results in enhanced expression levels of this enzyme in DS. This change increases the metabolizing rate of superoxide ions to hydrogen peroxide, thus affecting pH either directly or through damage to the mitochondria. (vi) Finally, abnormalities of mitochondria in DS [6] could also contribute to pH abnormalities.

We examined pH levels in hippocampal slices from trisomic Ts65Dn and control (2N) mice. Two approaches have been used: (i) Registration of the pH level with pH-sensitive microelectrodes and (ii) Optical registration with pH-sensitive fluorescent dyes (BCECF-AM and other). Transverse hippocampal slices (350 μm) were prepared and kept according to a standard protocol for electrophysiological recordings. For optical registration, slices were incubated for 10-30 min in artificial cerebro-spinal fluid (ACSF) containing BSECF-AM (5–10 μM), and then were washed-out in ACSF for 30–60 min, thus allowing for metabolizing the compound. The slices were transferred into the recording chamber for ratiometric evaluation of the pH level using dual-excitation (440 nm and 490 nm)/single emission (535 nm) configuration.

Steady-state pH level was more acidic in Ts65Dn slices

Steady-state pH level was measured in hippocampal slices from Ts65Dn and 2N mice at 24 C° and 32 C°. At both temperatures the slices from the Ts65Dn hippocampus were more acidic. Interstitial pH level measured with a pH-sensitive microelectrode at 24 C° was in 2N slices 7.34 ± 0.01, n = 15, and in Ts65Dn slices 7.29 ± 0.02, n = 12 slices ($p < 0.01$). The difference in the interstitial pH level was even greater at 32 C°: the pH level was in 2N slices 7.1 ± 0.1, n = 4, and in Ts65Dn slices 6.9 ± 0.04, n = 5 ($p < 0.05$). Measurements with pH sensitive fluorescent dye BCECF confirmed these data and showed that the slices from the hippocampus of Ts65Dn mice were more acidic in respect to the slices from control 2N mice. Thus, DS-specific genetic abnormalities result in excessive acidification of the brain of Ts65Dn model mice.

Evoked pH transients were greater in Ts65Dn vs. 2N slices

Activation of afferent fibers resulted in bi-phasic changes of the interstitial pH level (short-term alkalinization followed by later prolonged acidification) in both 2N and Ts65Dn slices. We found that the amplitudes of both phases of the pH transients were greater in the Ts65Dn slices. To examine which receptors are responsible for this difference, we examined activity-evoked pH transients after pharmacological suppression of a number of receptors and/or channels.

To compare pH shifts associated with activation of glutamatergic receptors, pH transients were measured before and after bath application the NMDA receptor antagonist APV (50 μM) and/or AMPA receptor antagonists NBQX (2 μM). The difference in pH transients recorded before and during application of an antagonist was attributed to the activation of the corresponding receptors. Antagonists of the glutamatergic receptors equally affected the pH transients in Ts65Dn and 2N slices. Using application of tetrodotoxin (1 μM), we next compared changes in pH transients associated with activation of Na+ channels. Again, the effects were similar in slices from Ts65Dn and 2N hippocampi. Finally, changes in pH transients associated with activation of the ionotropic $GABA_A$ receptors were compared. Application of the selective $GABA_A$ receptor antagonist picrotoxin (100 μM) significantly reduced both phases of the pH transients (the initial alkalinization and the later acidification) and abolished the difference between the slices from 2N and Ts65Dn mice. We conclude that the major difference of the activity-evoked pH transients in Ts65Dn and 2N hippocampus arises from greater activation of the $GABA_A$ receptors in the Ts65Dn model mice.

Possible consequences of abnormal pH regulation in Ts65Dn mice

It is known that extracellular pH effectively modulates currents through a number of receptors. Acidic pH blocks, while alkaline pH augments the currents through the NMDA receptors [7]. Modulation of the NMDA receptors results mainly from changes in number of channel openings, while unitary conductance remains largely unchanged. Extracellular pH significantly modulates also properties of GABAergic synapses and individual $GABA_A$ receptors. Thus, extracellular acidification may be an important factor contributing to reduced synaptic plasticity and enhanced efficiency of the inhibitory system in Ts65Dn model of DS.

Acknowledgements

The work was supported by grants from NIH (NS 38869, NS055371), the Hillblom Foundation, The Anna and John J. Sie Foundation, The Thrasher Foundation and the Down Syndrome Research and Treatment Foundation.

References

1. K. Gardiner, et al., *J. Neurosci*., 2010, **30**(45), 14943-5.
2. M.T. Davisson, C. Schmidt and E.C.Akeson, *Prog. Clin. Biol. Res*., 1990, **360**, 263-80.
3. N.P. Belichenko et al., *J. Neurosci*., 2009, **29**(18), 5938-48.
4. A.M. Kleschevnikov et al., *J. Neurosci*., 2004, **24,** 8153-8160.
5. Z. Galdzicki, R. Siarey, R. Pearce, J. Stoll, S.I. Rapoport, *Brain Res. Brain Res Rev*., 2001, **35**(2), 115-45.
6. J. Busciglio, A. Pelsman, C. Wong, et al., *Neuron*, 2002, **33**(5), 677-88.
7. S.F. Traynelis and S.G. Cull-Candy, *Nature*, 1990, **345**(6273), 347-50.
8. M. Dierssen et al., *Physiol Behav*., 2001, **73**, 859-871.

DYNAMICS OF NEURON NETWORK BIOELECTRICAL ACTIVITY CAUSED BY PERIODIC LOCAL ELECTRICAL STIMULATION

E.A. Koriagina[1,2,3], **A.S. Pimashkin**[1,2], **V.B. Kazantsev**[1,2], and **I.V. Mukhina**[1,3]

[1] Department of Neurodynamics and Neurobiology, Lobachevsky State University of Nizhny Novgorod Nizhny Novgorod, Russia
[2] Laboratory of Nonlinear Processes in Living Systems, Institute of Applied physics of RAS Nizhny Novgorod, Russia
[3] Normal Physiology Department, Nizhny Novgorod State Medical Academy, Nizhny Novgorod, Russia
katerina_neuron@mail.ru

Cultured neuron networks today are the perspective experimental models to investigate cellular mechanisms of signal propagation and information processing at the network level. It has been found that such networks generate synchronized bursting events (of 0.5–2 s duration) with high frequency spiking elicited by a large number of cells involved in the network. Bursting activity in cultures was broadly investigated in connection with many different problems including disease treatment [1], learning in neuron networks [2–4], signal processing at network level (Chiappalone M., 2008) [5, 6] and many others. The cultured networks show highly variable characteristics of bursting dynamics [7]. The presence of motifs in the activation patterns is especially interesting since such patterns can be repeated with a millisecond precision [8, 9]. It is particularly important for cellular mechanisms of learning when the motifs change during low-frequency electrical stimulation [10].

Stimulated bioelectrical activity of the neural networks was analyzed. The goal of our research is to test the possibility of training a neural network of a primary hippocampal culture grown in the multielectrode array MED64 (Alpha MED Sciences, Japan).

The methods include obtaining the neuronal culture directly at the multielectrode probe MED64 and consequent stimulation, multi-channel recording, and analysis of the extracellular activity of the networks. To stimulate the neuronal cultures, we use the standard protocols of the stimulation comprising the standard software of the multielectrode system MED64, and our original protocol of the simultaneous stimulation by two adjacent electrodes. All signals were statistically analyzed by the customized software.

In this paper, we pay primary attention to the patterns of spikes (isolated discharges) during spontaneous bioelectric activity by virtually all the neurons, which are called spontaneous network burst activity. The packets of the spikes appear in relatively large time intervals and consist of high-frequency sequences of the spikes.

The spikes were characterized by the time lag of their appearance in the packet (burst). As the functional characteristics of each packet, we built a 64-dimensional pattern of activation – the time lag of the first spike at each electrode from the start of the burst activity (Fig. 1).

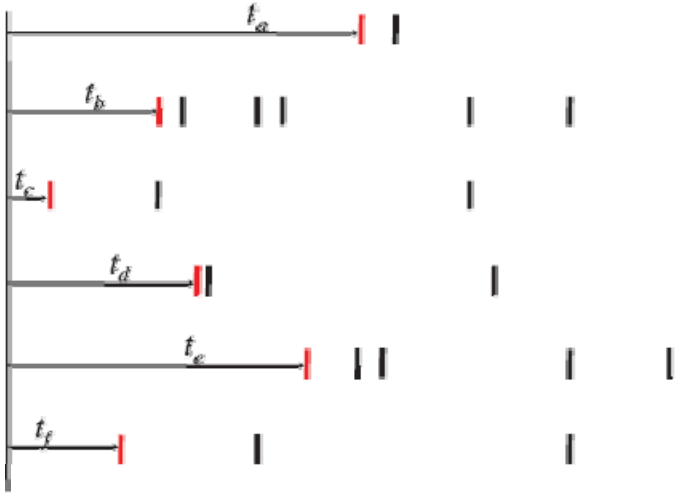

Fig. 1. The pattern of the neuronal activity. The bars denote time lags of the spikes at different electrodes. The red bars mark the first spikes in the packet and describe the pattern of activity

Further, we introduced the time interval (distance) between different packets of the spikes

$$S(p,q) = \frac{1}{N}\sqrt{\sum_{i=1}^{N}\left((t_i^p - t_i^q\right)^2},$$

where t_i^p and t_i^q are the times of the p^{th} and q^{th} packets of the spikes at the i^{th} electrode, $N = 64$ is the total number of electrodes.

The pattern of activity in spontaneous generation mode corresponds to the morphology of the neural networks and the signal paths in them which is manifested as a definite (constant) structure of time delays between pulses from different neurons.

The unique pattern of activity for different cultures of neurons is a functional indicator of the network. This indicator is required to assess the mechanisms of memory and learning.

The external stimulation caused new stable patterns of activity which are statistically distinguishable from the spontaneous activity. This indicates that the external stimulation switches over the dynamics of activity to a new steady state.

Thus, our experiments by the electrical stimulation of the neuronal culture reveal the existence of the mechanisms of formation of different responses of the neural network to the electrical stimuli. This indicates the possibility to change plasticity of the dissociated cultures of hippocampal neurons at the network level in the learning process and the formation of long-term functional changes.

References

1. D. Wagenaar, R. Madhavan, J. Pine, S. Potter, "Controlling bursting in cortical cultures with closed-loop multi-electrode stimulation", *J. Neurosci*., 2005, **25**(3), 680-688.
2. G. Shahaf, S. Marom, "Learning in networks of cortical neurons", *J. Neurosci*., 2001, Nov 15, **21**(22), 8782-8.
3. S. Marom, G. Shahaf, "Development, learning and memory in large random networks of cortical neurons: lessons beyond anatomy", *Q. Rev. Biophys*., 2002, **35**, 63-87.
4. J. le Feber, J. Stegenga, W.L.C. Rutten, "The Effect of Slow Electrical Stimuli to Achieve Learning in Cultured Networks of Rat Cortical Neurons", *PLoS ONE*, 2010, **5**(1), e8871. doi:10.1371/journal.pone.0008871.
5. D. Bakkum, Z. Chao, S. Potter, "Long-Term Activity-Dependent Plasticity of Action Potential Propagation Delay and Amplitude in Cortical Networks", *PLoS ONE*, 2008, **3**(5), e2088. doi:10.1371/journal.pone.0002088.
6. D. Wagenaar, J. Pine, S.M. Potter, "Effective parameters for stimula-tion of dissociated cultures using multi-electrode arrays", *J. Neurosci. Methods*, 2004, **138**, 27-37.
7. D. Wagenaar, J. Pine, S. Potter, "An extremely rich repertoire of bursting patterns during the development of cortical cultures", *BMC Neurosc*., 2006, **7**, 11.
8. D. Chao-Yi, L. Jisoon, N. Yoonkey, C. Kwang-Hyun, "Systematic analysis of synchronized oscillatory neuronal networks reveals an enrichment for coupled direct and indirect feedback motifs", *Bioinformatics*, 2009, **25**, no. 13, 1680–1685.
9. N. Raichman, E. Ben-Jacob, "Identifying repeating motifs in the activation of synchronized bursts in cultured neuronal networks", *J. Neurosci. Methods*, 2008, **170**(1), 96-110.
10. G. Shahaf, D. Eytan, A. Gal, E. Kermany, V. Lyakhov, et al., "Order-Based Representation in Random Networks of Cortical Neurons", *PLoS Comput Biol*., 2008, **4**(11), e1000228. doi:10.1371/journal.pcbi.1000228.

FRACTAL PROPERTIES OF PROTEINS

S.G. Lushnikov, **S.V. Strokov,** and **A.V. Svanidze**

Ioffe Physical Technical Institute RAS, S.-Petersburg, Russia, sergey.lushnikov@mail.ioffe.ru

The mechanism of protein functioning is of vital importance for the understanding of the activity of living organisms at the molecular level. At present research efforts of many teams all over the world are focused on the investigations of proteins, however, few attempts have been made to consider the protein structure and dynamics in the framework of a unified approach. In this report we demonstrate a successful use of the fractal approach for description of the protein properties from a single point of view. The fractal geometry is a suitable tool for analysis of the spatial organization and dynamics of disordered or partly ordered media [1, 2], and it is not surprising that from the moment of development of the fractal theory by Mandelbrot there have been numerous efforts to describe the protein topology by using the fractal approach. In more recent model the protein molecule is considered to be a "mass" fractal. Note that in the case of the "mass" fractal, the law of increase in the mass of a fractal object is described by the function of its linear sizes $M(r) \propto r^{D_f}$, i.e., the density becomes a decreasing function of the fractal object size $\rho(r) \propto r^{D-D_f}$, $D > D_f$, where D is the topological dimension of the space into which the fractal is embedded [1, 2].

If the case the fractal approach is used for description of a protein, its low-frequency part of vibration spectrum must contain a collective excitation at a fractal, i.e., a fracton (the properties of this excitation were described in detail in a review [2]), whose dispersion law in certain frequency range is $\omega \propto k^{D_f/\tilde{d}}$, where $\tilde{d}$ is the fracton dimension. The protein vibration spectrum was analyzed theoretically in [3]. The author obtained the numerical estimates of the fractal and fracton dimensions of g-actin and suggested an explanation of specific features of the low-frequency protein dynamics based on the fractality of their structure [3]. Model calculations have shown that fracton dimensions of proteins range from 1.3 to 1.9. Analysis of the generalized density of states function revealed that both the Debye and fracton regimes were realized in the low-frequency region of the vibration spectrum of lysozyme [4].

The goal of our work was to describe the protein structure and dynamics in the framework of the fractal approach and to demonstrate that this approach is applicable to protein. The objects were hen egg white lysozyme, bovine serum albumin (BSA) and g-actin. For the investigations, small-angle (SANS) and inelastic neutron scattering (INS) techniques were used.

SANS spectra were recorded in the range of scattering wave vectors q from 0.0401 to 0.5088 Å^{-1} by a small-angle neutron diffractometer «Yellow Submarine» (Budapest Neutron Center, Hungary). Solutions of lysozyme (Hen Egg White Lysozyme, Fluka), BSA and g-actine with concentrations 5 mg/ml, 50 mg/ml and 250 mg/ml were prepared by using heavy water (D_2O).

Inelastic neutron scattering experiments were performed at a time-of-flight FOCUS spectrometer placed at the LNS, Paul Scherrer Institute (Switzerland). The objects used in the INS experiments were powder-like samples of lysozyme, BSA and g-actin.

The dependence of scattering intensity on wave vector in the double logarithmic scale for the lysozyme solution in sodium acetate buffer with a protein concentration of 50 mg/ml obtained by SANS at 300 K (Fig. 1). The spectrum is similar to those published earlier. The $I(q)$ dependence can be conventionally divided into three regions: $q < 0.1$ Å^{-1} corresponds to the interparticle interaction between lysozyme molecules under a repulsive Coulomb potential, and the 0.1 – 0.2 and 0.3 – 0.6 Å^{-1} ranges reflect mainly the tertiary protein structure and interdomain correlation within the molecule, respectively. In the range of wave vectors $0.073 < q < 0.1215$ Å^{-1} the dependence of scattering intensity on wave vector is described by the Guinier's law

In this report we focus our attention on the wave vector range 0.1578 Å$^{-1} < q < 0.2574$ Å^{-1} that describes the structure of protein molecule. The dependence of the scattering intensity on wave vector for this region is well described by the power law

$$I(q) \propto q^{-D_f} \qquad (1)$$

The calculations using Eq. (1) yielded $D_f = 2.77 \pm 0.08$. This means that lysozyme at the scales $L < r < \xi$, where $L = 24$ Å and correlation length $\xi = 38$ Å, can be described as a mass fractal. This range is close to the lysozyme molecule sizes, which suggests that the lysozyme molecule is a fractal. Note that $D_f = 2.77 \pm 0.08$ is in good agreement with the model calculations of fractal dimensions of proteins. Similar values of D_f were obtained for BSA and g-actin.

In the inelastic neutron scattering investigations of lysozyme, a generalized density of states function $G(\omega)$ was obtained and analyzed correctly in the region from 1.5 to 20 meV because the contribution of the multi-phonon scattering is expected to be small (for experimental details and data processing method see [4]). The low-frequency region (from 1.5 to 20.0 meV) of the generalized density of states function of deuterated lysozyme $G(\omega)$ at 280 K in the double logarithmic scale. It is well seen that the curve in Fig. 2 has two linear regions with different power law dependences. For the region in the 1.5 to 3.5 meV energy range the exponent has been found to be 1.89, which $G(\omega)$ corresponds to a spectral dimension of 2.89±0.05. This result agrees with the Debye model for the density of states of acoustic modes of solids. The next linear region (Fig. 2) corresponds to the energy range from 7 meV to 14 meV. This region is characterized by an exponent of 0.4 and, hence, spectral dimension $\tilde{d}$ =1.4. This magnitude of $\tilde{d}$ corresponds to the fracton dimension of classical fractal systems.

To summarize, the fractal dimension of lysozyme, BSA and g-actin D_f has been determined in SANS experiments. The fracton dimension of the same proteins $\tilde{d}$ has been estimated by analyzing the generalized density of states function obtained by inelastic neutron scattering. Thus, we have succeeded in describing the proteins as a fractal object. This opens up great possibilities for the use of the fractal approach (and corresponding mathematical apparatus) for description of the spatial structure of proteins and their dynamics.

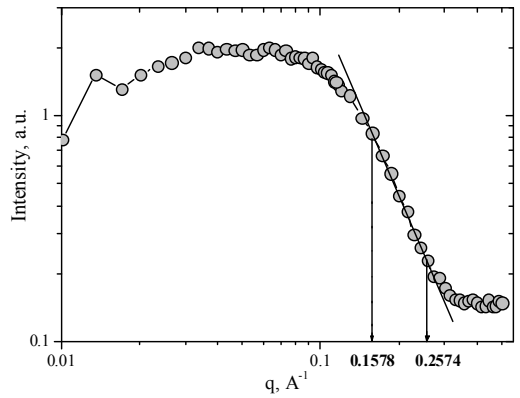

Fig. 1

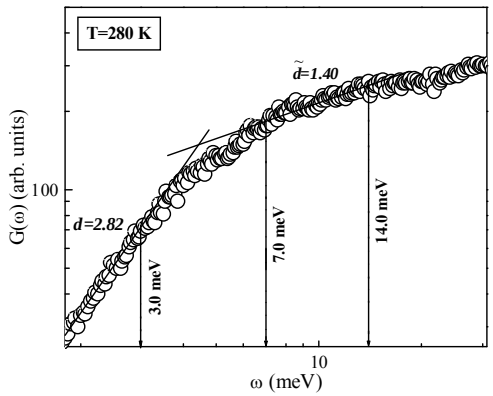

Fig. 2

Acknowledgements

The work was supported in part by Grant from RFBR 10-02-00511.

References

1. E. Feder, *Fractals Plenum*, New York, 1988, p. 283.
2. T. Nakayama and K. Yakubo, R.L. Orbach, *Rev. Mod. Phys*., 1994, **66,** 381-423.
3. D. ben-Avraham, *Phys. Rev. B*, 1993, **47,** 14559-14563.
4. S.G. Lushnikov, A.V. Svanidze, S.N. Gvasaliya, et al., *Phys.Rev. E*, 2009, **79,** 031913-9.

MATHEMATICAL MODEL OF NETWORK NAVIGATED NEURONAL CELL GROWTH

V.I. Mironov[1,2] and **V.B. Kazantsev**[1,2]

[1] Institute of Applied Physics of RAS, Nizhny Novgorod, Russia, mironov@neuro.nnov.ru
[2] University of Nizhny Novgorod, Russia

Evolutionary formation of network morphology is one of the important features of developing neuronal networks. Morphological configuration of neuronal networks (spatial configuration of neuronal processes – neurites) has a significant impact on the probability of forming synaptic contacts when the axon approaches a target dendrite. Hence, the morphological structure is one of the key determinants in the formation of signal transmission pathways in the brain systems. The process of developing neurites depends on many factors, including intracellular transport of building protein molecules (particularly, tubulin) and extracellular navigating growth cones [1].

We have proposed a mathematical model of growing network capable of configuring phenomenologically realistic geometry of neurites in development. The model takes into account the dynamical processes of elongation, branching, and spatial orientation of a neurite.

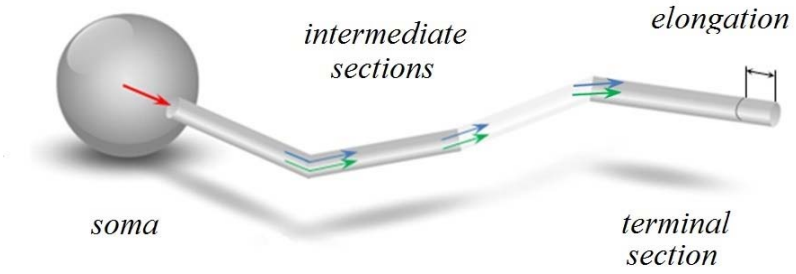

Fig. 1. Schematic view of compartmental model of neurite growth

We assume that the elongation process depends on the concentration of active substances (growth proteins) produced in the cell soma and delivered to the growth cone (neurite ending) by diffusion current and biological transport. The growing neurite is represented as a set of sequentially connected compartments as illustrated in Fig. 1. Then the concentration of active substances is calculated for each compartment as proposed in [2]. The maximal length of the whole neurite is saturated by the decay of building protein transport to the distal compartments. Hence, the neurite elongation is determined by the amount of tubulin available in the terminal section (e.g. growth cone).

Growth cone branching is described in the frame of a phenomenological stochastic model [3]. The probability of a branching event in a terminal segment (growth cone) in each moment of time is given by the following equation [3]:

$$P\left(t\middle|n(t),\gamma\right) = D\left(t\right)n\left(t\right)^{-E} C\left(\gamma,t\right). \qquad (1)$$

Here $D(t)$ is a baseline branching rate function decaying exponentially, $n\left(t\right)^{-E}$ describes the dependence of branching probability on the total number of terminal segments $n(t)$, E is the parameter accounting for the resource competition between different growth cones on neurite arborization, $C(\gamma,t)$ determines different branching probability depending on the distance to some. Branching results in the formation of two daughter branches, whose angles and diameters are defined by the parameters of the parent branch. Experimental facts describing the diameters at the branching points show a power-law relation between parent and daughter branches [4]. We used in the model the following relation:

$$d_0^2 = d_1^2 + d_2^2, \qquad (2)$$

where d_0 is the diameter of the parent branch, d_1 and d_2 are the emerging diameters of the daughter branches. Note that under the condition (2) the total cross-section area of the neurite is preserved after branching. In other words, (2) is the continuity condition when the total flux of building protein is not changing.

Spatial orientation of the neurite is realized by means of special signaling molecules (growth factors) that affect the neurite growth cone. These molecules are produced by the other network neurons and create in the extracellular space a diffusive field of growth factors. The gradient of this field is sensed by the growth cone. Integrating such signals coming from all network neurons the growth cone chooses the direction of further growths. This process is described by following equations [5]:

$$\phi_{gi} = \arg\left(\sum_{j=1}^{N} \lambda_{ji} \nabla \rho_j\right), \qquad \dot{\phi}_i = M_i \sin\left(\phi_{gi} - \phi_i\right) \tag{3}$$

where ϕ_{gi} is the preferred growth direction of the *ist* neuron, ϕ_i – current growth direction of the *ist* neuron, M_i is growth cone mobility, ρ_j is growth factors of the *jst* neuron, λ_{ji} is the intensity of the influence of growth factors of the *jst* neuron on the growth cone of the *ist* neuron.

In our simulations we assumed that the network contains three different types of cells relative to the attractiveness of the growth cones. In particular, the influence of the network neurons to the growing neurite can be attractive *(λ_{ji}=1)*, repulsive *(λ_{ji}=-1)* and neutral *(λ_{ji}=0)*. We simulated the growing neuronal network consisting of N=20 neurons located initially in random position 3D cubic area. Depending on the model parameters, the network originated from the same initial conditions shows the formation of different morphologies. Figure 2 illustrates typical shapes of the neurons created in the network navigated model for different branching probability.

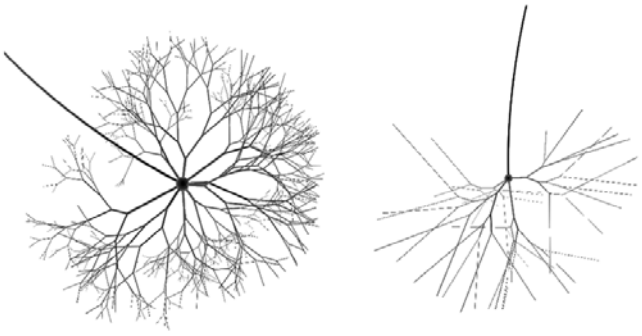

A B

Fig. 2. The shapes of the neurons grown in the network navigated model for high branching probability (A) and for low branching probability (B)

Acknowledgements

This work was supported by the Russian Federal Program (grants 16.512.11.2136, 14.740.11.0075) and by the grant of the President of the Russian Federation (MD-5096.2011.2).

References

1. E.R. Kandel, J.H. Schwartz, T.M. Jessell, *Principles of neural science*, N.Y.: McGraw-Hill, Health Professions Division, 2000, 1414 pp.
2. G. Kiddie, D. McLean, A. Ooyen, and B. Graham, *Progress in Brain Research*, 2005, **147**, 67.
3. J.V. Pelt and H.B.M. Uylings, *Brain and Mind*, 2003, **4**, 51.
4. J.V. Pelt and H.B.M. Uylings, *Natural variability in the geometry of dendritic branching pattern*, 2005, **4**, 85-115.
5. J.K. Krottje, A. Ooyen, *Bulletin of Mathematical Biology*, 2007, **69**, 3.

Invited

MONITORING OF FUNCTION NETWORK ACTIVITY *IN VITRO*

I.V. Mukhina[1,3], **A.S. Pimashkin**[1,2], **E.A. Koriagina**[1,2,3], **E.V. Mitroshina, Ya.I. Kalintseva, Yu.N. Zakharov,** and **V.B. Kazantsev**[1,2]

[1] Department of Neurodynamics and Neurobiology, Lobachevsky State University of Nizhny Novgorod, Russia
[2] Laboratory of Nonlinear Processes in Living Systems, Institute of Applied physics RAS Nizhny Novgorod, Russia
[3] Normal Physiology Department, Nizhny Novgorod State Medical Academy, Russia
mukhinaiv@mail.ru

Signaling in neuronal networks plays a crucial role in regulating processes of proper network formation during development and learning in the mature nervous system. Mechanisms of resulting network signals, e.g. spatio-temporal activity patterns, associated on the one hand with molecular signaling and with systemic function on the other hand still remain generally unknown. Dense cultured neuronal networks today is one of the perspective experimental models to investigate cellular mechanisms of signal propagation and information processing at the network level. It has been found that such networks generate synchronized bursting events (of 0.5–2 s duration) with high frequency spiking elicited by a large number of cells involved in the network. Bursting activity in cultures was broadly investigated in connection with many different problems, including disease treatment [1], learning in neural networks [2, 3], signal processing at network level [4], and many others.

Developing cultured networks show highly variable characteristics of bursting dynamics. At the same time, it has been noted that the burst consists of quite well-organized spatio-temporal spiking sequences. Generation of spontaneous burst discharges can be also treated as a kind of self-organized criticality (e.g. neuronal avalanches) [5]. When the burst develops spikes from different neurons form an avalanche, leading to a high frequency sequential population discharge. Such avalanches also reflect the presence of a certain synaptic organization in the cultured networks at a certain stage of development. When sufficient synaptic recourses are available, spontaneous spikes may activate signal transmission pathways generating a definite direction of the avalanche development which decays due to the synaptic depression at the end of the burst. Then, theoretically both processes of burst initiation and decay should go along the same synaptic connectivity cluster and, hence, should demonstrate a certain level of similarity in their spiking times during the whole burst. The statistical properties of the spiking patterns are reproduced from burst to burst indicating the presence of well-defined organization in the underlying synaptic signalling pathways.

Adaptation of neuronal networks to the cultured conditioning in the absence of external drive stimulates appearance of self-sustained spiking patterns without any specific stimuli. Some alteration, like electrical stimulation, medium changing, metabolic activation or depression of mature culture evoke novel properties of spiking pattern. These properties are reversible usually and may be considered as a new function system occurring as a consequence of strong stimulations. Irreversible alterations indicate network homeostatic plasticity.

To identify function neuronal networks in vitro we investigated spontaneous electrical activity and intracellular calcium transients in mouse hippocampal networks cultured on MEA for a month after plating. Some experiments were compared with the network activity in acute hippocampal slices.

A spike correlation graph method, activation pattern, and analysis of the burst intrinsic structure using similarity measures between the spiking patterns as the vector of spiking times relative to some reference time line were used for determination of spike timing profiles of population bursts obtained by MEA recording (Fig. 1).

The existence of stable hub distributions and spatio-temporal profiles of spike distribution in the bursts for crucial period of network development and their stimulus-dependent alteration were established. The external stimulation like short-term glucose deprivation, glutamate treatment, extracellular matrix disintegration, repetitive electrical stimulation caused the new stable patterns of activity which are statistically distinguishable from the spontaneous activity. This indicates that the stress external stimulation switches the dynamics of activity to the new steady state only.

Simultaneously with electrical recoding to measure the level of network organization we examined the degree of functional connectivity between $[Ca^{2+}]_i$ events in different cells of hippocampal cultures and acute slices (Fig. 2).

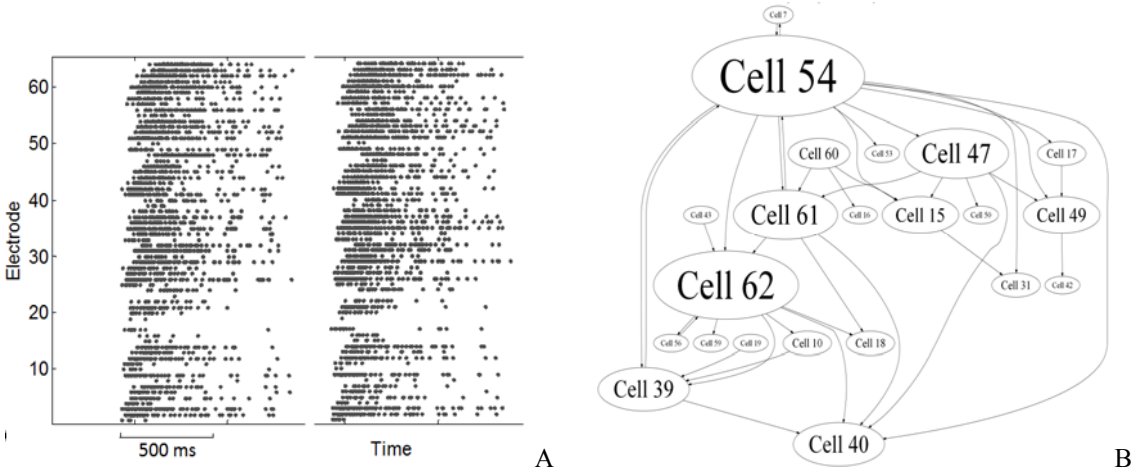

Fig. 1. A – raster plot of the bursts, with similar activation patterns;
B – spike correlation graphs of hippocampal culture spontaneous activity (45th day *in vitro*)

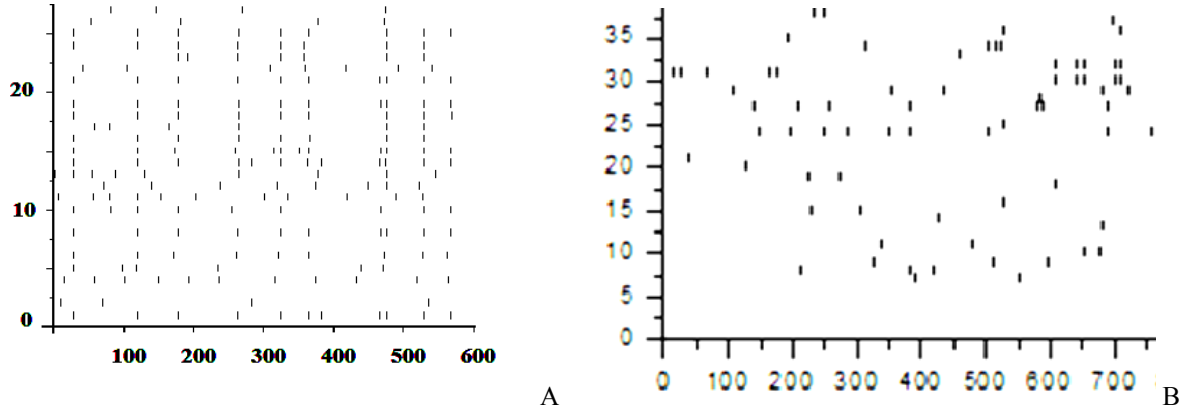

Fig. 2. Raster plot of the spontaneous Ca^{2+} oscillations in:
A – hippocampal culture (11th day *in vitro*); B – acute hippocampal slice (P14)

We discuss how such properties of the spike and $[Ca^{2+}]_i$ events can be associated with self-organized criticality and synaptic plasticity in the cultured networks *in vitro*.

Acknowledgements

The research is supported by the Russian Department of Education and Science 2.1.1./6223.

References

1. D. Wagenaar, R. Madhavan, J. Pine, S. Potter, "Controlling bursting in cortical cultures with closed-loop multi-electrode stimulation", *J. Neurosci*., 2005, **25**(3), 680-688.
2. G. Shahaf, S. Marom, "Learning in networks of cortical neurons", *J. Neurosci*., 2001, Nov. 15, **21**(22), 8782-8.
3. S. Marom, G. Shahaf, "Development, learning and memory in large random networks of cortical neurons: lessons beyond anatomy", *Q. Rev. Biophys*., 2002, **35**, 63-87.
4. M. Chiappalone, P. Massobrio, S. Martinoia, "Network plasticity in cortical assemblies", *Eur. J. Neurosci.*, 2008, **28**(1), 221-37.
5. J.M. Beggs, D. Plenz, "Neuronal avalanches are diverse and precise activity patterns that are stable for many hours in cortical slice cultures", *J. Neurosci*., 2004, **24**(22), 5216-5229.

ROLE OF CALCIUM IONS IN GENERATION OF ELECTRICAL SIGNALS IN PLANTS INDUCED BY DAMAGING IRRITATION

L.A. Orlova[1], V.A. Vodeneev[1], E.A. Sergeeva[2] , and **A.L. Gribkov[1,2]**

[1] N.I. Lobachevsky State University of Nizhny Novgorod
603950 Gagarin St., 23, Nizhny Novgorod, Russia; *kbf@unn.ru*
[2] Institute of Applied Physics RAS,
603950 Ulyanov St., 46, Nizhny Novgorod, Russia

Calcium ions play an important role in the majority of processes taking place in higher plant cells. It is known that calcium ions take part in transduction of many signals acting as secondary messengers [1]. However, a calcium signaling system of higher plants still needs to be studied better. One of the main questions connected with calcium signaling in plants is its involvement in the process of generation of electrical impulses, is a primary reaction reaction to external irritation. It is known that these reactions or excitation potentials in higher plants are represented by two types of electric impulses: action potential (AP) which has a lot in common with APs in animals – a response to external non-damaging irritation, and variable potential (VP) – a unique plant electrical response to damaging irritation. Unlike AP, the mechanisms of generation and propagation of VP are not well studied [2, 3]. VP generation is considered to be connected with transient inhibition of plasmatic membrane H^+-ATPase activity [4]. However, judging from the form of electric reaction and appearance of several spikes in some cases in repolarization phase of VP, the mechanism of its generation is more complicated.

The goal of our work is to investigate whether a calcium signaling system also takes part in the process of VP generation in higher plants.

Materials and methods

The objects of study were 3–4-week seedlings of pumpkin (Cucurbita *pepo* L.) Changes of calcium concentration were registered by calcium-dependent fluorescent probe Fluo-4/AM. Loading of the probe into the plant was performed by the low-temperature technique for loading AM-esters [5]. The seedling was placed into the probe solution for 12-14 hours at 4°C for loading Fluo-4/AM into cells and then for 2 hours into the IPW solution (containing 10^{-3}M KCl, $5*10^{-4}$M $CaCl_2$, and $5*10^{-4}$ M NaCl) at 20-25°C for hydrolysis of AM-compound.

The seedling was placed on a microscope table; a fragment of stem with removed strips of epidermis was fixed on the object glass. The uninjured stem site faced the object glass and its fluorescence intensity was recorded. The seedling roots were immersed into the Petri dish with the IPW solution. Fluorescence of the whole plant was observed and recorded by the laser scanning microscopy system Carl Zeiss LSM 510 equipped with spectral module META 23. Excitation of fluorescence was performed by argon laser at the wavelength of 488 nm; fluorescence of Fluo-4 was detected in the 500-550 nm spectral range.

VPs were generated by open fire exposure on a cotyledon leaf. Electric activity was registered extracellularly and intracellularly. The extracellular measurements were made by chlorine-silver (Ag/AgCl) macroelectrodes (EVL-1M3). An IPL-112 universal ionomer served as an amplifier. The measuring electrode was located in the zone of recording of fluorescence; the comparison electrode was in contact with the root-washing solution. The exracellularly measured potential difference represented integral changes of the cell membrane potential in the recording zone. For intracellular measuring microelectrode technique was used. Micropipettes were filled with 0.1 KCl. Registration was made by means of the microscope Olympus BX51 with automatic micromanipulators (amplifier Axon Inst. Multiclamp 700 B).

Results and discussion

It has been shown that loading of probe Fluo-4 into plant cells which results in sufficient intracellular concentration requires incubation for 12–14 hours at 4°C. Such an accumulation period is sufficient for esterase reactivation and for AM hydrolysis (fig. 1). Increase of Fluo-4 fluorescence intensity has been registered after VP produced by open fire (fig. 2). Based on these results we conjectured that the depolarization phase of VP is connected with intracellular free calcium concentration increase when calcium ions enter a cell.

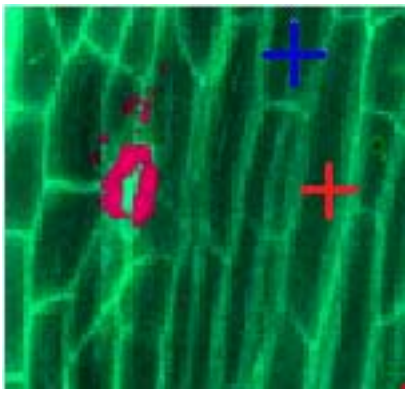

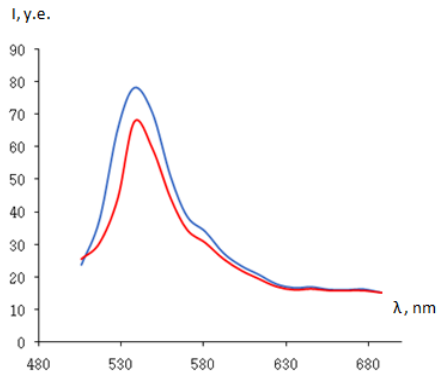

Fig. 1. Localization of Fluo-4 in cells (left) and its spectrum of fluorescence excited at 488 nm (right). Markers show points at which fluorescence spectra have been registered

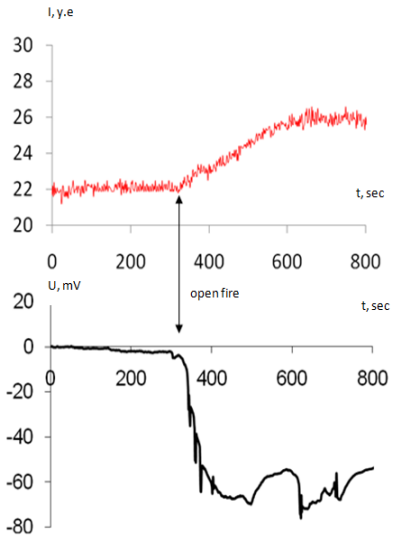

Fig. 2. Change of fluorescence intensity of Fluo-4 loaded into plant stem at generation of VP

To verify the results of fluorescent analysis stimulation of VP, generation was performed in a medium without calcium. Chelator of calcium ions EGTA (0.1 mM) was added to washing stem solution. VP was registered 1 hour after EGTA addition. Statistically approved data showed that the absence of calcium ions in extracellular space VP amplitude is much lower than VP control amplitude and velocity of VP depolarization phase is decreased.

Results of this work show that generation of VP of higher plant is provided by increasing intracellular calcium concentration; moreover, parameters of VP dramatically change when calcium ions are removed from extracellular space. We can consider that VP as a primary reaction to external damaging irritation is a complex response, which includes several signaling systems in its generation.

Acknowledgements

The work is partially supported by the Russian Foundation for Basic Research (project 09-04-97085) and by the Federal Agency of Science and Innovations (GK № 02.740.11.0086).

References

1. A.S.N. Reddy, *Plant Science. Review*, 2001, **160**, 381-404.
2. J. Fromm, S. Lautner, *Plant Cell Environ*., 2007, **30**, 249-257.
3. F. Baluska, S. Mancuso., *Cogn Process.*, 2009, **10**(1), 3-7.
4. M.R. Zimmermann, H.H. Felle, *Planta*., 2009, **229**, 539-547.
5. W.H. Zhang, Z. Rengel, J. Kuo, *The Plant Journal.*, 1998, **15**(1), 147-151.

Invited

REGULATION OF ANXIETY BY EXTRACELLULAR PROTEOLYSIS IN THE AMYGDALA

R. Pawlak

University of Leicester, Leicester, UK, rp135@le.ac.uk

Fear is a highly conserved emotion which evolved to help organisms recognize, memorize and predict danger, thereby promoting their long-term survival. While fear is generally evolutionarily beneficial, prolonged or severe stress can trigger maladaptive forms of neuronal remodeling leading to generalization of fear and high anxiety. Anxiety disorders, in their whole diversity, affect about 25% of adults at least once in their lives. Such a high prevalence of anxiety disorders, combined with high co-morbidity with depression, generates an enormous personal, social and economic burden across the world. The most dramatic form of anxiety, the posttraumatic stress disorder (PTSD), is characterized by cognitive impairment, depression, fear, anxiety, and may eventually lead to suicide.

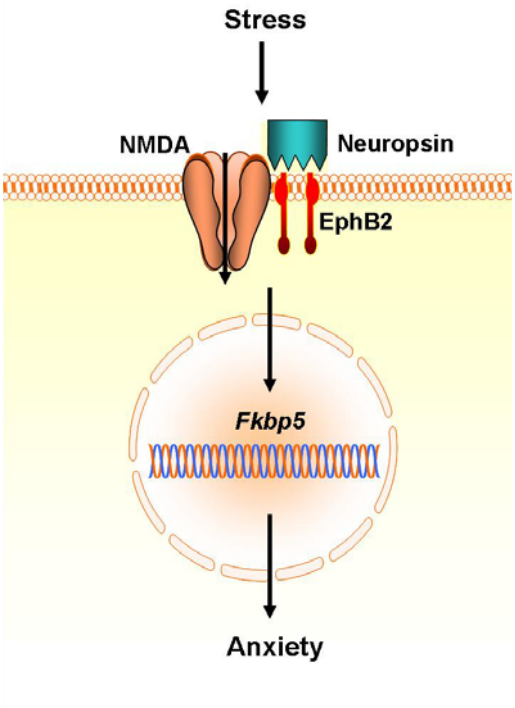

Fig. 1. The mechanism of facilitation of stress-induced anxiety by neuropsin. Our studies favor a model where, after stress, Neuropsin cleaves the extracellular portion of EphB2 and facilitates the dynamic interaction of EphB2 with the NR1 subunit of the NMDA receptor. The resulting enhancement of the NMDA current causes an upregulation of *Fkbp5* and promotes the development of anxiety

Traumatic events are memorized due to neuronal plasticity, the capacity for synaptic connections in the amygdala to undergo experience-dependent functional or morphological changes. While mechanisms utilized to mediate stress-induced plasticity are quite diverse, extracellular proteases are uniquely poised to remodel the neuron-extracellular matrix interface and may facilitate fear and anxiety [1-4]. One important group of molecules that are subject to modulation by extracellular proteases are Eph-receptor tyrosine kinases. In mammals the Eph protein family consists of fourteen members divided into two classes, A and B, determined by their sequence conservation and binding affinity. The Eph proteins are enriched in highly plastic areas of the brain that are such as the amygdala and the hippocampus where they promote neuronal plasticity [5-7].

Neuropsin (KLK8) is a kallikrein-like serine protease uniquely positioned to facilitate stress-induced plasticity due to its unusual forebrain-specificity and high levels of expression in the amygdala and hippocampus [8]. In order to better understand the effect of neuropsin in the amygdala we used a multidisciplinary approach at the molecular and systems level to examine its role in stress-induced neuronal plasticity and behavioral changes.

We found that neuropsin is critical for stress-related plasticity in the amygdala by regulating the dynamics of EphB2/NMDA receptor interaction, the expression of *Fkbp5* and anxiety-like behaviour [9]. Stress results in neuropsin-dependent cleavage of EphB2 in the amygdala causing dissociation of EphB2 from the NR1-subunit of NMDA receptor and promoting membrane turnover of EphB2 receptors. Dynamic EphB2/NR1 interaction enhances NMDA receptor current and E-LTP, induces the *Fkbp5* gene expression and enhances behavioral signatures of anxiety. Upon stress, neuropsin-deficient mice do not show EphB2 cleavage and its dissociation from NR1 resulting in a static EphB2/NR1 interaction, attenuated induction of the *Fkbp5* gene and low anxiety. The behavioral response to stress can be restored by intra-amygdala injection of neuropsin into neuropsin-deficient mice and disrupted by the injection of either anti-EphB2 antibodies or silencing the *Fkbp5* gene in the amygdala of wild-type animals. Our findings established a novel neuronal pathway linking stress-

induced proteolysis of EphB2 in the amygdala to anxiety. This novel pathway, highlighting the ability of Eph and NMDA receptors to respond to activity dependent signals from the extracellular milieu, opens new possibilities for treatment of stress-associated disorders, including various forms of anxiety disorders.

Methods

Restraint stress was performed by placing the mice in wire mesh restrainers while control animals were left undisturbed. Anxiety was measured using the elevated-plus maze by counting the number of entries to closed or open arms during 5 min. *Fkbp5* gene was silenced by intraamygdala injection of lentiviral shRNA construct followed by behavioral assessment two weeks later. LTP was recorded from the lateral-basal pathway and whole-cell recordings made from basal amygdala neurons. Data were analyzed by Student t-test or ANOVA followed by Tukey's post-test. P values of less than 0.05 were considered significant.

Acknowledgements

Research in my laboratory is supported by Medical Research Council, Marie Curie Excellence Grant from European Commission and by Medisearch.

References

1. N. Gogolla, P. Caroni, A. Luthi, & C. Herry, "Perineuronal nets protect fear memories from erasure", *Science*, 2009, **325**, 1258-61.
2. T. Matys, et al., "Tissue plasminogen activator promotes the effects of corticotropin-releasing factor on the amygdala and anxiety-like behavior", *Proc. Natl. Acad. Sci. U S A*, 2004, **101**, 16345-50.
3. R. Pawlak, A.M. Magarinos, J. Melchor, B. McEwen, & S. Strickland, "Tissue plasminogen activator in the amygdala is critical for stress-induced anxiety-like behavior", *Nat. Neurosci*., 2003, **6**, 168-74.
4. R. Pawlak, et al., "Tissue plasminogen activator and plasminogen mediate stress-induced decline of neuronal and cognitive functions in the mouse hippocampus", *Proc. Natl. Acad. Sci. U S A*, 2005, **102**, 18201-6.
5. M.B. Dalva, et al., "EphB receptors interact with NMDA receptors and regulate excitatory synapse formation", Cell, 2000, **103**, 945-56.
6. I.C. Grunwald, et al., "Kinase-independent requirement of EphB2 receptors in hippocampal synaptic plasticity", *Neuron*, 2001, **32**, 1027-40.
7. R. Klein, "Bidirectional modulation of synaptic functions by Eph/ephrin signaling", *Nat. Neurosci*., 2009, **12**, 15-20.
8. Z.L. Chen, et al., "Expression and activity-dependent changes of a novel limbic-serine protease gene in the hippocampus", *J. Neurosci*., 1995, **15**, 5088-97.
9. B.K. Attwood, et al., "Neuropsin cleaves EphB2 in the amygdala to control anxiety", *Nature*, 2011, **473**, 372-5.

Invited

HETERODIMERIZATION OF SEROTONIN 5-HT_{1A} AND 5-HT_7 RECEPTORS AND REGULATION OF RECEPTOR TRAFFICKING AND SIGNALLING

E. Ponimaskin, U. Renner, A. Zeug, F. Kobe, M. Niebert, E. Wischmeyer, E. Neher, and **D.W. Richter**

Cellular Neurophysiology, Medical School Hannover, Germany
Ponimaskin.Evgeni@mh-hannover.de

An increasing number of G protein-coupled receptors (GPCRs) have been shown to form oligomers. Presently, the existence of GPCR homo- and heterodimers has become generally accepted, and a growing body of evidence indicates a functional importance of oligomeric complexes for the receptor trafficking, receptor activation as well as G-protein coupling in native tissues. Also the clinical significance of GPCR oligomerization became more evident during the last years leading to identification of receptor oligomers as a novel important therapeutic target.

Serotonin receptors 5-HT_{1A} and 5-HT_7 are highly co-expressed in brain regions implicated in depression, anxiety and stress. However, their functional interaction has not been established. In this study, using biochemical and microscopic approaches we show that 5-HT_{1A} and 5-HT_7 receptors form heterodimers both *in vitro* as well as *in vivo*. The resonance energy transfer-based assays further verified specific 5-HT_{1A}-5-HT_7 interaction and also revealed that, in addition to 5-HT_{1A}-5-HT_7 heterodimers, two types of homodimers composed either by 5-HT_{1A} or 5-HT_7 receptors co-exist in cells expressing both types of receptor. Noteworthy, the affinity to form defined dimers is different with the highest value obtained for 5-HT_7-5-HT_7 homodimers, followed by the 5-HT_7-5-HT_{1A} heterodimers and 5-HT_{1A}-5-HT_{1A} homodimers. Functionally, heterodimerization decreases the 5-HT_{1A} receptor-mediated activation of G_i-protein without affecting 5-HT_7 receptor-mediated G_s-protein activation. Moreover, heterodimerization markedly decreases the ability of 5-HT_{1A} receptor to activate G-protein gated inwardly rectifying potassium channel in a heterologous system. The inhibitory effect on potassium current was preserved in hippocampal neurons, demonstrating a physiological relevance of heteromerization *in vivo*. In addition, heterodimerization markedly enhances the internalization of the 5-HT_{1A} receptor as well as its ability to mediate ERK activation. Finally, we found that production of 5-HT_7 receptor continuously decreases during postnatal development, suggesting that the relative concentration of 5-HT_{1A}-5-HT_7 heterodimers and, consequently, their functional importance undergoes pronounced developmental changes.

Invited

PROPERTIES OF THE CALCIUM TRANSIENT IN THE NERVE ENDINGS OF PERIPHERAL SYNAPSES

D.V. Samigullin[1], **N.F. Fatikhov**[1], **E.F.Khaziev**[1], **E.A. Bukharaeva**[1,2], and **E.E. Nikolsky**[1,2]

[1] Kazan Institute of Biochemistry and Biophysics of Kazan Science Centre of RAS, Kazan, Russia
samid75@mail.ru
[2] Kazan State Medical University, Kazan, Russia

In the vertebrate neuromuscular junction, calcium ions play the primary role in promoting the stimulus-induced secretion of acetylcholine from nerve terminals [1]. Calcium influx into the axoplasm through the voltage dependent calcium channels during each action potential triggers an intracellular machine of exocytose of synaptic vesicles and plays a key role in the modulation of the secretory process [2]. Therefore the investigations of the calcium entry into nerve endings are essential for understanding the process of the mediator secretion. Until recently, direct measurements of the calcium current were made only in some objects, such as squid axon [3]. Lately, for large synapses in the central nervous system and lobster neuromuscular junction a method of assessing fast calcium transient with fluorescent dyes was described [4]. In this connection the question arises on realization of this technique and possibility of its application to small neuromuscular junctions for estimation of calcium transient and comparison of its changes with data obtained at simultaneous electrophysiological registration of synapse activity. There is evidence that calcium transients, obtained in preparations loaded with dyes of different affinity to calcium have different dynamic characteristics [5]. In this regard, the task of this study was the selection of optimal calcium dye for neuromuscular preparation and analysis of the calcium transient during rhythmic activity of the synapse.

The method of registration of the fast changes of calcium ions concentration was based on the application of a fluorescent marker with high affinity to calcium – Oregon Green 488 BAPTA-1 hexapotassium salt or low affinity to calcium Magnesium Green pentapotassium salt. Marker (50 mmol/l) was loaded into the terminal of the cutaneous pectoris preparation of a frog from the cut end of the nerve bundle [6].

Measurements of changes in the fluorescence of calcium dye (calcium transient) in response to single nerve impulse were carried out using a highly sensitive and high-speed photodiode recording system. The photodiode(S1087, Hamamatsu Photonics, Japan) was used to record fluorescence transients on an upright microscope (Olympus BX51WI) with an ×40 water immersion lens (0.80 NA, Olympus, Japan) and a filter set consisting of a 505 dcxt dichroic mirror and an E5201p emission filter (Chroma Technology Corp., USA) were used to detect fluorescent signals. A viewfinder optical system (Till Photonics, Germany) was used to select the region of interest. A Polyhrom V monochromator (Till Photonics, Germany) set at 488 nm excitation amplitude was used.

For images acquisition during rhythmical activity we used confocal microscope Leica TCS SP5 (Leica, Germany). Observations were performed using a 20x water immersion lens (1,0 NA, Leica, Germany). Excitation of calcium fluorochrome was performed by argon laser at 488 nm.

Nerve action potentials and extracellular endplate currents were recorded using standard electrophysiological techniques.

In response to single nerve stimulation calcium transient was registered from nerve terminals loaded with high affinity or low affinity dyes. In low affinity dye loaded terminal calcium transient had faster rise time and faster time of decay.

Also we recorded simultaneously calcium transient and extracellular currents from the same nerve terminal in both low and high affinity loaded terminals. In both cases calcium transient reached its maximum later than postsynaptic response.

For explanation of this effects computer simulation was used. Computer model describes the interaction of calcium with low or high affinity dye and intracellular calcium buffer systems. Also simulation accounts for the diffusion time and the geometric dimensions of the presynaptic terminals.

Computer simulations showed that the observed differences in the time course of calcium transients in preparation loaded with different dyes explained the different diffusion time of calcium and different dye properties.

The results of computer simulations have shown that during high-frequency nerve stimulation calcium transient obtained in the presence of low affinity dye reproduces the dynamics of presynaptic calcium more accurately. This was confirmed by experimental results. In high affinity dye loaded terminal during 50 hz stimulation each next signal in train had smaller amplitude. This indicates that under this condition calcium dye is saturated. But in low affinity dye loaded preparation each next calcium transient in train had approximately the same amplitude. So low affinities dye does not reach saturation during high frequency stimulation and more accurately reproduces calcium dynamics.

Chemical synapses, including neuromuscular junction, in vivo operate in a mode of rhythmic activity in a wide range of frequencies [7]. During stimulation of motor nerve at the frog neuromuscular junction within one minute, with frequencies ranging from 20 to 70 Hz registration of changes in the calcium transient was performed. With increasing frequency stimulation the character of the calcium signal significantly changed. Smooth growth of the basal concentration of calcium at 20 Hz was replaced by two-phase increasing of the calcium signal at 50 Hz and a subsequent sharp growth at the 70 Hz frequency. No monotonous character of the change of the calcium signal with increasing frequency stimulation suggests additional source of calcium, which may be the intracellular calcium stores. Adding to the solution ryanodine at a concentration of 10 μM, at which it blocks the ryanodine receptors, eliminated the second phase of increase of calcium signal, where a first phase remained the same.

It can be concluded that for correct estimation of the calcium transient in the peripheral synapses in response to single action potential, as well as to rhythmic stimulation the calcium dye with low affinity is preferable. The data obtained allow us to conclude that during prolonged high frequency stimulation the endoplasmic reticulum is involved in the regulation of presynaptic calcium levels via ryanodine receptors.

Acknowledgements

Supported by grants of RFBR (10-04-00765, 11-04-00602) and "Leading scientific schools" grant (64631.2010.7).

References

1. B. Katz and R. Miledi, *J. Physiol*., April 1967, **189**(3), 535-544.
2. S.J. Smith, G.J Augustine, *Trends Neurosci*., 1988, **11**, 458-464.
3. G.J. Augustine and R. Eckert, *J. Physiol*., January 1984, **346**, 257-271.
4. W.G. Regehr and D.W. Tank, *The Journal of Neuroscience*, November 1992, **12**(11), 4202-422.
5. A. Vyshedskiy, J.W. Lin, *J. Neurophysiol.*, Jan. 2000, **83**(1), 552-62.
6. Y.-Y. Peng, R.S. Zucker, *Neuron.*, 1993, **10**, 465-473.
7. R. Hennig, T. Lømo, *Natur.,* 14-20 Mar. 1985, **314**(6007), 164-6.

ADULT THORACIC NEUROMUSCULAR JUNCTION OF DROSOPHILA: ARE PCREB AND PCOFILIN GLIAL OR NEURAL?

A.N. Kaminskaya[1,2], T.L. Payalina[1], A.V. Medvedeva[1], E.A. Nikitina[1], and **E.V. Savvateeva-Popova[1]**

[1] Pavlov Institute of Physiology RAS, St. Petersburg, Russia, esavvateeva@mail.ru
[2] Sechenov Institute of Evolutionary Physiology and Biochemistry RAS, St. Petersburg, Russia

One of the crucial regulators of actin remodeling is LIM kinase 1 (LIMK1), a target of Rho GTPases via PAK1, PAK2, PAK4, and MRCKα (myotonic dystrophy kinase)-related Cdc42-binding protein kinase. LIMK1 phosphorylates cofilin at Ser3 inhibiting its binding to G-actin (monomeric actin) and F-actin and thereby affects actin filament dynamics leading to axon reorganization. LIMK1 also phosphorylates transcriptional factor CREB which initiates gene expression during memory formation. Interestingly, the integration of current understanding of cofilin regulation and cellular function leads to the conclusion that cofilin is a functional node in cell biology [1]. Many of the factors that regulate cofilin activity are themselves modulated by cofilin and phospho-cofilin. Thus cofilin is emerging as an agent of cellular homeostasis. Quite recently it has turned out that cofilin has a number of functions surprisingly unrelated to actin-assembly regulation.

The crucial cellular roles of cofilin are:

1) chaperoning actin to the nucleus, thereby affecting gene expression;

2) translocation to mitochondria necessary for the opening of the mitochondrial permeability transition pore and subsequent release of cytochrome **c**, an early step in apoptosis,

3) direct activation of phospholipase D1 (PLD1, an enzyme essential for chemotaxis) required for cell migration toward growth factors during neuronal development;

4) mediation of oxidative stress;

5) the ability to act as a cellular pH sensor;

6) breaking the symmetry of neurons during axon specification;

7) bridging cytoskeleton and extracellular matrix [1–3].

The finding that cofilin is connected to extracellular matrix is quite new and up to now predominantly focuses on Reelin [3].The extracellular matrix molecule Reelin, a large glycoprotein secreted by Cajal-Retzius cells during early cortical development, is required to control proper migration and positioning of cortical neurons and cofilin is presumed to be an effector molecule of the Reelin signalling cascade. Taken together, these facts strongly confirm the statement "What could be more efficient than having a single component in the cell with such a diversity of functions? It secures the certainty of the two activities needed being coincidentally present since they both reside in one molecule!" [1]. This might explain, why presently the neurodegenerative diseases, such as Alzheimer's, Parkinson 'sand Huntington's diseases are named "cofilinopathies".

Experimental evidence indicate that when neurons in culture are transiently stressed by inhibition of ATP synthesis, they rapidly form within their neurites rodlike actin inclusions that disappear when the insult is removed. Oxidative stress, excitotoxic insults, and amyloid beta-peptide oligomers also induce rods. Immunostaining of neurites indicates that these rods also contain the majority of the actin filament dynamizing proteins and cofilin. If the rods reappear within 24 h after the stress is removed, the neurite degenerates distal to the rod but with no increase in neuronal death [4]. Luckily, many of the aforementioned functions could be analyzed with a help of *Drosophila* mutants. For instance, the *Drosophila agnostic* locus, as we have shown previously contains the CG1848 gene for LIMK1.

Temperature-sensitive mutation agn^{ts3} leads to:

1) significant alterations in gene structure of LIMK1 as witnessed by our sequencing data;

2) increased expression of actin cascade components – LIMK1 and cofilin;

3) severe defects in short-term and long-term memory (mainly due to defects in orientation and courtship song) assessed in the conditioned courtship suppression paradigm;

4) increased formation of Congo Red-positive amyloid-like inclusions which line the cytoskeleton.

Interestingly, the inclusions disappear and the memory formation is improved 1 hr after heat shock. Using our setup for automatic registration of courtship song parameters, we evaluated learning ability by calculating learning indices (LIs) as in the conditioned courtship suppression paradigm but based

only on singing index (courtship song or wing vibration produced by a male during courtship). *agn*^{ts3} demonstrated negative learning indices. To estimate a possible involvement of the *agn*^{ts3} mutation in memory formation after 5-hr massive training we analyzed distribution pCREB at adult thoracic NMJs at basalar and subalar muscles fields responsible for courtship song production. Using confocal microscopy, we found different distribution of pCREB in Canton-S and *agn*^{ts3}. First, both in Canton-S and *agn*$^{ts\ 3}$pCREB was detected in thin nerve terminals but not at the synaptic boutons before learning, after learning pCREB level increased and bridges between axons were formed. Contrary, in *agn*^{ts3} pCREB was detected in nuclei of nervous and muscular cells before and after learning. Surprisingly, pCofilin was predominantly expressed in glial sheaves. Moreover, pCofilin and pCREB are localized in thin axonal terminals, forming junctions with the wing muscle. The central space of axon was free of both pCofilin and HRP that can be seen as an empty channel within the axonal terminal. The data are discussed in the light of new findings concerning the role of cofilin as a functional node in cell biology.

Acknowledgements

This research was supported by RFBR Grant 09-04-01208, RAS Program "Biodiversity and Genofonds, Contract with Ministry of Science and Education P-316.

References

1. B.W. Bernstein and J.R. Bamburg, *Trends Cell Biol*, 2010, **20**(4), 187-195.
2. S. Tahirovic and F. Bradke, *Cold Spring Harb perspect Biol*, 2009, **1**(3), a001644.
3. E. Förster, H.H. Bock, J. Herz, X. Chai, M. Frotscher and S. Zhao, *Eur J Neurosci*, 2010, **31**(9), 1511-1518.
4. B.W. Bernstein, H. Chen, J.F.Doyle, J.R. Bamburg, *Am J Physiol Cell Physiol*, 2006, **291**(5), C829-839.

Invited

PATTERNS OF THETA SYNCHRONIZATION IN AMYGDALA-HIPPOCAMPAL-PREFRONTAL CORTICAL NETWORK DURING FEAR MEMORY CONSOLIDATION AND EXTINCTION

T. Seidenbecher

Institute of Physiology I, Westfälische Wilhelms-University Münster, D-48149 Münster, Germany?
seidenbe@uni-muenster.de

Synchronized rhythmic network activities are considered to be key elements of brain function and have been associated with sensory information processing, mnemonic functions, and expression of distinct behavioral states. Through their coordinated effects on brain activity patterns they appear to be particularly well-suited to support the formation and selective activation of distributed cell populations and neuronal circuits in the brain, a process fundamental to information processing and memory formation.

Key structures of the mammalian brain determining fear memory and extinction include the amygdala (LA), the CA1 subfield of the hippocampus (CA1) and the medial prefrontal cortex (mPFC). The regulation of fear and anxiety behaviour relies on a multi-modular neural network, which can be experimentally assessed through Pavlovian fear conditioning and extinction paradigms.

Rhythmic oscillatory activities comprise a principal mechanism of network communication in the brain; specifically, rhythms in the theta frequency range (2–12 Hz) have been shown to be of particular relevance to different states of information processing, induction of synaptic plasticity and behavioral memory. Furthermore, recordings of human EEG have provided indirect support for the role of theta oscillation in memory functions. It is widely accepted that theta oscillations provide spatiotemporal codes, which support the temporal compression from the rather long time scale of behavior into the milliseconds timescale required for synaptic plasticity. Theta oscillations are observed during electrophysiological recordings at levels of individual neurons and in large neural networks. Furthermore, in the amygdala, a subpopulation of parvalbumin-positive GABAergic interneurons seems to be capable of synchronizing principal neurons in the theta frequency range.

Multi-site local field potential (LFP) and single unit recordings, related to conditioned fear responses, were obtained from the LA, CA1 and the mPFC in freely behaving mice after Pavlovian fear conditioning. Presentation of the conditioned stimulus, in the absence of the aversive unconditioned stimulus, elicited an increase in theta frequency (4-8 Hz) correlations between all pairs of recording sites during early retrieval, declined during extinction learning and rebounded during extinction recall. Rhythmically synchronized activity at theta frequencies increased between the LA and the CA1 subfield of the hippocampus during consolidation and reconsolidation of conditioned fear, and returns to baseline at remote stages of fear memory. During extinction recall, theta synchrony rebounded in LA-mPFC and CA1-mPFC, and remained at a low level in the CA1-LA circuit. Simultaneous recordings of LFPs and unit activity revealed theta phase-related unit activity, occurring in all three brain regions.

According to Lachaux et al. (Human Brain Mapp. 8, 1999), using a straightforward method to estimate the synchrony and lag (directionality) of signals in different brain areas, these data revealed that, directed theta oscillations may play a central role in spatiotemporal coordination of populations of cells in LA, CA1 and mPFC, possibly via tight amplitude correlations during consolidation. Here, theta amplitude coupling prevailed in a regionally and directionally specific manner during retrieval of learned fear and recall of extinction, while low directional oscillatory interactions persisted throughout the extinction learning phase. As proof of principle, experimental manipulation through electrical micro-stimulation (LA-CA1 'in-phase' and 'anti-phase' theta burst stimulation) was performed during extinction learning. Animals stimulated 'in-phase' showed a delay in extinction learning and poor extinction recall whereas animals that were stimulated anti-phasic did not show any impaired extinction learning and recall of extinction. Additionally, in animal models of disturbed anxiety behavioral expressions, enhanced theta synchrony has been shown in conjunction with increased anxiety and impaired fear extinction and recall.

In summary, these results support the hypothesis that theta synchrony in the amygdala-hippocampal-prefrontal cortex network provides a means for inter-areal coordination in conditioned behavioral responsiveness. More specifically, theta oscillations seem to contribute to a population code indicating conditioned stimuli during recall of fear memory and extinction.

Acknowledgements. These studies were sponsored with funding from the Deutsche Forschungsgemeinschaft (SFB-TRR58, A01, A02).

Invited

SUBCELLULAR MECHANISMS OF CA^{2+} ACTIVITY IN ASTROCYTES

X. Tang[1], Y.-W. Wu[1], I. Patrushev[1], S. Asatryan[2], M. Arizono[1], H. Bannai[1], K. Mikoshiba[1], V. Kazantsev[2], and **A. Semyanov[1]**

[1] RIKEN Brain Science Institute, Wako-shi, Saitama, Japan, semyanov@brain.riken.jp
[2] Institute of Applied Physics RAS, Nizhny Novgorod, Russia

Current view holds that neurons communicate to astrocytes through activation of astrocyticmGluRs. Being activated by synaptically released glutamate mGluRs trigger synthesis of inositol 1,4,5-trisphosphate (IP_3). IP_3 reaches IP_3 receptors (IP_3Rs) on endogenous Ca^{2+} stores (e.g. endoplasmic reticulum (ER) or mitochondria) and activates Ca^{2+}release from them. Using cultured rat astrocytes transfected with genetically encoded Ca^{2+} sensor (GCaMP2) we monitored spontaneous Ca^{2+} activity (Ca^{2+} sparks) in astrocytic processes even when the mGluRs were blocked. Our further experiments suggested that these Ca^{2+} sparks are triggered by the stochastic Ca^{2+}influx through the plasma membrane which directly activates IP_3Rs. Interestingly, the frequency of Ca^{2+}sparks was significantly higher in thin astrocytic processes (Fig.1). With a mathematical model we showed that fluctuations of intracellular Ca^{2+} due to the influx through the plasma membrane depend on the number of open Ca^{2+} channels and the volume of the cytoplasm. Thus, for uniformly distributed Ca^{2+} channels, Ca^{2+} influx is proportional to the surface-to-volume ratio (SVR) which is larger in thin astrocytic processes. Then we analysed 3D reconstruction of spines and astrocytic processes obtained from electron microscopy (EM) serial images of CA1 *str.radiatum* in rat hippocampus. Interestingly, SVR of astrocytic processes was larger in the proximity of the synapses. Moreover, perisynaptic processes did not have Ca^{2+} stores suggesting their specialization for detection of synaptic activity rather than for astrocytic Ca^{2+} excitation. Such specialization is reminiscent of the function of dendritic spines in neurons, the main function of which is detection of synaptic input. Because Ca^{2+} influx through voltage-sensitive Ca^{2+}channels is triggered by depolarization we suggest that astrocytic processes can by depolarized by K^+ increases during synaptic signalling and thus detect neuronal activity. Therefore, synaptic release of K^+ may serve as a mechanism for neuron-astrocyte communication in addition to glutamate.

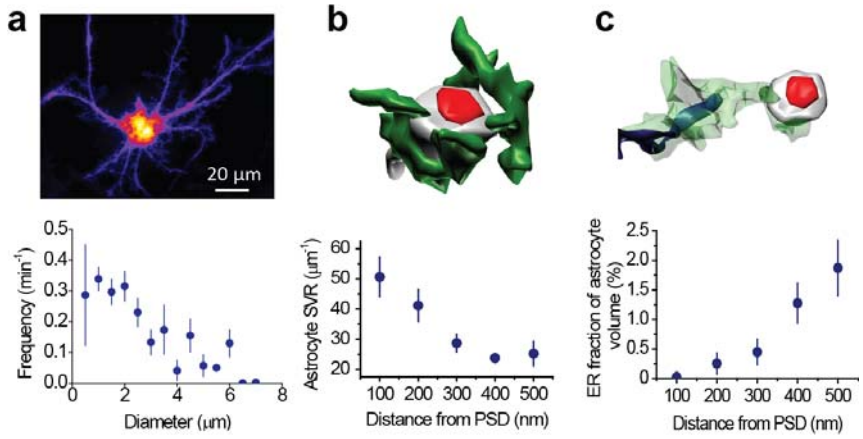

Fig. 1. Ca^{2+} sparks are more frequent in thin astrocyte processes which have larger SVR (**a**, GCaMP2 imaging). Astrocytic SVR is higher around synapses (**b**, EM). Perisynaptic processes lack Ca^{2+} stores (**c**, EM). PSD – postsynaptic density (red spot in **b**, **c**)

Astrocytes generate two types of Ca^{2+} transients – local Ca^{2+} sparks and generalized events. It remains unclear if generalized events are triggered by Ca^{2+} sparks or built of spark summation. We found that mGluRs activation by t-ACPD increases the duration of Ca^{2+} sparks without changing their frequency, but increased the frequency of generalized events. This suggests that activation of mGluRs may not be responsible for the triggering of Ca^{2+} sparks. Using the mathematical model we have demonstrated that the increase in IP_3 is responsible for synchronization of Ca^{2+} sparks and their manifestation as generalized events. Thus, we suggest that activation of astrocyticmGluRs by synaptically released glutamate can modulate both duration and synchronization of Ca^{2+} sparks. Synchronized Ca^{2+} sparks are recorded as generalized events in the soma using low resolution imaging techniques and disappear when mGluRs are blocked or genetically deleted.

DETECTION AND CHARACTERIZATION OF DIRECTIONAL COUPLINGS FROM TIME SERIES: METHODS AND APPLICATIONS TO NEURODYNAMICS

D.A. Smirnov[1,2] and **B.P. Bezruchko**[2,1]

[1] Saratov Branch, V.A. Kotel'nikov Institute of RadioEngineering and Electronics
Russian Academy of Sciences, Saratov, Russia, smirnovda@info.sgu.ru
[2] Saratov State University, Saratov, Russia

Detection and characterization of interaction between complex systems solely from their time realizations is an interdisciplinary problem which has attracted much attention of researchers for a long time [1]. Several approaches to coupling detection have been suggested within the framework of linear time series analysis and information theory, including cross-correlation function, coherence, and mutual information. To reveal directionality of coupling, their generalizations exist, such as Granger causality [2] and transfer entropy [3]. Recently, there have been developed new approaches in nonlinear dynamics which are based either on state space analysis [4-8] or phase dynamics modeling [9–12]. The latter are very promising techniques since they are often more sensitive to weak couplings than any other methods.

The techniques for detection and characterization of directional couplings are highly demanded in neuroscience. In particular, they are required to reveal functional neural assemblies or detect interactions between brain areas during cognitive tasks [13]. Next, many neurological diseases, including epilepsy and Parkinson's disease, seem to result from the fact that brain function becomes severely impaired by synchronization processes. In particular, Parkinsonian resting tremor appears to be caused by a population of neurons located in the thalamus and basal ganglia [14]. Epileptic seizures are often accompanied by the influence of low-frequency activity of hippocampus on different cortex areas and low-frequency synchronization of the latter [13]. As well, low-frequency synchronization of different thalamic and cortical areas is observed in absence epilepsy [15]. The exact mechanisms of these phenomena are largely unknown. Thus, getting reliable empirical evidence for the existence of directional couplings between different brain areas is the problem of great significance.

However, the existing methods are often insufficient to characterize couplings under realistic neurophysiological settings: different time scales of the processes and relatively low sampling rates, short and non-stationary data series, characterization of dynamical importance of couplings, detection of weak couplings in large ensembles of neural oscillators. Therefore, appropriate generalizations of the methods are in order. In this work, we review our recent results concerning the development of such novel approaches and apply them to artificial neuron model data and experimental time series from epileptic rats and patients with Parkinsonian resting tremor.

Granger causality and the problem of time scales

There are time series from two processes $x_1(t)$ and $x_2(t)$ recorded at a sampling interval Δt. According to Granger's idea [2] to determine how strongly the processes affect each other, one constructs autoregressive models to predict the future value of a process x_i based on the previous values of x_i and (possibly) of the other process x_j. If the prediction gets better when x_j is taken into account, one says that the process x_j "Granger causes" x_i. The approach can be generalized to multivariate processes [16] and nonlinear equations [8].

However, both processes may involve different characteristic time scales which can be in different ratios with the sampling interval. Such situations have not been carefully analyzed. We have shown that the results of coupling estimation may strongly depend on the value of the sampling interval, in particular, too a large sampling interval may even lead to erroneous detection of bivariate coupling. We have explained this effect and developed a special surrogate data test to distinguish between unidirectional and bidirectional couplings in case of low sampling rates.

Long-term causality

Another problem with the Granger causality is that it is often insufficient to assess physical or dynamical "importance" of coupling. Granger causality idea can be successfully used to *detect* couplings and quantify their *short-term* effects. However, it is often more important in practice to learn how *long-term* characteristics of x_i (e.g., its power spectrum, amplitude of oscillations, trends,

etc) would change if x_j behaved in a certain way? Thus, in studying Parkinsonian tremor one develops deep brain stimulation techniques [14] and reveals how the brain activity should be changed to provide a normal behavior of the limbs instead of their pathological high-amplitude oscillations. This problem relates to the characterization of long-term effects of couplings between the processes. To overcome the difficulty, we have introduced the concept of "long-term causality" [17] which extends the concept of Granger causality. The long-term causality is estimated from data via empirical modeling and analysis of the model dynamics under different conditions.

Phase dynamics analysis and its advantages

To get more sensitive characteristics of coupling, it appears fruitful to introduce the phase of the observed signals (a variable which characterizes repeatability of the processes, their basic "rhythms" [18]) and model the phase dynamics [10]. We have adapted this idea for the cases of (i) short time series by introducing analytic significance level to get reliable conclusions about coupling presence [19] and (ii) ensembles of oscillatory systems [20]. Moreover, we have shown that the phase dynamics modeling can be applied to the analysis of neural oscillators [21] and under certain conditions appears more sensitive to weak couplings than state space approaches and linear Granger causality [21, 22].

We have applied all the above mentioned techniques to artificial stochastic and deterministic, linear and nonlinear oscillatory systems to illustrate their performance under different idealized conditions. With the aid of the developed techniques, we have got quantitative characteristics of directional couplings (i) between brain activity and hand oscillations from local field potentials measured in sub-thalamic nucleus and accelerometer signals during strong spontaneous Parkinsonian tremor (data from the group of Prof. P. Tass, Research Center Juelich, Germany) [23,24], (ii) between different thalamic nuclei and cortical areas from local field potential recordings during spike-and-wave discharge in epileptic rats of the strain WAG/Rij (data from Dr. E. Sitnikova, Institute of Higher Nervous Activity and Neurophysiology of RAS, Moscow) [25].

Conclusions. We have reviewed several modifications of the methods based on the concept of Granger causality developed to detect and characterize directional couplings between complex systems under realistic settings. They include the concept of long-term causality to characterize long-term effects of couplings, special kind of surrogate data to avoid the problem of undersampling, characteristics of phase dynamics applicable to short time series and ensembles of oscillatory systems including the case of neural oscillators. These methods and settings are required in neuroscience as illustrated by their applications to epileptic rats and Parkinsonian patients.

Acknowledgements. The research was supported by the Russian Foundation for Basic Research (grant 11-02-00599), RAS and Federal Program "Scientific and pedagogical cadres of innovational Russia" (grant 2011-1.2.1-201-007/062).

References

1. J. Pearl, *Causality: Models, Reasoning, and Inference*, Cambridge University Press, Cambridge, 2000.
2. C. Granger, *Econometrica*, 1969, **37**, 424.
3. T. Schreiber, *Phys. Rev. Lett.*, 2000, **85**, 461.
4. A. Cenys, G. Lasiene, and K. Pyragas, *Physica D*, 1991, **52**, 332.
5. N.F. Rulkov et al., *Phys. Rev. E*, 1995, **51**, 980.
6. S.J. Schiff et al., *Phys. Rev. E*, 1996, **54**, 6708.
7. J. Arnhold et al., *Physica D*, 1999, **134**, 419.
8. U. Feldmann and J. Bhattacharya, *Int. J Bifurc. Chaos*, 2004, **14**, 504.
9. F. Mormann et al., *Physica D*, 2000, **144**, 358.
10. M.G. Rosenblum and A.S. Pikovsky, *Phys. Rev. E*, 2001, **64**, 045202R.
11. M. Palus and A. Stefanovska, *Phys. Rev. E*, 2003, **67**, 055201R.
12. T. Kiemel, et al., *J. Comput. Neurosci.,* 2003, **15**, 233.
13. F. Varela et al., *Nature. Neuroscience*, 2001, **2**, 229.
14. P.A. Tass, *Biol. Cybern.*, 2003, **89**, 81.
15. C.P. Panayiotopoulos, in *Epilepsy: a comprehensive textbook* (eds. J.J. Engel, T.A. Pedley), Lippincott-Raven Publishers, Philadelphia, 1997. P. 2327.
16. L.A. Baccala and K. Sameshima, *Biol. Cybern.*, 2001, **84**, 463.
17. D.A. Smirnov and I.I. Mokhov, *Phys. Rev. E*, 2009, **80**, 016208.
18. A. Pikovsky, M. Rosenblum, and J. Kurths, *Synchronization. A Universal Concept in Nonlinear Sciences*, Cambridge University Press, Cambridge, 2001.
19. D.A. Smirnov and B.P. Bezruchko, *Phys. Rev. E*, 2003, **68**, 046209.
20. D.A. Smirnov and B.P. Bezruchko, *Phys. Rev. E*, 2009, **79**, 046204.
21. D. Smirnov et al., *Chaos*, 2007, **17**, 013111.
22. D.A. Smirnov and R.G. Andrzejak, *Phys. Rev. E*, 2005, **71**, 036207.
23. D.A. Smirnov et al., *Europhys. Lett.*, 2008, **83**, 20003.
24. P. Tass et al., *J. Neural Eng.*, 2010, **7**, 016009.
25. E. Sitnikova et al., *J. Neurosci. Meth.*, 2008, **170**, 245.

INFLUENCE OF TERAHERTZ RADIATION WITH A FREQUENCY 0.05 ÷ 2 THZ ON THE GROWTH OF NEURITES OF SENSORY GANGLION

M.V. Tsurkan[1], O.A. Smolyanskaya[1], S.A. Kozlov[1], V.A. Penniyainen[2], A.V. Kipenko[2, 3], E.V. Lopatina[2, 3], and **B.V. Krylov[2]**

[1] Saint-Petersburg State University of Information Technologies, Mechanics and Optics, St.Petersburg, Russia
tsurkan.maria@yandex.ru
[2]Pavlov Institute of Physiology, Russian Academy of Sciences, St. Petersburg, Russia
[3]Almazov Federal Heart, Blood and Endocrinology Centre, St. Petersburg, Russia

Development of sources and detectors of terahertz (THz) radiation has led to a wide range of works, focusing on the influence of THz radiation on biological systems. From this point of view, the influence of THz radiation on the nerve fibers is of primary concern. Thus, several studies indicated both stimulating and depressive effect on nerve cells [1, 2]. However, the mechanism of this effect has not yet been studied, including defined dose and exposure time. In this regard, our work has been devoted to the influence of broadband pulsed THz radiation range 0.05 ÷ 2 THz on the growth of neurites. The object of our study was sensory ganglias of 10-12 days chicken embryos in organotypic tissue-culture. Ganglion – is a cluster of nerve cells, consisting of bodies, dendrites and axons of nerve and gliacytes. It is responsible for the relationship with the environment and reflects changes in the conditions of its existence. An optical scheme of the experiment was worked out.

The scheme of the experiment was the following: a laser beam (a femtosecond fiber laser EFOA-SH) passed a system of mirrors and was focused by the lens into the InAs crystal placed in the strong magnetic field of the magnet. Femtosecond radiation created free carriers, its motion in a magnetic field generated THz radiation. Laser power before the InAs crystal was 120 mW. Divergent THz radiation was collected by off-axis parabolic mirrors and directed into a Petri dish with the object. The average THz power was 5 mW. The generated THz radiation had a frequency band from 0.05 to 2 THz.

The work is done on cultured sensory ganglia of 10 ÷ 12-day-old chick embryos prepared at the level of the lumbosacral spinal cord and cultivated for 3 days on substrates of collagen in Petri dishes at 36.5° WITH and 5% CO_2 (Sanyo, Japan). The nutrient medium contained 40% Hanks solution, 40% Eagle's medium, 5% of chicken embryonal extract and 15% of fetal cows serum with the addition of insulin (0.5 ea./ml), glucose (0.6%), glutamine (2 mM), gentamicin (100 ea/ml) [3]. Tools for eye surgery were used to prepare the material. Sensory ganglia were removed under a microscope. Then they were placed in a sterile plastic Petri dish on the cover glasses with the collagen substrate. A plastic cup was chose because of the transparency of the material to the radiance in the THz range. Explants were not exposed to THz radiation, and were considered as a reference. The time of exposure was a few minutes.

For the attachment of the explant the object was placed into a CO_2-incubator at a temperature of 36.8 ^{o}C. After three days the growing of neurites was investigated in vivo by using a microscope «Axiostar Plus» (Carl Zeiss, Germany). A morphometric method was used to quantify the effect of THz radiation on the growth of neurites in sensory ganglia. In order to unify finite exponents of the growing neurites, evaluation relative criterion was used – area index (AI), which was calculated as the ratio of the whole explant, including the peripheral zone of growth to the original area of the ganglion. AI values were expressed as percentage, the reference value AI taken for 100%. The results were processed with the help of t- Student's test.

References

1. P.H. Siegel and V. Pikov, *SPIE Photonics West, BiOS*, 2010, paper 7562-17.
2. U.S. Olshevskaya, A.S. Kozlov, A.K. Petrov, T.A. Zapara, A. S. Ratuwnyak, *Journal of higher nervous activity n.a. I.P. Pavlova*, 2009, **59**(3), 353-359.
3. V.A. Penniyainen, B.V. Krylov, N.I. Chalisova, I.I. Malevsky, Tsitologiya, 2003, **45**, 377-379.

ERROR-RELATED POTENTIAL FOR CORRECTING P300 SPELLER BRAIN-COMPUTER INTERFACE: IS IT REALLY WORTH IT?

A. Combaz, N. Chumerin, N.V. Manyakov, and **M.M. Van Hulle**

K.U. Leuven, Laboratorium voor Neuro- en Psychofysiologie, Herestraat 49, B-3000 Leuven, Belgium
marc@neuro.kuleuven.be

A P300 Mind Speller is a Brain-Computer Interface (BCI) that enables subjects to spell text on a computer screen by detecting P300 Event-Related Potentials in their electroencephalograms (EEG). Error-related Potentials (ErrP) are EEG signals generated by the subject's perception of an error. We report on the feasibility of using the ErrP for automatically correcting errors made with the P300 Mind Speller, and whether it is really beneficial.

Introduction

The BCI field has witnessed a tremendous development in recent years [1] and has led to solutions that could substantially improve the quality of life of neurologically impaired patients. BCIs exist in basically two versions: invasive ones that rely on neural signals recorded with a brain implant, and non-invasive ones that rely mostly on electroencephalograms (EEGs) recorded from the scalp. Several paradigms have been considered for EEG-based BCIs but here we focus on the P300 Event-Related Potential (ERP) [2]. It is elicited in the context of an oddball paradigm: when a subject performs the classification of two types of events, one of which is only rarely presented, then the rare event is expected to elicit an ERP with an enhanced positive-going component at a latency of about 300 ms. A popular application is the P300 Mind Speller originally described in [3]: the subject focuses on the symbol he/she wishes to communicate, among all other possible symbols, arranged in a matrix display, while the rows and columns of the matrix are consecutively and randomly intensified. The intensification of a row or column containing the target symbol elicits a P300 ERP and, by detecting it, the BCI can detect the target row and column and, thus, identify the symbol the subject has in mind.

An elegant way to improve the performance of an EEG-based BCI is with the so-called Error-related Potentials (ErrPs). They are related to the subject's perception of an error. The error could be made by the subject him/herself [4], or by the BCI [5]. The latter is what we will focus on. We will report on experiments we performed to study the possibility of detecting the ErrP in real-time, and discuss whether including it in a P300 Mind Speller is beneficial or not.

Recording

The EEG recordings were performed using a prototype of an ultra low-power 8-channels wireless EEG system developed by imec, Leuven (Belgium) [6]. The data is transmitted with a sampling frequency of 1 kHz, for each channel. We used a brain-cap with large filling holes and sockets for active Ag/AgCl electrodes (ActiCap, Brain Products). The first step in the recording was to familiarize the subjects with our P300 Mind Speller BCI [7] and to train the system (i.e., classifier) to recognize each subject's P300 ERPs elicited when selecting each one of 8 mandatory symbols. In the second step, the subjects used the trained P300 Mind Speller to type symbols of their choice.

Experiment

Two series of experiments were performed. For the first series, 6 healthy subjects (4 male, 2 female, age 22-34, 5 right handed and 1 left handed) were recruited (for details, see [7]). They all performed one session during which they spelled between 32 and 65 symbols during which 6 to 19 errors occurred. For the second series of experiments, 3 new subjects were tested (2 female, 1 male, age 24-27, 2 right handed and 1 left handed); they performed between 6 and 7 sessions. The second series was set-up specifically to study the feasibility of on-line ErrP detection.

Shape of ErrP

When looking at the grand average error-minus-correct EEG responses, of both series of experiments, we observe a negative peak followed by positive one at about 320 ms and 450 ms, respectively, which was most prominent at electrodes Fz and FCz. The high variability of the responses between subjects motivated us to train the ErrP classifiers on individual subjects.

On-line detection of ErrP

Here, we focus on the results obtained from the second series of experiments. We aim here at gaining insight into the possibility of correctly classifying the EEG responses as ErrP (incorrect feedback) and non-ErrP (correct feedback). We performed the ErrP classification using a Fisher Linear Discriminant Analysis (FLDA) and a linear Support Vector Machine (10-folds cross-validation, [8]). Our findings indicate a significant variability of the way the brain processes errors across subjects for a given context. Nevertheless, our observation was that the responses to both types of feedback were significantly different, giving us good hopes about the possibility of classifying accurately those EEG responses. We also studied the influence of the amount of training data on the accuracy of the ErrP/non-ErrP classification. We found that it more influenced the sensitivity than the specificity and that, in order to reach a sensitivity of at least 50%, we needed training sets with at least 25 ErrPs.

Discussion

The question arises about the viability of ErrP detection for the P300 Mind Speller. One simple strategy could be, after an ErrP is detected, to simply repeat the sequence of intensifications, but this would lead to an important increase in the time taken to communicate a symbol. Another strategy would be to select the second best letter according to the classifier's ranking. This approach has the advantage not to increase the stimulation time. However, one has also to take into account that not all ErrPs are correctly detected and new mistakes can appear when responses to correct feedbacks are wrongly classified. We have tested this by comparing the performance of the linear SVM classifier and the FLDA to the theoretically maximal classifier performance. We observed that, for all 3 subjects, in the second series of experiments, the SVM outperforms the FLDA. Our results also indicate the importance of minimizing the proportion of False Negatives, and of having a classifier biased towards the non-ErrP class. Several strategies could be though of to improve ErrP detection itself: one could consider weighting the scores of each symbol with a probability of occurrence given the previous symbol. The disadvantage is that the result would be language specific and not suitable for proper nouns or non-text based communication (e.g., using icons).

Conclusion

A first step towards the integration ErrP detection in the P300 Mind Speller BCI was presented. Besides the undeniable practical advantage of ErrP-based error correction, the necessity of gathering a substantial amount of training data, the importance of minimizing false positives, and the fact that we need to perform single trial detection, makes this a very challenging task. If hours of training are not acceptable, one could let the subject work with the P300 Mind Speller, and in the meantime collect ErrP examples, and train the ErrP/non-ErrP classifier, before correcting errors from ErrP detection.

Acknowledgements

AC is supported by IWT (Flanders), NC by IST-2007-217077, NVM by IST-2004-027017, MVH by PFV/10/008, CREA/07/027, G.0588.09, IUAP P6/29, GOA 10/019, IST-2007-217077, and the King Baudouin Foundation of Belgium (SWIFT prize). The authors wish to thank Refet Firat Yazicioglu, Tom Torfs and Chris Van Hoof from imec, Leuven, for providing us with the wireless EEG system.

References

1. P. Sajda, K.-R. Muller, K. Shenoy, *IEEE Signal Processing Magazine,* 2008, **25**, 16–17.
2. W.S. Pritchard, *Psychological bulletin*, 1981, **89**, 506–40.
3. L.A. Farwell, E. Donchin, *Electroencephalography and clinical neurophysiology*, 1988, **70**, 510–23.
4. W.J. Gehring, M.G.H. Coles, D.E. Meyer, E. Donchin, *Electroencephalography and clinical neurophysiology. Supplement,* 1995, **44**, 261–72.
5. P.W. Ferrez, J. del R. Millan, *Advances in Neural Information Processing Systems,* 2007, **20**, 1–8.
6. R. Yazicioglu, P. Merken, R. Puers, C. Van Hoof, *Proc. 32nd European Solid-State Circuits Conference*, IEEE, 2006, 247–250.
7. A. Combaz, N. Chumerin, N. Manyakov, A. Robben, J. Suykens, M. Van Hulle*, Proc. 2010 IEEE International Workshop on Machine Learning for Signal Processing, IEEE*, 2010, 65–70.
8. S. Keerthi, D. DeCoste, *Journal of Machine Learning Research,* 2006, **6**, 341.

HYALURONIDASE POTENTIATION OF EPILEPTIFORM ACTIVITIES CAUSED BY 4-AMINOPYRIDINE IN CULTURED MICE HIPPOCAMPAL NEURONS

M.V. Vedunova[1], T.A. Sakharnova[1], S.A. Korotchenko[2], I.V. Mukhina[1,2], and **A.E. Dityatev[3]**

[1] Cell Technology Science Group, Nizhny Novgorod State Medical Academy, Russia
[2] Department of Neurodynamics and Neurobiology, Lobachevsky State University of Nizhny Novgorod, Russia
[3]Department of Neuroscience and Brain Technologies, Italian Institute of technology, Genoa, Italy
MVedunova@yandex.ru

Extracellular matrix plays an important role in regulating use-dependent synaptic plasticity. Distinct aggregates of extracellular matrix (ECM) molecules surround cell bodies and proximal dendrites of some central neurons, forming the perineuronal nets [1]. These nets are heterogeneous in their structure and composition, secreting from both neurons and astrocytes [2] and consisting of hyaluronic acid (HA), chondroitin sulfate proteoglycans of the aggrecan family, and tenascin-R [3]. HA is a large, negatively charged, non- branched polymer composed of repeated disaccharides of glucuronicacidand N-acetylglucosamine. Recently, HA has been shown to affect both the mobility of a-amino-3-hydroxyl- 5-methyl-4-isoxazolepropionate (AMPA) glutamate receptors and paired-pulse modulation in hippocampal cultures [4]. Also it was established that HA facilitates LTP induction by increasing the activity of L-type voltage-dependent Ca^{2+} channels (L-VDCCs) in hippocampal slices.

To investigate the role of HA in epileptiform activities, we used enzymatic pretreatment of hippocampal culture with hyaluronidase (Hyase). Epileptiform activities were induced by 4-aminopyridine (4-AP) in cultured mice hippocampal neurons. 4-AP is blocker of K^+ channels, which are key modulators of neuronal excitability, and mutations in certain types of these channels are known to cause epileptic seizures both in vitro and in vivo, including in humans (Stork, 1994; Kobayashi, 2008). Hippocampal cells were dissociated from embryonic mice (E18) and plated on microelectrode arrays (MEAs) pre-treated with adhesion promoting molecules of polyethyleneimine (Sigma). C57BI6 mice were killed by cervical vertebra dislocation, according to protocols approved by the National Ministry of Public Health for the care and use of laboratory animals. Embryos were removed and decapitated. The entire hippocampus was dissected under sterile conditions. After enzymatic treatment for 25 min by 0.25% trypsin at 37°C (Invitrogen) cells were separated. Dissociated cells were seeded in 40µl droplet covering the center of the culture dish with $1mm^2$ electrode region of the MEA, forming a dense monolayer. After cells had adhered (usually in 2 hrs), the dishes were filled with 0.8 ml Neurobasal medium (Invitrogen) supplemented with B-27 (Invitrogen) and 0.5 mM Glutamine (Invitrogen) with 10% fetal calf serum (PanEco). Glial growth was not suppressed, because glial cells are essential to long-term culture health. One half of the medium was changed every day. Cells were cultured under constant conditions of 37°C, 5% CO_2 and 95% air at saturating humidity in a cell culture incubator (MCO-18AIC, SANYO). Experiments were done when the cultures were 16 days in vitro (DIV). Local application of drugs to the culture was performed using a feeder. Hyase (from Streptomyces hyalurolyticus, Sigma; 75 U/ml), which is specific for hyaluronic acid and cleaves b-GlcNAc [1-4] glycosidic bonds yielding 4,5-unsaturated tetra-and hexasaccharides was added on 17th DIV. Glutamat transmission were blocked by adding10 mcM CNQX, 10 mcM CPP, and L-type voltage-dependent Ca^{2+} channel (L-VDCC) blocker 10 mcM diltiazem to the extracellular solution. All reagents were purchased from Sigma or Tocris.

Extracellular potentials were collected through 64 planar indium tin-oxide (ITO) with platinum black electrodes simultaneously with the integrated MED64 system (Alpha MED Science, Japan). The MED probe (MED-P5155) had 8 x 8 (64) electrode arrays with 50µm x 50µm micro-electrode measured and the 150 µm spacing. Data was recorded simultaneously on 64 channels at sampling rate of 20kHz/channel. All signal analysis and statistics were performed using custom made software (Matlab®). Detected spikes were then plotted in a raster diagram. Note that the minimal interspike interval was set to 1.5 ms to avoid the overlap of the neighbouring spikes. To detect bursts we calculated the quantity called total spike rate (TSR(t)) accounting for the total number of spikes at all electrodes within the 50 ms bin. The signal TSR(t) was analyzed to estimate burst beginning and ending points. Burst threshold was set to $T_{Burst} = 0.1 \times \sigma_{TSR}$, where σ_{TSR} - standard deviation of TSR(t). This method permits to minimize the burst event detection error caused by the constant level of spontaneous spikes.

Hyaluronidase treatment on 17th DIV changed neuronal network activity in hippocampal primary cultures grown on multielectrode arrays. The increase of mean burst frequency and the decrease in inter-burst intervals and mean burst duration were observed (Fig. 1).

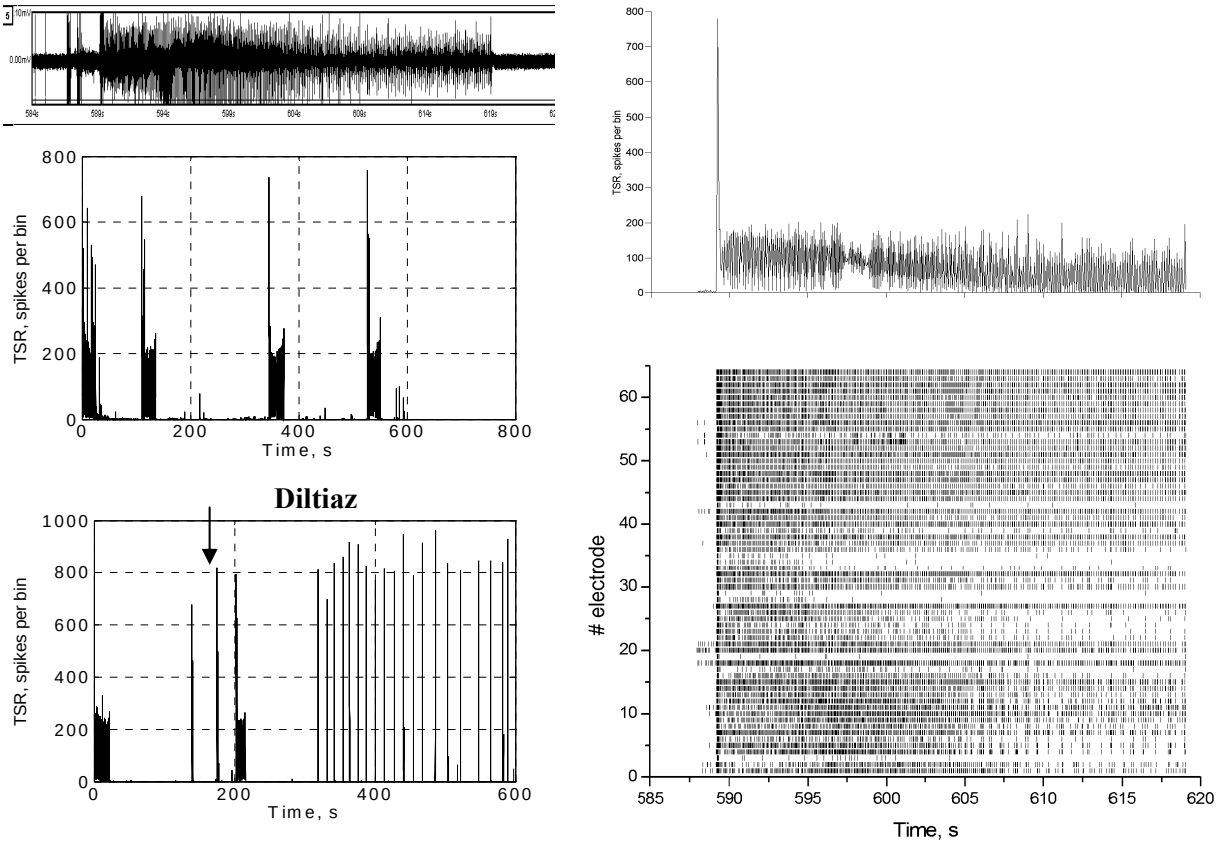

Fig. 1. The pattern of the neuronal network activity in cultured mice hippocampal neurons, 33 DIV. A – recording of spontaneous seizures from 4th electrode of MED64 probe; B – burst rate after hyaluronidase treatment (75 U/ml); C – seizure block by diltiazem (10 mcM); D – total spike rate TSR(t) and raster diagram of hyaluronidase–induced seizure

Our findings revealed that hyaluronidase potentiated epileptiform activities caused 4-AP in cultured mice hippocampal neurons. Apart from that, enzymatic pretreatment of hippocampal culture with hyaluronidase stimulated a hyaluronidase–induced epileptogenesis independently. Spontaneous seizures were observed during 2 weeks and were blocked by L-type voltage-dependent Ca^{2+} channel (L-VDCC) blocker

These results suggest a novel *in vitro* model of epileptogenesis that may help elucidate some of the mechanisms that underlie ECM-induced epilepsy.

Acknowledgements

The research is supported by the Russian Department of Education and Science 2.1.1./6223 and 11.G34.31.0012.

References

1. G. Kochlamazashvili, et al., "The extracellular matrix molecule hyaluronic acid regulates hippocampal synaptic plasticity by modulating postsynaptic L-type Ca2+ channels", *Neuron*, 2010, **67**, 116-128.
2. A. Dityatev, et al., "The dual role of the extracellular matrix in synaptic plasticity and homeostasis", *Nat Rev Neurosci*., 2010, **11**, 735-46.
3. C.M. Galtrey, J.W. Fawcett, "The role of chondroitin sulfate proteoglycans in regeneration and plasticity in the central nervous system", *Brain Res Rev*., 2007, **54**, 1-18.
4. R. Frischknecht, et al., "Brain extracellular matrix affects AMPA receptor lateral mobility and short-term synaptic plasticity", *Nat Neurosci*., 2009, **12**, 897-904.

QUANTITATIVE CALCIUM ION CONCENTRATION MEASUREMENTS WITH THE HELP OF SINGLE WAVELENGTH DYES

Yu.N. Zakharov and **A.V. Ershova**

N.I. Lobachevsky State University of Nizhny Novgorod, Russia, zhrv@rf.unn.ru

Calcium ion concentration ($[Ca^{2+}]_i$) dramatically influences brain cells vital activity. Critical evaluation of the role of calcium as an intracellular messenger requires quantitative measurements of $[Ca^{2+}]_i$ and comparisons of varied stimuli and cell responses. So, reliable information of calcium ion concentration dynamics is of great importance for investigations of brain cell functional activity. This work is devoted to the problem of data reliability in experiments on rat and mouse hippocampal cells by means of laser scanning fluorescence microscopy for neuron-glial networks signaling processes. We use Zeiss LSM510 NLO Duoscan confocal and two-photon microscope system for recording and preprocessing fluorescence signals from hippocampal slices or cell cultures dyed by specific calcium indicator.

The most popular approach to measuring intracellular free calcium ion concentration is ratiometric imaging using the UV excited calcium indicators offered by Grynkiewicz et. al. [1]. With this method, calcium ion concentration is calculated from a ratio of fluorescences at two excitation wavelengths. We propose to determine $[Ca^{2+}]_i$ by single-wavelength specific calcium indicator Oregon Green BAPTA1 AM whose intensity of green fluorescence changes upon binding to calcium ions inside neuronal and glial cells. To distinguish neurons and glia, Suiforodamin 101 as astrocytic marker is used. It penetrates into astrocytes and its red fluorescence together with green fluorescence of Oregon Green give a composite yellow color of calcium-active glia along with green live neurons. By filtering Oregon Green fluorescence and measuring its intensity it is possible in principle to calculate calcium ion concentration but is difficult to use in practice the known relationships between fluorescence and calcium ion concentration [1] because it is necessary to know fluorescence intensities at maximum and minimum $[Ca^{2+}]_i$ for every concrete experimental situation.

We suggest $[Ca^{2+}]_i$ quantification method based on high affinity single-wavelength calcium indicator fluorescence intensity in situ measurement subject to dye loading protocol and fluorophore excitation conditions without calcium saturation and reduction of resting $[Ca^{2+}]_i$ in every *in vitro* experiment. Fluorescence intensity F is determined by the product of dye concentration n, excitation intensity I_0, molar extinction coefficient α, fluorescence quantum yield Q_F, quantum yield of the photodetector Q_D, and **Φ** – number of photons acquired by the optics :

$$F = \Phi Q_D Q_F \alpha I_0 n \ .$$

Since α and Q_F of free and Ca^{2+}-bounded dye molecules is different, $F = S_f n_f + S_b n_b$, where n_f and n_b are concentrations of free and Ca^{2+}-bounded dye, and $S = \Phi Q_D Q_F \alpha I_0$.

According to the dissociation constant concept, $K_d = \frac{n_f [Ca^{2+}]_i}{n_b}$, $[Ca^{2+}]_i = K_d \frac{n_b (S_b - S_f)}{n_f (S_b - S_f)}$

and subject to total dye concentration $n_\Sigma = n_b + n_f$, we finely have:

$$[Ca^{2+}]_i = K_d \frac{F - S_f n_\Sigma}{S_b n_\Sigma - F} \ .$$

Thus, we can determine calcium ion concentration from parameters of using dye, instrument function of microscopy equipment, total amount of loaded dye that is the result of fill up protocol and measuring fluorescence intensity.

This work was supported by the Program of the Russian Ministry of Education (No. 2.1.1/6223), RFBR grant 09-04-01432-a and the RF Government grant No. 11.G34.31.0012.

References

1. G. Grynkiewicz, M. Poenie, and R.Y. Tsien, *J. Biol.Chem.*,1985, **260**, 3440 –3450.

THE DISTRIBUTION OF THE PHOSPHORYLATED CYCLIC AMP-RESPONSIVE ELEMENT BINDING PROTEIN (p-CREB) IN THE BRAIN STRUCTURES OF *DROSOPHILA MELANOGASTER*

A.V. Zhuravlev[1], **A.A. Petrov**[2] and **E.V. Savvateeva-Popova**[1]

[1] Pavlov Institute of Physiology RAS, St. Petersburg, Russia, beneor@mail.ru
[2] Zoological Institute RAS, St. Petersburg, Russia

Introduction

CREB is an important nuclear factor regulating long-term memory (LTM) formation in mammals and invertebrates [1]. The *D. melanogaster* protein dCREB2, CREB homolog, is activated upon cAMP/protein kinase A-dependent phosphorylation of Ser^{231} residue, which corresponds to phospho-Ser^{133} of mammalian CREB [2]. dCREB2 has been shown to induce the process of LTM following courtship conditioning [3]. In *D. melanogaster* head, however, the whole pool of dCREB2 is in phospho-Ser^{231} form [4]. Thus, the additional posttranslational modifications or local dCREB2 displacements within the brain structures might be involved in cAMP-dependent memory formation. We investigated the distribution of phospho-Ser^{231} dCREB2 (pCREB) in the 5 day imago male brains before and after the LTM formation in the conditioned courtship-suppression paradigm [5].

Methods

To induce the process of LTM formation following courtship-suppression [6] the naive 5 day *Canton-S* males were placed in the food vials together with the fertilized females for 5 hours. To analyze the pCREB distribution the brains were isolated [7] and fixed in 10% paraformaldehyde solution in 0.3% Triton X-100-PBS buffer (PBT) for 20-25 min. After washings the brains were incubated in 10% normal donkey serum in PBT for 1 hour and stained with mouse antibodies against *Drosophila* brain neuropile marker cystein string protein (dilution 1:20) and rabbit polyclonal antibodies against human phospho-Ser^{133}-CREB (dilution 1:100) in PBT for 5 days at 4º C. After washings the brains were stained with FITC- and Rhodamine-conjugated secondary antibodies against mouse and rabbit antibodies, respectively (dilution 1:100, 1:100) in PBT for 1 day at 4º C. After washings the brains were stained with DAPI (~1.2 mg/L) in PBS for 40 min at room temperature. The brains were enclosed into the mounting medium and scanned in the frontal with the confocal laser scanning microscope Leica TCS SP5, using the 20x/63x immersion lens. The multiphoton laser was used to induce DAPI fluorescence in nuclei. FIJI software was used for the image visualization.

Results

In the adult *Drosophila* brain pCREB mainly concentrates in the cell bodies and axons of several neurons in the area of the subesophageal ganglion (SEG) (Fig. 1a). These neurons extend their axonal processes towards the esophagus (ES) and the superior medial protocerebrum (SPb), forming the glomerular-like structures (Fig. 1b,c). Two neuronal tracts (Fig. 1d) connect the glomerular structure 2 with the V-shaped structure of the SPb (Fig. 1g), conjoining above the central complex (CC) (Fig. 1e) and extending laterally (Fig. 1h). All these pCREB-enriched structures seem to form the integral brain system, morphologically resembling that involved in the regulation of fly taste sensitivity and nutrition behavior [8]. Two clusters of pCREB-enriched neurons were found in each brain hemisphere in the area of the antennal nerve (AN) (Fig. 1i), connected by the commissure tract under the esophagus (Fig. 1j). pCREB was also detected in the cytoplasm of some neurons near the surface of the brain. Surprisingly, it was not detected in the cell nuclei, except for the pCREB-enriched neurons of SEG. In these nuclei pCREB was found to localize beyond the transcriptionally repressed chromocenters. No visible differences in pCREB distribution and number of pCREB-positive neurons were observed before and after the courtship-suppression conditioning.

Discussion

dCREB2 distribution area in the *Drosophila* brain is mainly restricted to the taste sensitivity and nutrition regulating system, interconnecting the neuropile structures of SEG, esophagus and SPb. As the taste sensitivity plays an important role in the courtship suppression, this system may be involved

in the LTM formation following courtship conditioning together with the antennal lobes (AL), the mushroom bodies, the CC and the other brain structures. The high level of nutrition system functional activity (fly on a food media) may also result in the elevated pCREB level within these structures. The brain distribution of dCREB2 does not visibly change after learning – probably, its activity during LTM formation is regulated by some additional posttranslation modifications [4]. In contrast to the well-known role of the mammalian CREB in the nuclear transcription activation, we did not observe dCREB2 in the nuclei, except for the dCREB2-enriched neurons in SEG where it functions within the genetically active euchromatin area. The localization of pCREB within the neuronal processes has been also shown for the hyppocampal neurons [9]. Possibly, it provides the basis for the synaptic activity-dependent regulation of gene expression.

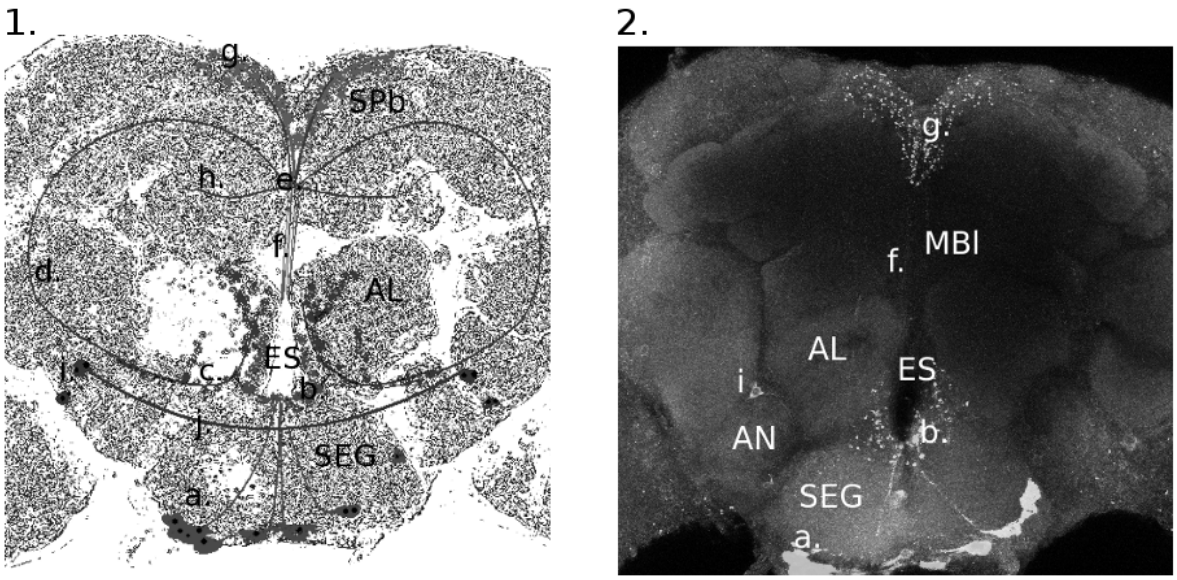

Fig. 1. The distribution of pCREB within the brain of *D. melanogaster*.

1. The scheme of pCREB distribution (dark grey). 2. pCREB-enriched structures (white). a. SEG neurons; b. esophageal glomerular structure 1; c. glomerular structure 2; d. neuronal tracts; e. neuronal tracts connected to V-shaped structure; f. – medial bundle (MBl); g. – V-shaped structure of SPb; h. the lateral tracts; i – the cell clusters near AN; j – commissure

Acknowledgements

This research was supported by the RFBR Grant 09-04-01208, RAS Program "Biodiversity and Genofonds", Contract of the Ministry of Science and Education P-316. We thank Prof. E. Buchner and Dr. A. Houfbauer for kindly supplying antibody to *D. melanogaster* cystein string protein.

References

1. J.C. Yin., M. De Vecchio, H. Zhou and T. Tully, *Cell*, 1995, **81** (1), 107-115.
2. J.C.P. Yin., J.S. Wallach, E.L Wilder, J. Klingensmith, D. Dang, N. Perrimon, H. Zhou, T. Tully and W.G. Quinn, *Mol. Cell. Biol.*, 1995, **15** (9), 5123-5130.
3. H. Ishimoto, T. Sakai and T. Kitamoto, *Proc. Natl. Acad. Sci. USA*, 2009, **106** (15), 6381-6386.
4. J. Horiuchi, W. Jiang, H. Zhou, P. Wu and J.C.P. Yin, *J. Biol. Chem*., 2004, **279** (13), 12117-12125.
5. R.W. Siegel and J.C. Hall, *Proc. Natl. Acad. Sci. USA*, 1979, **76** (1), 3430-3434.
6. T. Sakai, T. Tamura, T. Kitamoto and Y. Kidokoro, *Proc. Natl. Acad. Sci. USA*, 2004, **101** (45), 16058-16063.
7. J.S. Wu and L. Luo, *Nature protocols*, 2006, **1** (4), 2110-2115.
8. C. Melcher and M.J. Pankratz, *PLoS Biology*, 2005, **3** (9), 1618-1629.
9. P. Crino, K. Khodakhan, K. Becker, S. Ginsberg, S. Hemby and J. Eberwine, *Proc. Natl. Acad. Sci. USA*, 1998, **95** (5), 2313-2318.